Cooperation of p300 and iASPP in apoptosis and tumour suppression

Dissertation

for the award of the degree

“Doctor rerum naturalium”

of the Georg-August-Universität Göttingen

within the doctoral program

Molecular Biology of Microbial, Animal and Plant Cells

of the Georg-August University School of Science (GAUSS)

submitted by

Daniela Kramer

born in

Goslar, Germany

Göttingen 2013

Thesis Committee

Prof Dr. Matthias Dobbelstein,
Institute for molecular oncology, Faculty of medicine

Prof. Dr. Heidi Hahn,
Tumour genetics, Department of human genetics, Faculty of medicine

Prof Dr. Ralph Kehlenbach,
Department of biochemistry, Faculty of medicine

Members of the Examination Board

Referee: Prof. Dr. Matthias Dobbelstein, Institute for molecular oncology

2nd Referee: Prof. Dr. Heidi Hahn, Tumour genetics, Department of human genetics

Further members of the Examination Board

Prof. Dr. Ralph Kehlenbach, Department of Biochemistry

Prof. Dr. Holger Reichardt, Department of experimental immunology

PD. Dr. Wilfried Kramer, Department for microbiology and genetics

PD Dr. Roland Dosch, Department of developmental biochemistry

Date of oral examination: 29.11.2013

AFFIDAVIT

Herewith I declare, that I prepared the PhD Thesis: "Cooperation of p300 and iASPP in apoptosis and tumour suppression" on my own and with no other sources and aids than quoted.

Göttingen, 30.09.2013

Table of contents

List of Figures

List of Tables

Abbreviations

°C	Degree Celcius
∆N	Delta N
µg	Microgram
µL	Microliter
µM	Micromolar
aa	aminoacid
Ac	Acetylation
APS	Ammonium persulfate
ASPP	Apoptosis stimulating proteins of p53 or ankyrin repeat, SH3-domain, proline-rich region containing proteins
ATM	Ataxia telangiectasia mutated
ATR	ATM- and Rad3-related
BCI	*(E)*-2-Benzylidene-3-(cyclohexylamino)-2,3-dihydro-1H-inden-1-one; MKP-1/ MKP-3 inhibitor
BH-3	Bcl-2 Homology 3 (domain)
bp	Base pair
B-RAF	v-raf murine sarcoma viral oncogene homolog B
BRMS1	Breast cancer metastasis suppressor 1
bromo	Bromodomain
BSA	Bovine serum albumine
CBP	CREB-binding protein
CDDP	cisplatin
CDK1	Cyclin-dependent kinase 1
cDNA	Complementary DNA
cDNA	copyDNA
CH	Cysteine-histidine rich region
ChIP	Chromatin immunoprecipitation
ChIPseq	Chromatin immunoprecipitation coupled with deep sequencing
Chk1	Checkpoint kinase 1
CHX	Cycloheximide
CMV	Cytomegalievirus
CoIP	Co-immunoprecipitation
Ct	Cycle threshold
CTB	N-(4-Chloro-3-trifluoromethyl-phenyl)-2-ethoxy-benzamide; p300 activator
C-terminus	Carboxy terminus of a protein
Ctrl	control
DBD	DNA-binding domain
DMEM	Dulbecco`s modified Eagle medium
DMSO	Dimethylsulfoxide
DNA	Deoxyribonucleic acid
dNTP	Deoxynucleotide triphosphate
DTT	Dithiotreitol

E.coli	Escheria coli
EDTA	Ethylene diamine tetraacetic acid
EGTA	Ethylene glycol tetraacetic acid
ERK	Extracellular signal-regulated kinase
EtOH	Ethanol
FACS	Fluorescence-activated cell sorting
FCS	Fetal calf serum
G	Gauge
GFP	Green fluorescent protein
h	hour
HAT	Histone acetyl transferase
hc	High concentrated
Hepes	4-(2-Hydroxyethyl)piperazine-1-ethanesulfonic acid
HRP	Horseradish peroxidase
iASPP	Inhibitory ASPP
IBID	Interferon-binding domain
ID	Inhibitory domain
IP	immunoprecipitation
K	lysine
kd	knockdown
kDa	Kilodalton
LiCl	Lithium chloride
luc	luciferase
M	Molar
MAP	Mitogen activated protein
Max.	maximal
MEF	Mouse embryonic fibroblast
mg	milligram
MG132	N-(benzyloxycarbonyl)leucinylleucinylleucinal Z-Leu-Leu-Leu-al, proteasome inhibitor
min	minute
mL	milliliter
mM	millimolar
MMulv	Moloney murine leukemia virus
MRN	Mre11-Rad50-Nbs1
mRNA	messenger RNA
myo	myoglobulin
n	ample size
n.s.	not significant
NaDoc	Sodium deoxycholate
$NaHCO_3$	Sodiumhydrogencarbonate
ng	nanogram
nM	nanomolar
nm	nanometer
No.	number
NP-40	Nonidet P-40 substitute
N-RAS	Neuroblastoma Ras viral oncogene homolog
N-terminus	Amino-terminus of a protein

OD	Oligomerisation domain
P	Phosphorylation
PBS	Phosphate buffered saline
PBS	Phosphate buffered saline
PCR	Polymerase chain reaction
PHD	Plant homeo domain
PIC	Protease inhibitor cocktail
PML	promyelocytic leukemia protein
pmol	Pico-mol
PP1	Protein phosphatase 1
PP2A	Protein phosphatase 2A
Q/P	Glutamine/proline-rich domain
qPCR	Quantitative real-time PCR
R	Arginine
RAI	RelA associated inhibitor
RelA	P65, NF-kB subunit, v-rel reticuloendotheliosis viral oncogene homolog A (avian)
RNA	Ribonucleic acid
rpm	Rounds per minute
RT	Room temperature; Reverse transcriptase
S2	Safety level 2
SAM	Sterile alpha motif
SB203580	P38 inhibitor
SDS	Sodium dodecyl sulfate
SDS-PAGE	Sodium dodecyl sulfate polyacrylamide gel electrophoresis
sec	Second
shRNA	Small hairpin RNA
siRNA	Small interfering ribonucleic acid
siRNA	Small interfering RNA
TA	transactivation
TAZ	Transcriptional adapter zinc binding
TBST	Tris buffered saline + Tween 20
TEMED	Tetramethylethylenediamine
Tm	Melting temperature
Tris	Trisamine
U	Unit
UCSC	University of California Santa Cruz
UV	Ultraviolet
V600E	Mutation from valine (V) to glutamic acid (E) at position 600
VSV-G	Vesicular stomatitis virus glycoprotein
WB	Western Blot
WT	Wild type
YAP-1	Yes associated protein 1
zVad	carbobenzoxy-valyl-alanyl-aspartyl-[O-methyl]-fluoromethylketone; caspases inhibitor
ZZ	Zinc finger domain

Abstract

Mutation or functional inactivation of tumour suppressors represents a key event in the transformation of cells and contributes to the development of cancer. P300 and CBP constitute two histone acetyltransferases with tumour suppressor functions that are frequently mutated or functional inactivated in cancer. Accordingly, after chemotherapy-induced DNA damage, for example, p300 and CBP can co-activate the key tumour suppressor proteins p53 and TAp73, thereby contributing to tumour cell apoptosis.

Here we investigated the impact of the co-factor protein iASPP on p300 and TAp73 function, after treatment of tumourigenic cell lines with the chemotherapeutic drug cisplatin. iASPP belongs to the ASPP-family, another class of co-factors that contribute to p53-family-mediated apoptosis induction. Direct interaction of iASPP with p300 and TAp73 has been revealed before; functional consequences of these interactions remain elusive though and are therefore subject of our analyses.

By investigating the consequences of stable iASPP knockdown in tumourigenic cell lines, we found that direct interaction of iASPP and p300 in cisplatin-treated cells led to enhanced protein stability of p300 and TAp73. Correspondingly, iASPP depletion resulted in decreased protein amounts of p300, reduced induction of pro-apoptotic p73 target genes and impaired apoptosis.

BRMS1 represents a recently discovered E3 ubiquitin ligase for p300. Hence, we observed that BRMS1 depletion rescued the degradation of p300 and CBP in cisplatin-treated, iASPP-depleted cells. Therefore, we hypothesize that BRMS1 inhibition constitutes the molecular mechanism underlying the increased protein stability of p300 in the presence of iASPP. Furthermore, we discovered, that malignant melanoma are characterized by down-regulated iASPP expression level. Follow-up studies on melanoma cell lines revealed that low iASPP expression correlated with decreased protein levels of p300 in cisplatin-treated cells. BRMS1 knockdown in some of these cell lines could up-regulate p300 protein level, suggesting that down-regulation of iASPP expression leads to functional inactivation of p300 in melanoma, by allowing BRMS1 activity on p300. Treatment of the cells with the MKP-1 inhibitor BCI, could re-establish p300 level and induce p300-dependent apoptosis by yet unknown mechanisms.

Summing up, iASPP represents a regulator for p300 function. It contributes to p300-dependent apoptosis induction by enhancing its protein stability after DNA damage. Re-establishment of p300 levels in low iASPP-expressing melanoma might represent a novel strategy to overcome chemoresistance.

1. Introduction

1.1 Regulation and function of TAp73 in cancer

1.1.1 The p53-family and its role in the prevention of cancer

In 2008 approximately 7.6 million people died due to cancer (according to fact sheet No.297 of World Health Organization, www.who.int). Therefore, cancer accounts for 13% of all deaths world-wide. In general cancer is mostly caused by accumulation of DNA mutations and following, uncontrolled proliferation of the cells. Mutations in the DNA arise from virus infections, bad nutrition, stroke or other environmental insults (Hanahan and Weinberg 2000). Moreover, gene aberrations or other genomic cancer pre-dispositions can be inherited (Garber and Offit 2005). However, non-cancerous cells harbour proteins, the so called guardians of the genome that become activated upon DNA damage or DNA mutations. Upon activation, these proteins trigger DNA repair mechanisms or, in case DNA is too severely damaged, induce the programmed death of a cell. One major protein family that prohibits such an accumulation of DNA mutations or replication errors constitutes the p53-family.

The p53-family, consisting of p53, p73 and p63 are tumour suppressor proteins that control cell cycle arrest and apoptosis induction by transcriptional regulation of cell-cycle related and pro-apoptotic target genes (Smeenk, van Heeringen et al. 2008; Allocati, Di Ilio et al. 2012). Moreover, the p53-family is also involved in a variety of other cellular processes such as differentiation, senescence or autophagy due to transcriptional regulation of different sets of target genes (Levrero, De et al. 2000).

As primarily p53 represents such a crucial inhibitor of cell transformation, 50% of all solid tumours display mutations in the p53 gene which lead to a functional inactivation of wild-type p53 (Soussi and Wiman 2007). Interestingly, these mutations comprise point mutations in the DNA-binding domain of the protein. They result in the expression of dominant-negative mutant p53, thus leading to the inactivation of the remaining wild-type p53 allele (Blagosklonny 2000; de Vries, Flores et al. 2002). Moreover, other tumours that retain wild-type p53 expression often harbour mutations in up-stream regulators of the p53 signalling pathway, thereby mediating a functional inactivation of wild-type p53 as well (Michael and Oren 2002; Brosh and Rotter 2009).

1.1.2 The p53-family members TAp73 and TAp63 constitute tumour suppressors.

The p53-family members p73 and p63 also constitute transcription factors that can partially regulate the same set of p53 target genes. Therefore, in case of inactive, deleted or mutated p53, both proteins can trigger tumour cell apoptosis as well (Rufini, Agostini et al. 2011; Allocati, Di Ilio et al. 2012).

P73 and p63 exist in multiple isoforms due to usage of an internal promoter and alternative splicing that occurs at the C-terminus of both proteins (Figure 1.1). In general, p73/p63 isoforms can be classified into two main groups. The first group of p73/p63 isoforms constitute the N-terminal truncated variants called ΔNp63 and ΔNp73. ΔNp73 and ΔNp63 may act in an oncogenic fashion, as they can inhibit the transcription factor function of p53, TAp73 and TAp63. Molecular basis of this inhibition represents the formation of dominant-negative hetero-tetramers and by blocking the DNA-binding sites of p53-family target genes (Muller, Schleithoff et al. 2006).

The other main group comprises the full-length TAp73/TAp63 isoforms that may function as classical tumour suppressors due to their overlapping function with wild-type p53. Interestingly, studies of TAp73 knockout mice revealed an important role for TAp73 in the prevention of chromosomal instability, as TAp73 knockout mice displayed increased aneuploidy in oocytes (Tomasini, Tsuchihara et al. 2008). Thus, TAp73-mediated apoptosis of chromosomal instable cells represents another aspect of the presumed tumour suppressive functions of TAp73, which contribute to the prevention of cell transformation.

Perhaps due to this dual role of tumour suppressor and proto-oncogene, the p73 and p63 gene loci are rarely mutated in cancer (Rufini, Agostini et al. 2011). Therefore, classical chemotherapy such as treatment of tumour cells with the chemotherapeutic drug cisplatin, Etoposide or doxorubicin mostly leads to an activation of TAp73 (or wild-type p53, if present), followed by induction of apoptosis and regression of the tumour (Irwin, Kondo et al. 2003).

1.1.3 Structure of the p73 and p63 gene locus

P73 and p63 proteins were discovered in 1997 and 1998, over 30 years after the discovery of p53 (Kaghad, Bonnet et al. 1997; Yang, Kaghad et al. 1998). Both proteins consist of a transactivation domain (TA) and a central DNA-binding domain (DBD) at the N-terminus (Figure 1.1). The DNA-binding domains of p53, p73 and p63 share high sequence homology which partially explains the overlapping sets of target genes (Lokshin, Li et al. 2007; Smeenk, van Heeringen et al. 2008). Additionally, all p53-family members harbour an

oligomerisation domain (OD) at the C-terminus, as the proteins bind to DNA as tetrameric complexes.

Due to intensive splicing at the C-terminus, p73 and p63 exist in multiple isoforms that differ in their C-terminal structure. Therefore, full-length isoforms of p73/ p63, called p73α/ p63α and p73β/ p63β contain a unique SAM motif (sterile-α-motif) for mediation of protein-protein interactions, as well as an extra, C-terminally located inhibitory domain (ID) that regulates their transcriptional activity (Luh, Kehrloesser et al. 2013).

Instead of the N-terminal located transactivation domain of TA-isoforms, ΔN isoforms comprise a more internally localized transactivation domain. (Liu, Nozell et al. 2004; Toh, Logette et al. 2008). Therefore, ΔNp73 and ΔNp63 can actively regulate specific sets of target genes as shown for example for ΔNp63α in keratinocytes (King, Ponnamperuma et al. 2003; Birkaya, Ort et al. 2007).

The composition of the p73 gene locus is depicted in Figure 1.1 (Deyoung and Ellisen 2007).

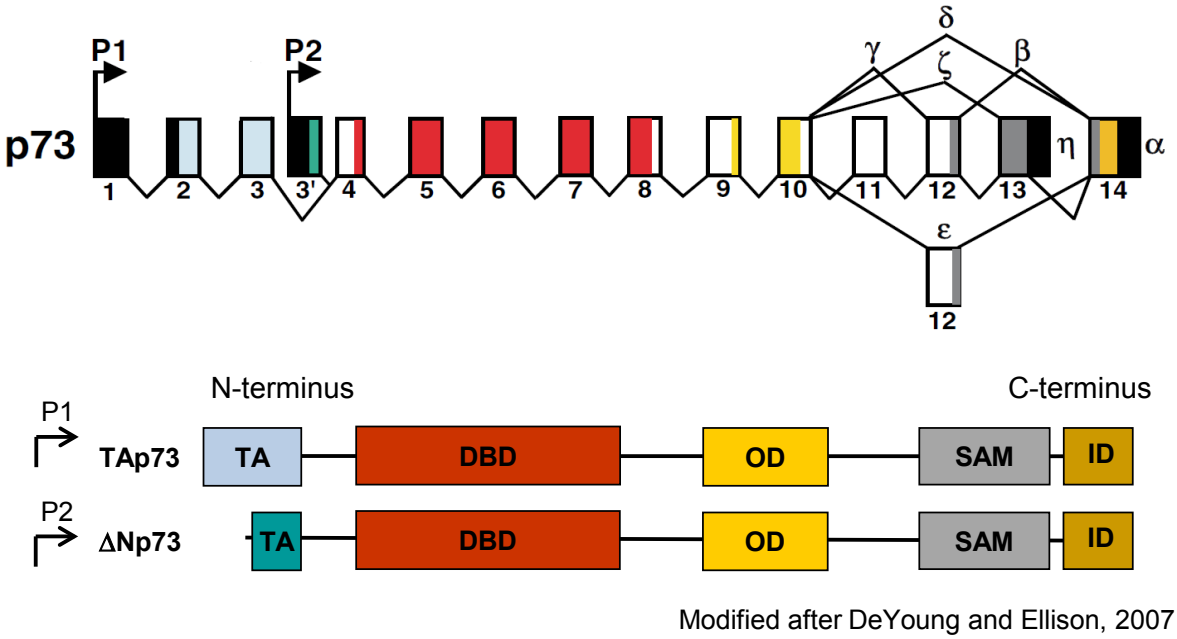

Figure 1.1. Structure of the p73 gene locus. *The gene locus of p73, including the exon structure as well as both promoter regions and the multiple splicing events at the C-terminus are displayed. Moreover the domain structure of TAp73 and ΔNp73 is illustrated. The exons which resemble the corresponding domains can be identified due to equal colouring. P1, P2 = promoter region; TA = transactivation domain; DBD = DNA-binding domain; OD = oligomerisation domain; SAM = sterile-α-motif, ID = Inhibitory domain.*

1.1.4 The expression pattern of p73 isoforms in cancer

In-vitro experiments have elucidated a more pronounced role for p73 in cancer compared to p63. The expression of different p73 isoforms is highly variable in different tumour types, though. In detail, high expression of full-length TAp73 isoforms was found in breast cancer, hepatocellular carcinoma and prostate cancer so far (Tannapfel, Wasner et al. 1999; Zaika, Kovalev et al. 1999; Su, Ouyang et al. 2009). In leukemia, high expression of short TAp73 isoforms (for example TAp73δ and TAp73ε) was commonly detected although functional consequences of this over-expression remain elusive (Tschan, Grob et al. 2000). In contrast, expression of the oncogenic splice variant ΔNp73 is often found to be up-regulated in neuroblastoma as well as in head and neck cancer (Guan and Chen 2005; Faridoni-Laurens, Tourpin et al. 2008). Interestingly, this over-expression of ΔNp73 isoforms can be correlated with increased chemoresistance in the respective tumours (Kovalev, Marchenko et al. 1998; Casciano, Mazzocco et al. 2002; Douc-Rasy, Barrois et al. 2002). However, most gene expression studies lack a differentiating analysis of the expression levels of single p73 isoforms. Therefore, future analyses will have to dissect the expression patterns of the pro- and anti-apoptotic p73 isoforms in more detail.

1.1.5 The role of TAp73 in classical chemotherapy

TAp73 becomes active by treatment of the cells with classical chemotherapeutics such as cisplatin, Taxol, doxorubicin or Etoposide, leading to TAp73-dependent apoptosis induction (Irwin, Kondo et al. 2003). The underlying signalling pathway of chemotherapy-induced, TAp73-mediated apoptosis induction involves a cascade of different proteins (Figure 1.2).

In summary, most of the TAp73-activating agents primarily cause DNA damage that is recognized then by the multiprotein complex MRN (protein complex of Mre11-Rad50-NBS1) (Uziel, Lerenthal et al. 2003; Adams, Medhurst et al. 2006). As a consequence, the kinases ATM and ATR are getting activated, leading to the phosphorylation and therefore activation of multiple down-stream kinases (Basu and Krishnamurthy 2010). Most importantly, the p73-specific, tyrosine receptor kinase c-abl is activated by ATR/ ATM which in turn triggers a variety of phosphorylation events that ultimately lead to the accumulation and activation of TAp73 (Agami, Blandino et al. 1999; Gong, Costanzo et al. 1999). Next, TAp73 transcriptionally up-regulates a panel of pro-apoptotic BH3-only genes, including *puma* and *pig3* (Fontemaggi, Kela et al. 2002; Melino, Bernassola et al. 2004). Due to this accumulation of pro-apoptotic proteins, BAX and BAK proteins are released from inhibitory complexes with the anti-apoptotic BCL-2 family member proteins. Subsequently, BAX and BAK can

translocate to the mitochondria which in turn initiates the release of cytochrome C and therefore the induction of tumour cell apoptosis. Figure 1.2 summarizes TAp73-mediated apoptosis after DNA damage.

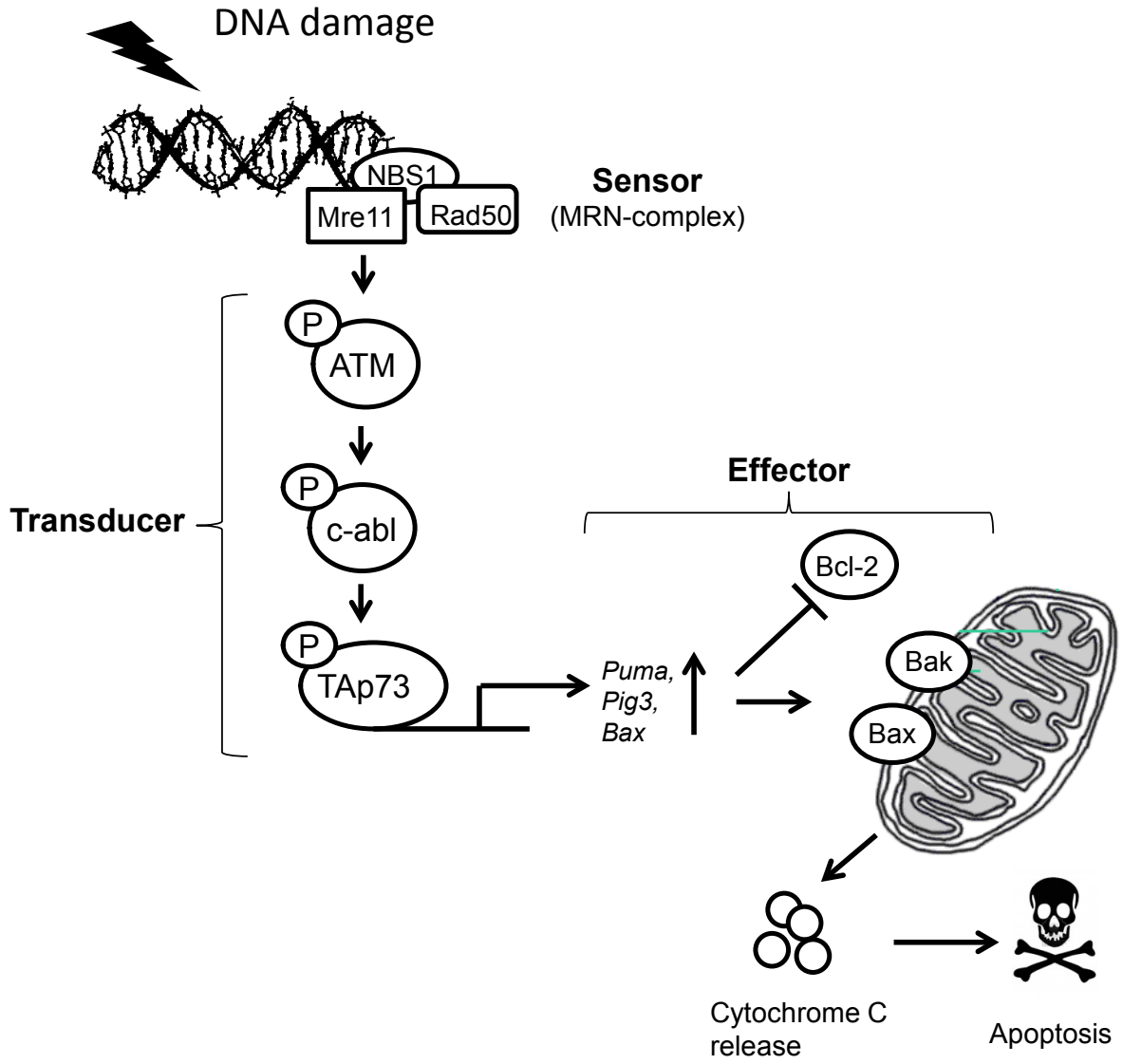

Figure 1.2. Overview of TAp73-dependent apoptosis induction after DNA damage.
After DNA damage, the MRN complex senses DNA lesions. Thereafter, a cascade of kinases, including ATM and c-abl are activated, leading to the transduction of the signal. Finally, TAp73 is activated by post-translational modifications, which subsequently mediates the transcriptional up-regulation of pro-apoptotic genes. Next, due to increased expression of pro-apoptotic proteins, BCL-2 is repressed and Bax and Bak can translocate to the mitochondria. Hence, cytochrome C is released, which induces apoptosis.

Nevertheless, classical chemotherapy often confers high toxicity and patients frequently lack a full response to the drug treatment (Serrone and Hersey 1999; Yao, Panichpisal et al.

2007; Galluzzi, Senovilla et al. 2012). Moreover, some tumours acquire chemoresistance during repeating cycles of chemotherapy. One of the causes for this acquired chemoresistance constitutes the functional inactivation of TAp73 due to an newly developed interaction of TAp73 with oncogenes such as mutant p53, or due to mutations of TAp73-associated co-factors (Bergamaschi, Gasco et al. 2003; Rufini, Agostini et al. 2011). As TAp73-signalling pathways are not completely understood, new insights into the regulation of TAp73 function might provide the basis for new cancer therapies, thus circumventing chemoresistance that derives from an inactivation of TAp73 function.

1.1.6 Regulation of TAp73 function by phosphorylation

As the p53-family can mediate a variety of different cellular responses, the activity and specific functions of the proteins have to be tightly regulated. Two of the major mechanisms that regulate the function and activity of the p53-family comprise associating proteins (so called co-factors) and post-translational modifications. Post-translational modifications of the p53-family include phosphorylation, acetylation, ubiquitination, sumoylation and neddylation (Bode and Dong 2004; Conforti, Sayan et al. 2012). Some of the post-translational modifications are commonly found for all p53-family members, others are family-member specific.

A variety of different post-translational modifications for TAp73 have already been described. As we investigated the effects of cisplatin on TAp73 function, we will only summing up the most relevant post-translational modifications of TAp73 that have been elucidated after cisplatin treatment (Figure 1.3).

As shortly mentioned before, a major phosphorylation event of TAp73 is mediated by the tyrosine receptor kinase c-abl. Thus, active c-abl kinase represents a pre-requisite for TAp73 protein accumulation, followed by activation of the protein and TAp73-mediated apoptosis induction (Agami, Blandino et al. 1999; Gong, Costanzo et al. 1999). In detail, upon DNA damage, especially after cisplatin treatment of primary and tumour cells, c-abl gets activated, thus leading to a direct interaction of c-abl and TAp73. Consequently, c-abl phosphorylates TAp73 at tyrosine residue 99 (Yuan, Shioya et al. 1999) which triggers activation and accumulation of the protein.

In parallel, the p38 MAP kinase pathway is activated by c-abl as well, due to the phosphorylation and activation of the MKK3/ MKK6 kinases. In turn, MKK3 and MKK6 activate p38 by its phosphorylation at threonine residue 180 and tyrosine residue 182 then (Sanchez-Prieto, Sanchez-Arevalo et al. 2002; Galan-Moya, Hernandez-Losa et al. 2008).

Subsequently, p38 contributes to the induction and stabilization of TAp73 protein by phosphorylating its threonine residues 167, 442 and 482 (Sanchez-Prieto, Sanchez-Arevalo et al. 2002; Rufini, Agostini et al. 2011). Interestingly, inhibition of p38 is already sufficient to prevent accumulation and induction of TAp73 protein, even in the presence of active c-abl protein (Sanchez-Prieto, Sanchez-Arevalo et al. 2002). This validates again the importance of phosphorylation-mediated regulation of TAp73 activity.

Furthermore, after previous phosphorylation of TAp73 by c-abl and p38, the TAp73 co-factor protein YAP-1 gets activated by c-abl-mediated phosphorylation as well, thereby inducing a complex formation of YAP-1 and TAp73 (Strano, Monti et al. 2005; Lapi, Di Agostino et al. 2008; Levy, Adamovich et al. 2008). Due to this complex formation, the p73-specific ubiquitin ligase Itch cannot bind and hence proteasomally degrade TAp73 anymore. Thus, TAp73 protein further accumulates due to an increase in its protein stability (Levy, Adamovich et al. 2007).

1.1.7 Regulation of TAp73 function by p300-mediated acetylation

After phosphorylation-mediated activation of TAp73, the histone acetyltransferase (HAT) p300 can associate with YAP-1/ TAp73 complexes, followed by p300-mediated acetylation of TAp73 at lysine residues 321, 327 and 331 (Costanzo, Merlo et al. 2002; Mantovani, Piazza et al. 2004). Hence, acetylation of TAp73 represents another type of post-translational modification that further contributes to the enhanced protein stability of TAp73. The underlying molecular mechanism of acetylation-mediated stabilization of TAp73 protein comprises the dissociation of the ubiquitin ligase MDM2 from TAp73, as binding of MDM2 and p300 to TAp73 is mutually exclusive (Zeng, Li et al. 2000). Furthermore, p300-mediated acetylation increases the DNA-binding affinities of TAp73. This partially explains the increased half-life of the TAp73 protein, as chromatin association of proteins anticipates their fast proteasomal degradation in general (Sakaguchi, Herrera et al. 1998; Martinez-Balbas, Bauer et al. 2000; Costanzo, Merlo et al. 2002).

Apart from enhanced protein stability, acetylation of TAp73 also dictates which groups of target genes are regulated by TAp73, as p300-dependent acetylation of TAp73 promotes the transcriptional up-regulation of pro-apoptotic p73 target genes instead of cell-cycle related genes (Costanzo, Merlo et al. 2002). This can be partially explained by the fact that this multi-protein complex consisting of p300, YAP-1 and TAp73 is localized to genomic p73 target sites. This causes p300-dependent acetylation of adjacent histones and formation of open and accessible chromatin regions (Levy, Adamovich et al. 2008). As p300 constitutes a

bridging factor for the basal transcription machinery with specific transcription factors, as well (Chen and Li 2011), chromatin localization of TAp73-YAP-1-p300 complexes also triggers the recruitment of RNA polymerase II to specific promoter regions. Consequently, transcriptional up-regulation of pro-apoptotic p73 target genes is initiated (Levy, Adamovich et al. 2008). Examples for genes that are transcriptionally up-regulated by TAp73-YAP-1-p300 complexes comprise the pro-apoptotic target genes *puma*, *pig3*, *bax*, *fas* or *noxa* (Fontemaggi, Kela et al. 2002; Koeppel, van Heeringen et al. 2011). Figure 1.3 summarizes the TAp73/ p300-mediated apoptosis induction after cisplatin treatment (Lunghi, Costanzo et al. 2009).

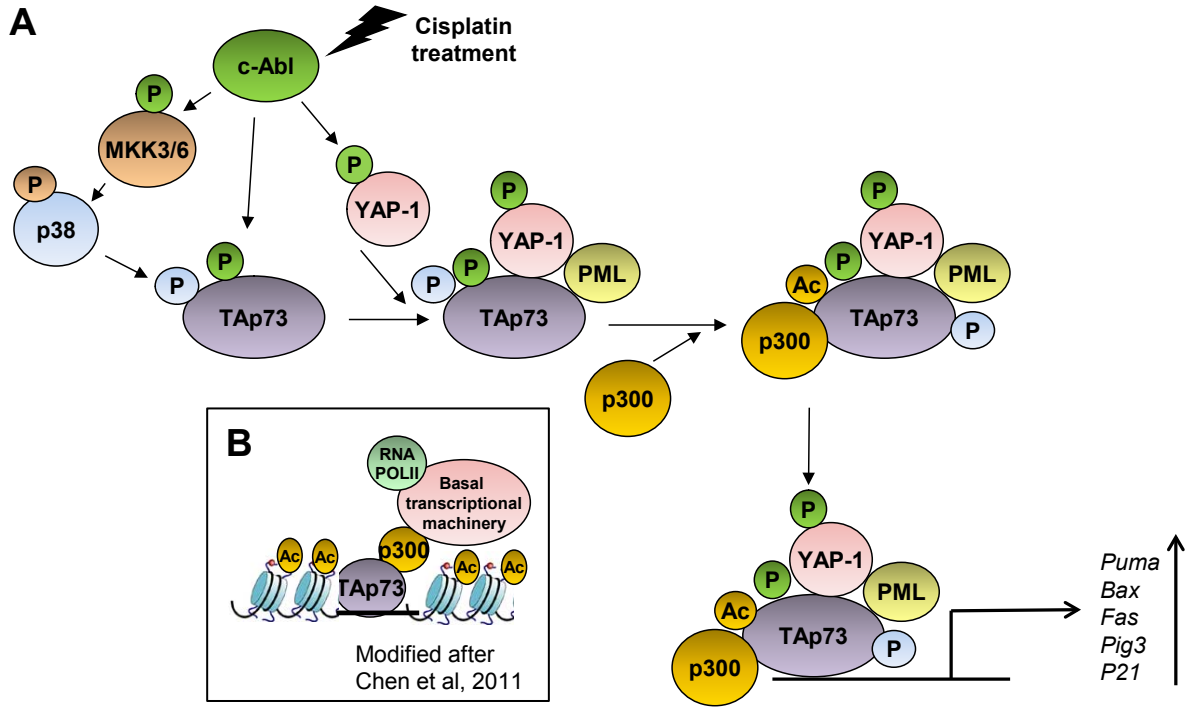

Modified after Lunghi et al, 2009

Figure 1.3. Activation of TAp73-mediated transcription after cisplatin treatment. A. *Upon cisplatin treatment of cells, c-abl and p38 are activated to mediate phosphorylation and therefore activation of TAp73. Moreover, c-abl-mediated YAP-1 phosphorylation triggers TAp73-YAP1 complex formation in PML bodies, followed by the recruitment of p300 to the protein complex and subsequent acetylation of TAp73.* ***B.*** *Additionally, p300 acetylates adjacent histones of p73 target gene promoters. This leads to the DNA-binding of the TAp73-YAP-1-complex to pro-apoptotic p73 target gene promoters as well as to the recruitment of the basal transcription machinery to pro-apoptotic p73 target gene promoters. (Ac = acetylation; P = phosphorylation, RNA Pol II = RNA polymerase II).*

Of note, TAp73-YAP-1-p300 complexes accumulate in distinct nuclear structures due to their association with PML protein (Lapi, Di Agostino et al. 2008). These nuclear structures are

composed of various proteins that form distinct, metabolically stable, sub-nuclear domains. The localization of TAp73-YAP-1-p300 complexes to the so called PML-bodies further protects p300, TAp73 and YAP-1 from proteasomal degradation, thus contributing to active transcription of p73-target genes and the subsequent induction of apoptosis (Bernassola, Salomoni et al. 2004; Shima, Shima et al. 2008).

Besides post-translational modifying enzymes, p73 as well as p53 and p63 can associate with other co-factor proteins that regulate distinct cellular responses of the p53-family as well. One important co-factor family constitutes the ASPP-family (**a**poptosis-**s**timulating **p**roteins of **p**53 or **a**nkyrin repeat-, **S**H3-domain- and **p**roline-rich region-containing **p**roteins).

1.2. The ASPP-family

1.2.1 Structure and interaction properties of the ASPP-family

The ASPP-family consists of three proteins, called ASPP2, ASPP1 and iASPP (Figure 1.4). The first protein of the ASPP-family that has been associated with p53 function was the ASPP2-deriving fragment 53BP2. Interestingly, binding studies between 53BP2 and wild-type p53 revealed that direct interaction of both proteins has a crucial impact on p53-mediated apoptosis induction (Iwabuchi, Bartel et al. 1994; Iwabuchi, Li et al. 1998; Lopez, Ao et al. 2000). Furthermore, point mutations in the DNA-binding domain of the p53 gene, that result in the expression of mutant p53, often target residues that mediate the interaction between p53 and 53BP2 (Iwabuchi, Bartel et al. 1994; Tidow, Veprintsev et al. 2006; Ahn, Byeon et al. 2009). Therefore, it is assumed that loss of 53BP2-p53 interaction due to p53 mutation contributes to the functional inactivation of wild-type p53 in respect to apoptosis induction. Follow-up analysis of the gene locus coding for 53BP2 (*TP53BP2*) revealed that 53BP2 only represents the N-terminal truncated version of the full-length protein ASPP2 and that ASPP2 has similar impact on p53 function than 53BP2 has.

Structural analysis discovered that all ASPP-family members are similarly composed of multiple ankyrin repeats, a SH3 domain and a proline-rich region at the C-terminus (Slee, Gillotin et al. 2004) (Figure 1.4). At the N-terminus, ASPP1 and ASPP2 harbour a unique α-domain region that is thought to mediate ASPP1- and ASPP2-specific protein-protein interactions (Sullivan and Lu 2007). Hence, ASPP1 and ASPP2 share a higher sequence homology compared to iASPP, thus indicating a functional difference between ASPP1/2 and iASPP.

Interestingly, in lower vertebrates such as *Caenorhabditis elegans* only one ASPP-family member is present (encoded by the *ape-1* gene) that displays high sequence homology to human iASPP (Bergamaschi, Samuels et al. 2003). Thus, the genes encoding for ASPP1 and ASPP2 (*PPP1R13B* and *TP53BP2*) are likely to be evolved from the iASPP encoding gene *PPP1R13L* (Trigiante and Lu 2006).

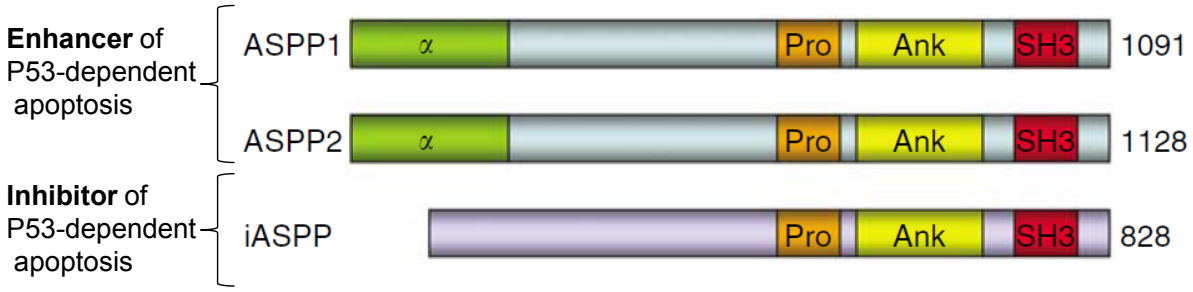

Figure 1.4. Structure of the ASPP-family (modified after Sullivan and Lu 2007).
All ASPP-family members, ASPP1, ASPP2 and iASPP, comprise a proline-rich region (Pro), multiple ankyrin repeats (Ank) and a SH3-domain (SH3) at the C-terminus. Moreover, ASPP1 and ASPP2 harbour a specific α–domain (α) at the N-terminus. IASPP is an inhibitor of p53-mediated apoptosis whereas ASPP1 and ASPP2 are stated as enhancers of p53-dependent apoptosis induction (the numbers left indicated the number of total amino acids and therefore size of the protein).

The main function of the ASPP-family includes the mediation of protein-protein interactions, the formation of multi-protein complexes and sub-cellular re-localization as well as conformational changes of their interaction partners (Sullivan and Lu 2007). By yeast two hybrid screens, several interaction partners of the ASPP-family have been identified. Apart from interaction of ASPP with BCL2, p65/RelA and Protein phosphatase 1 (PP1) (Naumovski and Cleary 1996; Yang 1999; Llanos, Royer et al. 2011), all ASPP family members are able to interact with the p53-family (Iwabuchi, Bartel et al. 1994; Samuels-Lev, O'Connor et al. 2001). Interestingly, binding studies of the ASPP- and p53-family members revealed that iASPP has a more potent binding affinity towards p63 and p73 than ASPP1 and ASPP2 display, which indicates that iASPP possesses p63/p73-specific functions (Robinson, Lu et al. 2008). On the other hand, binding affinities of ASPP2, ASPP1 and iASPP to p53 are equally strong.

1.2.2 The role of ASPP1 and ASPP2 as co-factors for the p53-family

ASPP1 and ASPP2 interactions with p53 result in enhanced DNA-binding properties of p53 followed by a stronger induction of pro-apoptotic target genes such as *puma* and *bax*

(Samuels-Lev, O'Connor et al. 2001*)*. Similar results were obtained from EMSA assays using recombinant ASPP1/2 proteins together with p73 and p63 (Samuels-Lev, O'Connor et al. 2001). In contrast, cell-cycle regulated target genes such as *p21* or *Mdm2* remained unaffected from ASPP1 and ASPP2 over-expression.

Moreover, a triple complex formation between ASPP1/2, p300 and p53 in untreated as well as doxorubicin-treated U2OS cells was discovered (Gillotin and Lu 2011). Luciferase assays using different combinations of these proteins showed that this triple interaction enhanced the transcriptional up-regulation of the pro-apoptotic gene *pig3* whereas *p21* expression remained unaffected. Therefore, ASPP1 and ASPP2 seem to promote the pro-apoptotic function of p53 by enhancing the interaction of p300 and p53.

In line, likely due to the p53-dependent, pro-apoptotic function of ASPP1 and ASPP2, mRNA levels of both genes were also found to be frequently down-regulated in tumours deriving from breast cancer patients (Bergamaschi, Samuels et al. 2003; Sullivan and Lu 2007). Down-regulation of ASPP1/2 mRNA levels is caused by methylation events at the promoter sequences and might partially explain the frequently observed functional inactivation of wild-type p53 in breast cancer beside the expression of mutant p53 (Mori, Ito et al. 2004; Liu, Lu et al. 2005; Zhao, Wu et al. 2010).

1.2.3 The cellular function of iASPP

In contrast to ASPP1 and ASPP2, iASPP is declared an inhibitor of p53-mediated apoptosis (Bergamaschi, Samuels et al. 2003). Originally, iASPP has been discovered as a smaller fragment called RAI (RelA-associated inhibitor) by using RelA/p65 as a bait in yeast two hybrid screens (Yang 1999). Follow-up studies depicted a role for RAI in the inhibition of the transcriptional activity of NF-κB (Takada, Sanda et al. 2002) (Figure 1.5). Four years later Bergamaschi and colleagues discovered that RAI only represents a small fragment of the full-length protein iASPP that is encoded by the *PPP1R13L* gene (Bergamaschi, Samuels et al. 2003). Of note, polymorphisms at the 19q13.2 gene locus (consisting out of *PPP1R13L,* ERCC*1* and *CD3EAP*) have been previously associated with increased susceptibility for the development of lung, breast and rectal cancer (Nexo, Vogel et al. 2008; Chae, Kim et al. 2013; Yin, Guo et al. 2013), thereby implicating a possible role of iASPP in the formation of cancer.

Expression studies of various iASPP fragments revealed an overall cytoplasmic localization of iASPP due to a nuclear export signal that is located at the N-terminus (Slee, Gillotin et al. 2004). However, Zhang and colleagues elucidated a pre-dominantly nuclear localization of

iASPP, likely due to the existence of a N-terminal truncated isoform of iASPP, called iASPP-SV (Zhang, Diao et al. 2007). Besides, it is not clear yet, whether iASPP-SV constitutes a new isoform of iASPP or whether it is a cleavage-product of the full-length iASPP protein.

Chikh and colleagues found a nuclear localization of iASPP in mouse keratinocytes as well, whereas in most of the analysed human cell lines iASPP localizes to the cytoplasm (Slee, Gillotin et al. 2004; Chikh, Matin et al. 2011). Interestingly, nuclear localization of iASPP could be clearly correlated with its inhibitory role on p53 and p63 function (Trigiante and Lu 2006). Thus, sub-cellular localization of iASPP seems to have a crucial impact on its specific function.

In U2OS and MCF-7 cells over-expression of full-length iASPP results in a complex formation of iASPP and wild-type p53 followed by inhibition of p53-dependent apoptosis after UV-radiation or treatment of the cells with cisplatin (Bergamaschi, Samuels et al. 2003) (Figure 1.5). Interestingly, it was recently discovered that a direct interaction of iASPP with PP1 seems to represent a pre-requisite for this inhibitory effects of iASPP, as mutation of the PP1 interacting phenylalanine residue 815 of the iASPP protein sequence prohibited the inhibitory effects of iASPP over-expression on p53 function (Llanos, Royer et al. 2011).

Nevertheless, an over-expression of iASPP in breast cancer tissue and breast cancer cell lines is frequently detected (Bergamaschi, Samuels et al. 2003). Moreover, rat transformation assays using full-length iASPP constructs revealed that iASPP can enhance cell transformation by its co-operation with Ras, E1A or E7, thereby validating iASPP as a proto-oncogene. Hence, the protein name iASPP can be also interpreted as the **i**nhibitory form of **a**poptosis **s**timulating **p**roteins of **p**53.

To assess the cellular role of iASPP more closely, iASPP knockout mice were recently generated. As the most obvious phenotype, iASPP knockout mice display abnormalities in the formation of the skin (Notari, Hu et al. 2011). Closer analysis of different skin layers revealed a crucial role for iASPP in prevention of cellular senescence, as loss of iASPP yielded a higher rate of differentiated keratinocytes (Notari, Hu et al. 2011). Further analysis showed that the underlying mechanism of iASPP function in skin homeostasis resulted from its nuclear interaction with p63, thus revealing a new, p53-independent function of iASPP (Chikh, Matin et al. 2011). In the analysed keratinocytes and MEF cells, iASPP was able to interact with TAp63 and ΔNp63, thereby inhibiting the transcription factor function of both proteins (Chikh, Matin et al. 2011; Notari, Hu et al. 2011), which in turn inhibited the expression of p63-specific target genes such as loricrin and involucrin (Figure 1.5).

Interaction of iASPP with p53 and p63 suggests similar, functional interactions between iASPP and p73, as direct binding of both proteins has been elucidated before. (Robinson, Lu et al. 2008). However, consequences of iASPP expression on TAp73 function have not been addressed yet. Moreover, a complex formation of iASPP and the TAp73 co-activator p300 has already been proven in untreated as well as doxorubicin-treated U2OS and H1299 cells (Gillotin and Lu 2011). The functional consequences of iASPP-TAp73 and iASPP-p300 interaction remain elusive, though. Figure 1.5 summarizes the cellular functions of iASPP that have been described so far.

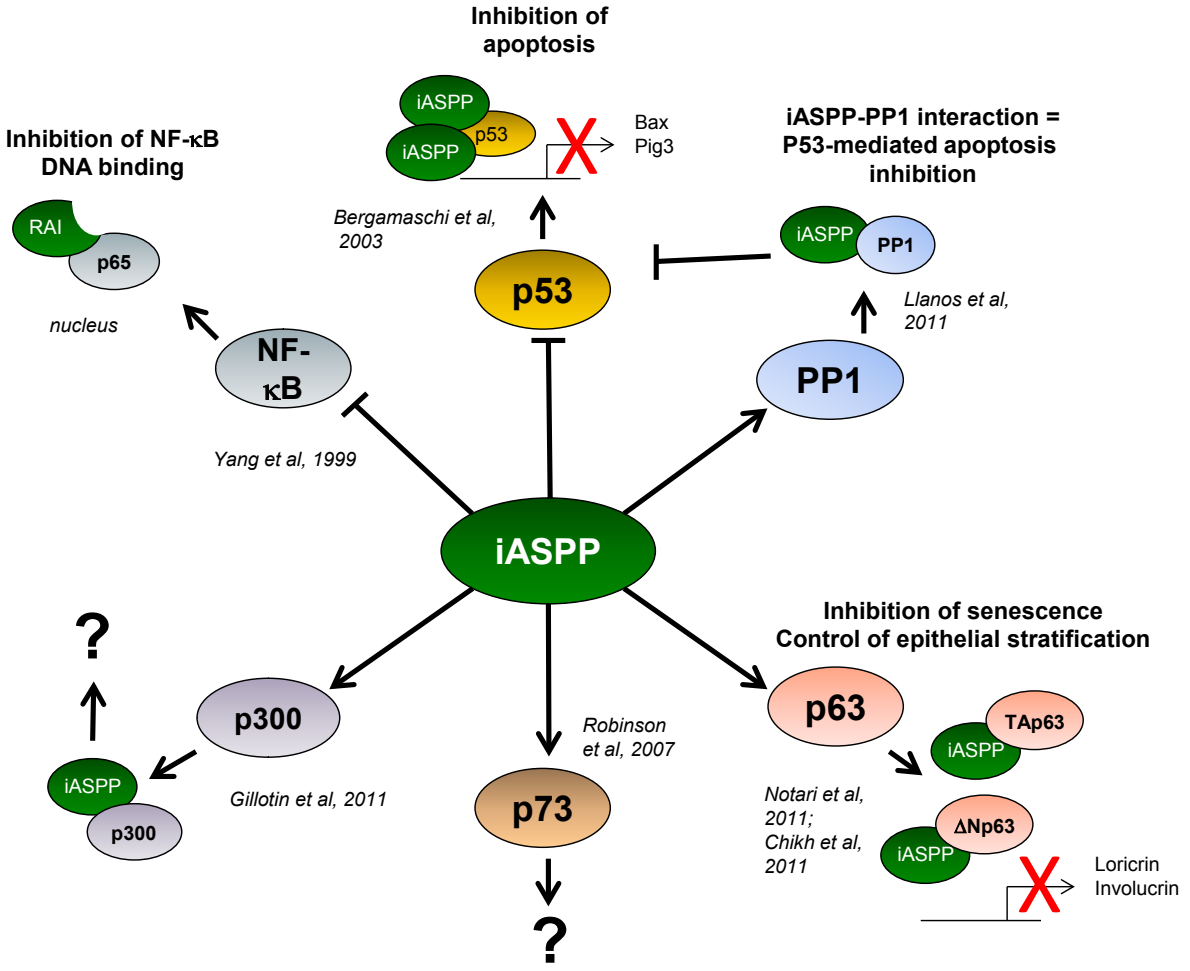

Figure 1.5. Protein interactions and cellular functions of iASPP. *iASPP interacts with a set of different proteins in the cell. One of the most important interactions represents the iASPP-p53 complex formation that leads to a functional inhibition of p53. The direct interaction of iASPP with PP1 represents a pre-requisite for this inhibitory function of iASPP on p53. In contrast, a fragment of iASPP (RAI) can also interact and inhibit RelA/ p65 and therefore NF-κB activity, which is likely to result in apoptosis induction. Additionally, in keratinocytes, iASPP binds to TAp63 and ΔNp63 which in turn leads to an inhibition of p63 function and therefore iASPP-mediated regulation of skin homeostasis. Other interactions of iASPP comprise those with p73 and p300; however, functional consequences of such interactions have not been addressed yet.*

1.3 Function and regulation of the KAT3-family members p300 and CBP

1.3.1 P300 and CBP mainly function as histone acetyltransferases

As stated before, p300 and CBP constitute another important co-factor family that modulates p53-family-dependent apoptosis induction (Costanzo, Merlo et al. 2002; Iyer, Chin et al. 2004). P300 and CBP are involved in various cellular processes. However we will only summarize the most relevant functions in respect to this project.

Originally, both proteins have been found as binding partners for the viral proteins E1A and E7 that cause the functional inactivation of p300 and CBP (Arany, Sellers et al. 1994; Eckner, Ewen et al. 1994). This at least suggests that CBP and p300 could be classified as tumour suppressor proteins. Moreover, aberrant CBP fusion products with other transcription factors are detected in haematopoietic malignancies due to chromosomal translocations (Blobel 2002; Chan, Hannah et al. 2011). Consequently, these aberrant fusion proteins (for example MOZ-CBP) induce the functional inactivation of wild-type CBP and constitute one of the main causes for the development of some subtypes of acute and chronic myeloid leukemia (Satake, Ishida et al. 1997; Crowley, Wang et al. 2005). P300, instead, lacks a significant role in the development of haematopoietic malignancies. However, mutations and truncations at the EP300 gene locus are frequently found in solid tumours of epithelial origin, which indicates a crucial role for p300 in tumour suppression as well (Gayther, Batley et al. 2000; Goodman and Smolik 2000).

P300 and CBP form the KAT3-family of histone acetyltransferases. Besides, they might possess additional, histone-acetylating independent functions (Shi, Pop et al. 2009).

Acetylation of N-terminal lysine residues of histones is normally associated with transcriptionally active genes, as histone acetylation results in a relaxation of chromatin packaging. P300- and CBP-mediated histone acetylation comprises acetylation of all 4 core histones (H2A, H2B, H3 and H4). Especially acetylation of H3K14, H3K18, H4K5 and H4K8 has been found to be solely mediated by p300 and CBP (Schiltz, Mizzen et al. 1999; Bedford and Brindle 2012) (Figure 1.6). Moreover, after DNA damage, p300 is likely to acetylate specific lysine residues, such as H3K56, thereby actively contributing to the recruitment of DNA repair complexes to DNA lesions (Das, Lucia et al. 2009; Ogiwara and Kohno 2012).

Apart from their function as histone acetyltransferases, p300 and CBP mediate the acetylation of over 100 non-histone proteins (Goodman and Smolik 2000). Therefore, p300 and CBP are proclaimed as factor acetyltransferases, as well. Generally, acetylation of non-

histone proteins is correlated with enhanced protein stability of the target protein as well as increased activity (Kalkhoven 2004). However, some single acetylation events, such as p300-mediated acetylation of the high mobility protein HMGI(Y), are functionally related to an inhibition of the respective target protein activity (Munshi, Merika et al. 1998).

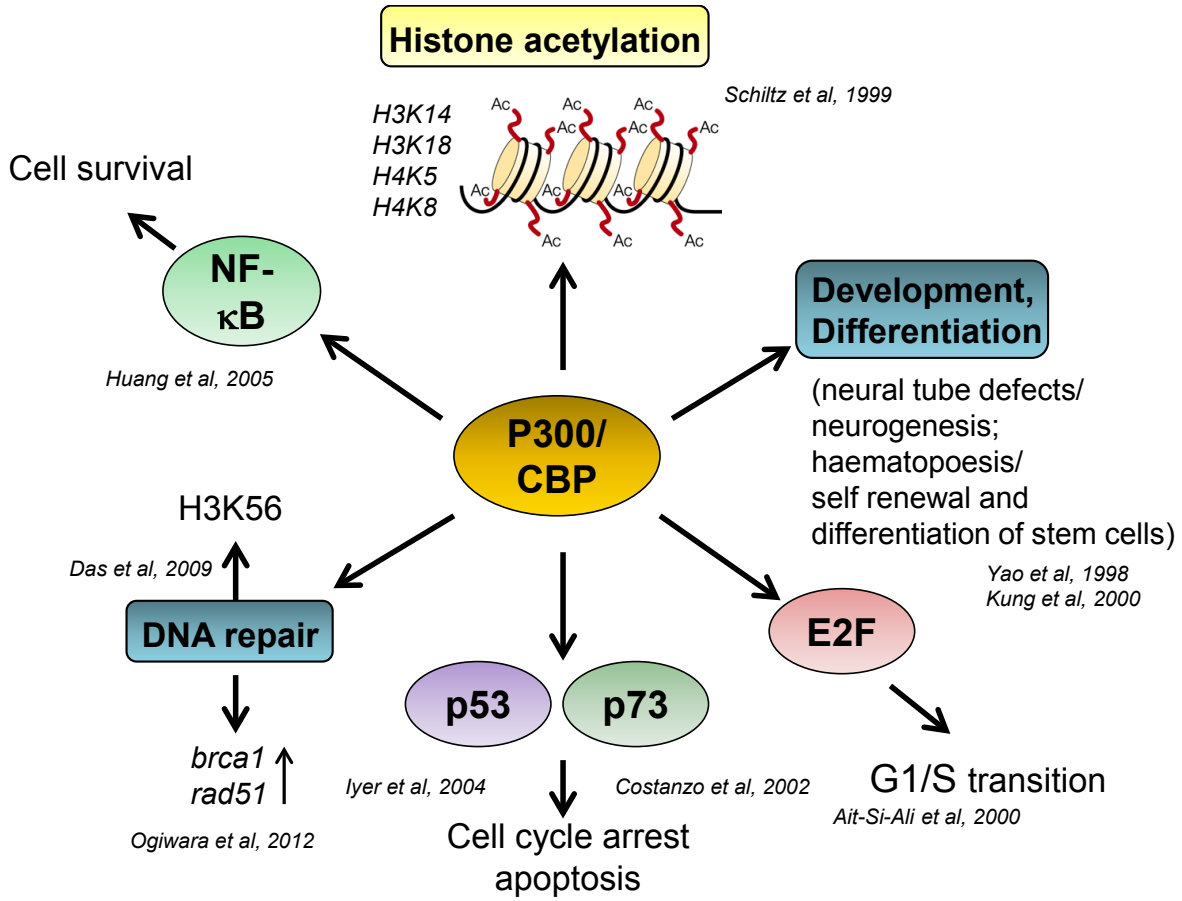

Figure 1.6. Overview of the main cellular substrates and functions of p300 and CBP. *Main function of p300 and CBP constitutes histone acetylation of different N-terminal lysine residues, thereby influencing transcription processes. Interaction of p300/ CBP with different proteins, including p53, p73, E2F or NF-κB, induces acetylation of the respective target protein and therefore contributes to the regulation of cell survival, apoptosis and cell cycle events. Moreover, p300 and CBP are involved in the control of different processes such as embryonic development and cell differentiation. Another important aspect of p300/CBP function represents their indirect involvement in DNA repair mechanisms. Recruitment of DNA repair proteins to DNA lesions (through specific histone marks) as well as the transcriptional regulation of DNA repair genes (for example brca1 and rad51) constitutes the molecular basis of p300/ CBP-dependent DNA repair.*

1.3.2 In-vivo studies of p300 and CBP confirm their important role in development

P300 and CBP knockout mice ($p300^{-/-}$ and $CBP^{-/-}$) die around day E11.5 and are therefore embryonic lethal (Yao, Oh et al. 1998; Goodman and Smolik 2000; Kung, Rebel et al. 2000). One major cause for death of the embryos derives from severe developmental defects, such as open neural tubes. Moreover, an increased portion of heterozygous p300 knockout mice ($p300^{+/-}$) die during development as well. This underscores the importance of the expression level of p300, as small changes in its expression are already likely to impair the full functionality of the p300 protein (Roth, Shikama et al. 2003; Shikama, Lutz et al. 2003).

Furthermore, p300 and CBP heterozygous knockout mice display similar as well as unique phenotypes. $P300^{+/-}$ mice show defects in the development of the heart, while $CBP^{+/-}$ mice display retarded growth and craniofacial abnormalities (Oike, Takakura et al. 1999; Kung, Rebel et al. 2000; Shikama, Lutz et al. 2003). Thus, in-vivo studies confirm an indispensable role of p300 and CBP in development and differentiation, and studies of heterozygous mice uncover overlapping but also unique functions of p300 and CBP. Figure 1.6 summarizes the role of p300 in different cellular responses.

1.3.3 P300 as a co-activator of the p53-family

As already mentioned, P300 and CBP mediate the acetylation of the p53-family, as well. Acetylation of the p53-family leads to the inhibition of the proteasomal degradation as well as the promotion of the transcriptional activity of p53, p73 and p63. This enhanced activity of the p53-family derives from increased DNA-binding affinities of p300-acetylated proteins to their respective genomic target sites (Figure 1.6). Furthermore, due to a re-localization of p300-p53 and p300-TAp73 complexes in metabolically stable PML bodies, p300-target protein complexes are fully protected from MDM2- and Itch-mediated degradation (Bernassola, Salomoni et al. 2004; Iyer, Chin et al. 2004), thus leading to a further increase of TAp73 and p53 protein levels.

Apart from direct acetylation of the p53-family, p300 and CBP also contribute to their activation in an indirect way, as both histone acetyltransferases are involved in the acetylation of TAp73- and p53-modifying proteins as well. In detail, p300-mediated acetylation of the TAp73-activating kinase c-abl has been described to cause a nuclear translocation of the protein. Hence, this sub-cellular re-localization of c-abl triggers a functional turn-over from its anti-apoptotic role in normally growing cells to its pro-apoptotic function after DNA damage (di Bari, Ciuffini et al. 2006). Thus, p300 also contributes to

TAp73 activation, through acetylation and re-localization of the TAp73-phosphorylating kinase c-abl.

Moreover, p38 is acetylated by p300 and CBP, which promotes a prolonged stabilization and therefore activation of the p38 kinase, thereby subsequently contributing to p53-family dependent induction of apoptosis (Pillai, Sundaresan et al. 2011).

Surprisingly, Zeng and colleagues reported that p300 is indeed crucial for TAp73 function; however, mutations in the HAT domain of p300 did not abolish its activating function of TAp73 (Zeng, Lee et al. 2001). Therefore, it is not clear yet, whether p300 needs to exhibit full HAT activity to display its effects on the p53-family.

As p300 and CBP can also acetylate and therefore activate transcription factors that promote uncontrolled proliferation and tumour growth, such as NF-κB, Stat-1 or c-myc, the question remains how p300 and CBP function is specifically regulated (Chen, Williams et al. 2005; Faiola, Liu et al. 2005; O'Shea, Kanno et al. 2005). One regulatory mechanism comprise a panel of post-translational modifications of the p300 and CBP proteins that influence their activity, protein level and interacting partners.

1.3.4 Regulation of p300 by post-translational modifications

P300 and CBP are subjects to a high degree of post-translational modifications including phosphorylation, acetylation and ubiquitination (Chen and Li 2011). Although p300 and CBP level can also be regulated by various mechanisms, we will only summarize the most important post-translational modifications that are relevant for our project.

As both proteins can regulate the acetylation and therefore the activity and protein stability of over 100 non-histone proteins, their specific function, cellular localization and expression levels have to be tightly regulated. Phosphorylation of p300 and CBP represents one of the major regulatory mechanisms.

Phosphorylation of p300 is conducted by various kinases, including p38, Akt, ERK1/2 and PKC and mostly occurs on serine residues at the C-terminus (Chen and Li 2011). In general, phosphorylated p300 can be detected in quiescent and proliferating cells (Yaciuk, Carter et al. 1991). Moreover specific phosphorylation events of p300 can be detected in specific phases of the cell-cycle, as these modifications are mediated by cyclin-dependent-kinases (Ait-Si-Ali, Polesskaya et al. 2000; Morris, Allen et al. 2000).

Phosphorylation of serine residue 89 of p300 was shown to be mediated by protein kinase C (PKC). Interestingly, this PKC-mediated phosphorylation at the consensus sequence RXXS results in inactive p300 and CBP proteins (Yuan and Gambee 2000) (Figure 1.7). Apart from this inhibitory phosphorylation, all other phosphorylation events that have been elucidated so far support the HAT activity of p300 and CBP.

One of the best-studied post-translational modification that enhances the HAT activity of p300 represents Akt- and p38-mediated phosphorylation at serine residue 1834 (Wang, Han et al. 2013) (Figure 1.7). Interestingly, phosphorylation of p300 by Akt kinase alone promotes the HAT activity of p300. This is followed by p300-mediated acetylation of NF-κB and subsequent transcriptional activation of NF-κB target genes (Huang and Chen 2005; Liu, Denlinger et al. 2006). Therefore, Akt-mediated phosphorylation of p300 results in the promotion of its pro-survival functions due to the activation of NF-κB signalling pathways.

In contrast, after UV radiation or cisplatin treatment, p300 is simultaneously phosphorylated by Akt and p38 kinases at serine residue 1834, followed by the activation and later degradation of the p300 protein. However, this phosphorylation and degradation of p300 only occurs after the generation of DNA lesions that are substrates for nucleotide excision repair. Thus, Akt- and p38-mediated phosphorylation of p300 represents a mechanism for activation and recruitment of the nucleotide excision repair process (Wang, Han et al. 2013). Chemical-based inhibition of one of these kinases is sufficient to inhibit p300 degradation. This is followed by impaired removal of UV-induced DNA lesions and diminished nucleotide excision repair.

Moreover, Poizat and colleagues showed that p38-mediated phosphorylation of p300 contributes to apoptosis induction in cardiac cells after doxorubicin treatment. This represents another cooperation of p38 and p300, thus controlling the level of p300-mediated apoptosis induction (Poizat, Puri et al. 2005).

Another important phosphorylation event of p300 is mediated by nuclear ERK1/ ERK2 (Gusterson, Brar et al. 2002). ERK1/ ERK2 is known to be activated after treatment of cells with DNA damaging agents such as Etoposide and cisplatin (Ley, Balmanno et al. 2003). Surprisingly, although activation of ERK1/ ERK2 is normally correlated with proliferation and cell survival, cisplatin treatment activates ERK1/ ERK2, which contributes then to the induction of apoptosis (Wang, Martindale et al. 2000; Pearson, Robinson et al. 2001). However, it is not elucidated yet under which conditions ERK1/ ERK2 phosphorylates p300 at the C-terminal residues serine 2279, serine 2315 and serine 2366 (Chen, Wang et al. 2007) (Figure 1.7). Moreover, it is unclear which functional consequences ERK1/ ERK2-

mediated phosphorylation of p300 will have and if the function of ERK1/ ERK2 in cisplatin-dependent apoptosis induction is related to p300 at all.

Besides phosphorylation as a regulatory mechanism of p300 and CBP activity, acetylation of both proteins promotes their HAT activity and elevates their expression levels. Auto-acetylation of p300 and CBP occurs at multiple lysine residues in the HAT domain, including lysine 1499 (for p300) and lysine 1535 (for CBP) (Thompson, Wang et al. 2004; Stiehl, Fath et al. 2007; Bhatia, Tykodi et al. 2009) (Figure 1.7). As auto-acetylation was found to be indispensable for p300/ CBP co-activator function, detection of acetyl-p300/ CBP can be utilized as a read-out for active p300 protein.

Figure 1.7 summarizes the most important post-translational modifications of p300 including localization of important interaction sites as well as the responsible kinase that mediates the specific post-translational modification (Teufel, Freund et al. 2007; Chen and Li 2011).

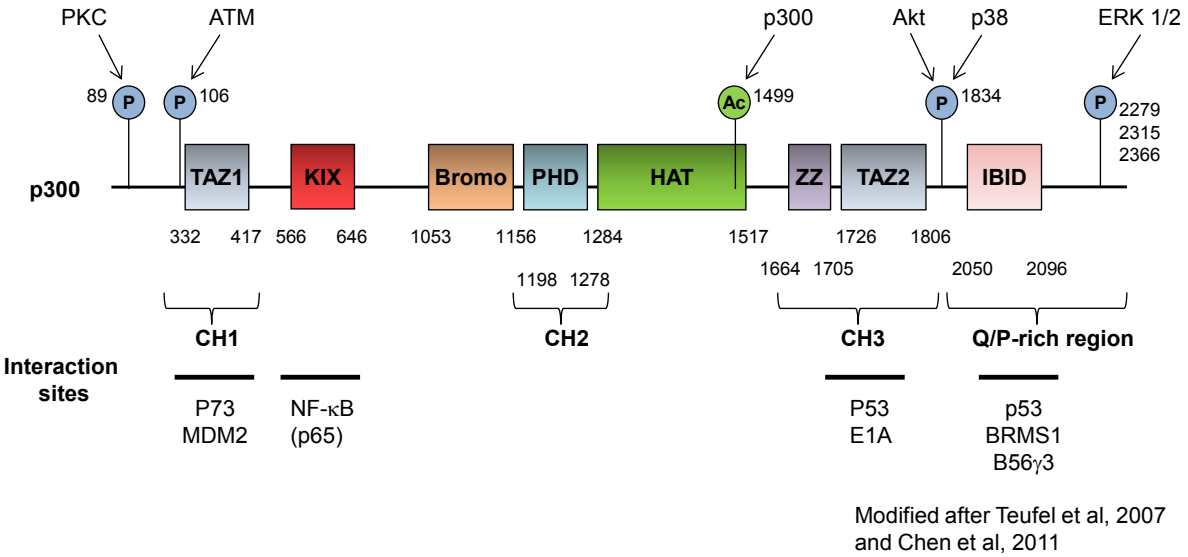

Figure 1.7. Post-translational modifications of p300. *The domain structure of p300 (N- to C-terminus) and the most important post-translational modifications are shown. The responsible enzymes that mediate these modifications are depicted above the respective residues. Below the domain structure and the most important interaction sites of some target proteins are displayed. (Ac = Acetylation, P = Phosphorylation, CH = cysteine-histidine-rich region, Q/P = glutamine-proline-rich region, TAZ = transcriptional adapter zinc binding domain, KIX = CREB-binding domain; ZZ = zinc finger domain, PHD = Plant homeo domain, Bromo = bromodomain; IBID = Interferon-binding domain)*

1.3.5 The protein stability of p300 is mainly regulated by poly-ubiquitination.

Poly-ubiquitination and therefore degradation of p300 and CBP represents another important post-translational modification that regulates the overall protein levels as well the stability of both proteins. Surprisingly, only a few studies discovered p300/CBP-specific E3 ubiquitin ligases yet. One such candidate ubiquitin ligase is Mdm2, which is one of the most important ubiquitin ligases of wild-type p53 (Haupt, Maya et al. 1997; Kubbutat, Jones et al. 1997). Mdm2 forms a complex with p300 (Grossman 2001), but this direct interaction does not trigger the proteasomal degradation of p300. Instead, Mdm2 is acetylated by p300, thereby preventing the degradation of p53 (Wang, Taplick et al. 2004).

Another E3 ubiquitin ligase that has been implicated in mediating the proteasomal degradation of p300 constitutes SCF^{Fbx3} (Shima, Shima et al. 2008). SCF E3 ligases are composed of Skp1, Cul1 and a F-box protein, the latter in this case Fbx3, dictating the substrate specificity of the respective SCF E3-ligase complex (Ahn, Byeon et al. 2009; Skaar, Pagan et al. 2013). Interestingly, association of p300 with PML in sub-nuclear structures inhibits the proteasomal degradation of p300 by SCF^{Fbx3} (Shima, Shima et al. 2008). Thereafter, when p300 completed its role in transcriptional regulation of specific cellular responses, it is subjected again to SCF^{Fbx3}-mediated proteasomal degradation in the nucleus. However, it is not clear yet which molecular signalling events lead to SCF^{Fbx3}-mediated degradation of p300 then (Shima, Shima et al. 2008).

As expected, phosphorylation of p300 indirectly regulates its protein stability and therefore its proteasomal degradation, as well. Chen and colleagues showed that over-expression of the protein phosphatase 2A (PP2A) subunit B56γ augments the proteasomal degradation of p300 (Chen, St-Germain et al. 2005). Hence, after treatment of cells with the histone deacetylase inhibitor valproic acid, B56γ directly binds to p300 and subsequently de-phosphorylates the protein. Thereafter, p300 is proteasomally degraded, thus possibly contributing to the frequently observed teratogenic side effects of valproic acid treatment, as p300 represents a key factor in embryonic development (Chen, St-Germain et al. 2005; Lloyd 2013).

However, major evidence for p300/CBP-specific E3-ubiquitin ligases is missing. Very recently Liu and colleagues discovered that the breast cancer metastasis gene 1 (BRMS1) harbours specific E3 ubiquitin ligase activity towards p300, thus identifying a new regulatory mechanism of p300 function (Liu, Mayo et al. 2013).

1.4. BRMS1 as a candidate ubiquitin ligase for p300/CBP

1.4.1 BRMS1 constitutes an E3 ubiquitin ligase for p300.

Breast cancer metastasis gene 1, shortly termed BRMS1, is a recently discovered gene that plays a role in the inhibition of metastasis whereas it has nearly no effect on tumourigenesis (Seraj, Samant et al. 2000; Shevde, Samant et al. 2002). Over-expression studies of BRMS1 in breast, lung and melanoma cell lines elucidated its crucial role in prevention of invasion, loss of cell adhesion and migration by transcriptional repression of metastatic genes (Robertson, Coleman et al. 1996; Shevde, Samant et al. 2002; Cicek, Samant et al. 2004). Molecularly, the BRMS1-mediated down-regulation of target genes is likely to derive from its interaction with the Sin3A-complex that can deacetylate histones and therefore silence gene expression (Hurst, Xie et al. 2013). However, further experiments still needs to prove that BRMS1-SIN3a complex formation indeed controls the transcriptional repression of pro-metastatic target genes.

In lung cancer cell lines, Liu and colleagues found that BRMS1 can also bind to p65, a subunit of the NF-κB complex, thereby leading to its transcriptional repression (Liu, Smith et al. 2006). It has been elucidated before that the transcriptional activity of NF-κB is mainly regulated through acetylation of p65 at lysine residue 310. P300 mediates this acetylation of p65, thereby inhibiting the IkBα-mediated cytosolic sequestration of NF-κB and thus positively regulating the transcription of NF-κb target genes (Chen, Williams et al. 2005). In contrast, BRMS1 was shown to mediate the deacetylation of lysine 310 due to recruitment of HDAC1 to p65 (Liu, Smith et al. 2006; Cicek, Fukuyama et al. 2009). Therefore, BRMS1 and p300 exhibit opposing roles in the regulation of NF-κB activity.

Correspondingly, it was recently discovered that BRMS1 can poly-ubiquitinate and therefore proteasomally degrade p300 (Liu, Mayo et al. 2013). BRMS1 is likely to possess E3 ubiquitin ligase activity due a conserved CXD motif that is structurally related to the bacterial Ipah E3 ligase family. Consequently, protein levels of p300 and BRMS1 are inversely correlated in lung cancer cell lines. Moreover, they also claimed that BRMS1-mediated degradation of p300 contributes to the suppression of metastasis, as mutation of the CXD motif is correlating with a higher migration potential of the cells. However, these observations did not correlate with a modulation in p300 activity, although some single reports proposed a role for p300 in the promotion of metastatic transformation before (Debes, Sebo et al. 2003; Li, Luo et al. 2011).

1.4.2 BRMS1 and its implication in melanoma development

Expression studies of the BRMS1 substrate p300 in melanoma lack so far. However, the anti-metastatic protein BRMS1 has been investigated in melanoma before, as their metastatic potential constitutes one of the most critical features of malignant melanoma. Initially, an increased frequency of chromosome breakage, mutations or deletion of chromosome 11 was discovered in malignant melanoma samples (Robertson, Coleman et al. 1996). Later, it was revealed that BRMS1 is encoded at chromosome 11q13 and that mutations at this genomic site might result in down-regulated BRMS1 expression. Analysis of the mRNA expression levels of BRMS1 revealed that BRMS1 expression is indeed dramatically down-regulated in the process of melanocyte transformation to primary tumours, followed by complete loss of BRMS1 expression in metastatic cell lines (Shevde, Samant et al. 2002). However, comparative analysis of protein and mRNA levels of BRMS1 in breast cancer cells revealed that mRNA level and protein level of BRMS1 do not always correlate, likely due to at least four different splice variants of BRMS1 (Hurst, Xie et al. 2009).

Lately, Slipicevic and colleagues revealed a more differentiated role for BRMS1 in malignant melanoma due to its sub-cellular localization within the cell (Slipicevic, Holm et al. 2012). While cytoplasmic BRMS1 expression accounts for an increased disease-free survival and decreased metastatic potential, nuclear localization of BRMS1 in some melanoma correlated with increased invasion and migration potential as well as a poor survival rate.

Concluding, it remains to be revealed whether BRMS1 constitutes an E3 ligase for p300 in melanoma as well. Therefore, it might be of therapeutical interest to investigate whether p300 expression in melanoma is altered, and whether changes in p300 expression correlate with the frequently observed high degree of chemoresistance in melanoma patients.

1.5 Scope of the thesis

Although p300 and CBP are implicated in many different signalling pathways and cellular responses, dissection of the molecular mechanisms underlying the specific regulation of p300/CBP function remains largely elusive. It has been revealed that p300 is frequently inactivated in certain tumour types (Goodman and Smolik 2000; Kalkhoven 2004). Therefore, re-establishment of p300 function might contribute to a re-activation and therefore enhancement of p53-family-dependent apoptosis induction. However, the question remains which treatment strategies re-establish p300 function and which types of tumours might respond to these treatments then.

Recently Gillotin and colleagues discovered a direct interaction of p300 with iASPP, another co-factor protein that can regulate p53-family dependent apoptosis induction (Gillotin and Lu 2011). However, the functional consequences of this interaction still need to be understood. Moreover, direct interaction of iASPP and TAp73 has been shown before; nevertheless, the functional consequences of iASPP expression on TAp73 function remain elusive as well (Bell, Dufes et al. 2007; Robinson, Lu et al. 2008).

Therefore, this project investigated the impact of iASPP-p300 interaction on the expression levels and acetyltransferase function of p300, in untreated as well as cisplatin-treated tumour cell lines. We hypothesized that iASPP might change the expression levels, sub-cellular localization or cellular function of p300 and that iASPP-p300 interaction might have implications for new therapy approaches in specific tumour types. Furthermore, we analysed the effects of iASPP expression on TAp73 expression levels and transcription factor function, as well as TAp73-mediated tumour cell apoptosis, as TAp73 constitutes an important downstream target protein of p300.

2.1 Material

2.1.1 Technical devices

Table 2.1. Technical Devices

Device	Company
Autoclave DX-200	Systec GmbH
Blotting chamber	Biozym, Hessisch Oldendorf, Germany
Cell counting chamber *Neubauer improved*	Brand, Wertheim, Germany
Centrifuge *5415R*	Eppendorf, Hamburg, Germany
Centrifuge *5810R*	Eppendorf, Hamburg, Germany
Centrifuge Megafuge *1.0R*	Heraeus, Thermo Scientific, Waltham, MA, United States
Chemiluminescence imager *Chemocam HR 16 3200*	Intas Science Imaging Instruments, Göttingen, Germany
Electrophoresis system Mini Format 1D, for SDS-PAGE	Bio-Rad Laboratories, Hercules, CA, United States
FACS machine Guava PCA-96 Base System	Millipore, Merck, Darmstadt, Germany
Freezer -20°C	Liebherr, Bulle, Switzerland
Freezer -80°C	Heraeus, Thermo Scientific
Incubator for bacteria	Memmert, Schwabach, Germany
Incubator for cell culture *Hera Cell 150*	Heraeus, Thermo Scientific, Waltham, MA, United States
Laminar flow cabinet *Hera Safe*	Heraeus, Thermo Scientific
Liquid nitrogen tank *LS 4800*	Taylor-Wharton, Theodore, AL, United States
Magnetic stirrer *MR Hei-Standard*	Heidolph, Schwabach, Germany
Microscope *Axovert 40C*	Zeiss, Oberkochen, Germany
Microwave	Cinex, Lippstadt, Germany

Mini Centrifuge *MCF-2360*	LMS, Tokyo, Japan
PCR machine for qPCR *CFX96, C1000*	Bio-Rad Laboratories
PCR machine *Thermocycler T personal*	Biometra, Göttingen, Germany
Personal computer	Dell, Round Rock, TX, United States
pH-meter *WTW-720*	WTW, Weilheim, Germany
Pipets Eppendorf Research Series 2100 (0.1-2.5 µL; 2-20 µL; 20-200 µL; 100-1000 µL)	Eppendorf, Hamburg, Germany
Power supply unit *Powerpack P25T*	Biometra
Refrigerator 4°C	Liebherr
Roller RM5 V-30	CAT, Staufen, Germany
Rotator *PTR 300*	Grant Instruments
Scales *Acculab ALC-6100.1*	Sartorius, Göttingen, Germany
Scales *LE623S*	Sartorius, Göttingen, Germany
Shaker *PROMAX 2020*	Heidolph
Sonication device *Bioruptor*	Diagenode, Liège, Belgium
Spectrophotometer *NanoDrop ND-1000*	PeqLab, Erlangen, Germany
Thermomixer *comfort*	Eppendorf, Hamburg, Germany
Timer	Oregon Scientific, Portland, OR, United States
UV-transilluminator Intas UV system Gel Jet Imager	Intas Science Imaging Instruments
Vacuum pump	IBS Integra Biosciences, Fernwald, Germany
Vortex *Genie 2*	Scientific Industries, Bohemia, NY, United States
Water bath *TW 20*	Julabo Labortechnik, Seelbach, Germany

2.1.2 Consumables

Table 2.2. Consumables

Product	Company
96-well plates for qPCR	4titude, Wotton, United Kingdom
Bacteria culture dishes	Sarstedt, Nümbrecht, Germany
Bacteria culture vials (14 cm)	Becton Dickinson
Cell culture dishes (10 cm, 15 cm)	Greiner, Frickenhausen, Germany
Cell culture plates (6-well, 12-well)	Greiner, Frickenhausen, Germany
Cell scraper (16 cm, 25 cm)	Sarstedt, Nümbrecht, Germany
Cryo tubes *Cryoline*	Nunc, Thermo Scientific
Filter tips (10 µL)	Starlab, Hamburg, Germany
Filter tips (20 µL, 200 µL, 1000 µL)	Sarstedt, Nümbrecht, Germany
Parafilm	Brand
Pipet tips (10 µL, 20- 200 µL, 1000 µL)	Greiner, Frickenhausen, Germany
Protran nitrocellulose transfer membrane	Whatman, Dassel, Germany
Reaction tube (0.2 mL)	Sarstedt, Nümbrecht, Germany
Reaction tube (0.5 mL, 1.5 mL, 2.0 mL)	Eppendorf, Hamburg, Germany
Falcon reaction tube (15 mL, 50 mL)	Greiner, Frickenhausen, Germany
Safe-lock reaction tube (1.5 mL)	Eppendorf, Hamburg, Germany
Sterile filter (0.2 µM and 0.45 µM)	Millipore, Merck
Syringe, 1 mL, 5 mL, 10 mL, 50 mL	Henke-Sass, Wolf, Tuttlingen, Germany
Syringe canules (23G)	B.Braun, Melsungen, Germany
Transparent sealing foil for 96-well plate	4titude, Wotton, United Kingdom
Whatman paper	Whatman, Dassel, Germany

2.1.3 Chemicals and reagents

Table 2.3. Chemicals and reagents

Substance	Article No.	Company
Albumin Fraction V (Bovine Serum Albumine, BSA) for molecular biology	80763	Roth
Ammonium persulfate (APS) p.a.	9592.1	Roth
Ammonium sulphate ($(NH_4)_2SO_4$) >99.5%, p.a.	3746.1	Roth
Ampicillin	K029.1	Roth
Bromophenol blue	B0126	Sigma-Aldrich
Calcium chloride dihydrate ($CaCl_2$ x $2H_2O$) >99%, p.a., ACS	52391	Roth
Chloroform, Rotipuran	3313.1	Roth
Complete Mini Protease Inhibitor EDTA free	11836170001	Roche, Basel, Schweiz
Dimethyl sulfoxide (DMSO)	A3672	AppliChem
Dithiotreitol (DTT)	6908.3	Roth
deoxynucleotide triphosphates (dNTPs)	Cat 1201,1202, 1203, 1204	Primetech
Ethanol 99.8%	K928	Roth
Ethanol 99.9% p.a. (EtOH)	1009672500	Merck
Sodium Ethylene diamine tetraacetatic acid (Na-EDTA)	80432	Roth
Ethylene glycol tetraacetic acid (EGTA)	3054.2	Roth
Formaldehyde, 37% solution	4979.1	Roth
Glucose	X997.2	Roth
Glycerol, >99%, p.a.	3783.2	Roth
Glycerophosphate (ß-) dissodium salt hydrate	G5422	Sigma-Aldrich
Glycine, >99%, p.a.	3908.3	Roth

Glycogen, molecular biology grade	HP51.2	Roth
Guava ICF Cleaning Solution	4200-0140	Millipore, Merck
HEPES Pufferan >99%, p.a.	3908.3	Roth
Hydrogen chloride (HCl)	0992.1	Roth
Igepal (NP-40), Ca-630	I3021	Sigma-Aldrich
Isopropanol	6752.4	Roth
Lithium chloride	P007.1	Roth
Lipofectamine 2000	11668-019	Invitrogen, Life Technologies
Magnesium chloride hexahydrate ($MgCl_2$ x $6H_2O$)	2189.1	Roth
Methanol >99% (MetOH)	4627.2	Roth
Milkpulver, blotting grade	T1454	Roth
Nonidet P-40 substitute (NP-40)	74385	Fluka
Phenol solution (pH 8.0) for ChIP	P4557	Sigma-Aldrich
Phenol solution (pH 4.3) for RNA	P4682	Sigma Aldrich
Potassium chloride (KCl)	A1362	Applichem
Potassium hydrogenphosphate (KH_2PO_4)	3904.1	Roth
Prestained Protein Ladder	26616	Fermentas, Thermo Scientific
Propidium iodide solution (PI), 1 mg/mL in water	P4864	Sigma-Aldrich
Protein-G-Sepharose,4 Fast Flow	17-0618-01	GE healthcare
Protein A/G Agarose	Sc2003	Santa Cruz
Puromycin	P9620	Sigma-Aldrich
Random Hexamer Primer (0.2 µg/µL)	SO142	Thermo Scientific fisher
Rotiblock 10x concentrate	A151.1	Roth
Rotiphorese Gel 30	3029.1	Roth
Sodium acetate (NaAc)	6773.1	Roth

Sodium hydrogen carbonate ($NaHCO_3$), >99,5%, p.a., ACS, ISO	6885.1	Roth
Sodium chloride (NaCl)	3957.2	Roth
Sodium deoxycholate	30970	Applichem
Sodium dodecyl sulphate (SDS)	161-0302	Biorad
Sodium hydrogenphosphate monohydrate ($NaHPO_4$ x H_2O), p.a.	K300.2	Roth
Sodium (di-) hydrogenphosphate dihydrate (Na_2HPO_4 x $2H_2O$) >99%, p.a.	4984.1	Roth
Sodium hydroxide (NaOH), pellets	221465	Sigma-Aldrich
SYBR green	S7567	Invitrogen, Life Technologies
Tetramethylethylenediamine (TEMED)	11.073.100.100	Merck
Trehalose dihydrate	22515	Usb corporation, Cleveland
Trisamine (Tris) Pufferan, >99% p.a.	4855.3	Roth
Triton X-100, molecular biology grade	A4975	Applichem
Trizol	15596-018	Invitrogen, Life Technologies
Tryptone	8952.2	Roth
Tween 20	A4974.0500	Applichem
Yeast extract	2363.2	Roth

Table 2.4. Chemotherapeutics and inhibitors

Name	Target/ Function	Article No.	Company
SB203580	P38	EI-286	Biomol
MG132	Proteasome	474791	Merck-Calbiochem
BCI	MKP-1, MKP-3	B4313	Sigma-Aldrich
CTB	P300, CBP	C6499	Sigma-Aldrich
Cisplatin (CDDP)	DNA intra/		Teva

	interstrand crosslinks		
Cycloheximide	Proteinsynthesis inhibitor	C1988	Sigma
Etoposide	Topoisomerase II inhibitor	E1283	Sigma
z-VAD-FMK	Caspases	ALX-260020M005	Enzo

2.1.4 Buffer and Solutions

Table 2.5. Buffer and Solutions

6x Laemmli buffer	
Tris pH 6.8	0.35 M
Glycerin	30.00%
SDS	10.00%
Dithiotreitol	9.30%
Bromophenol blue	0.02%
dissolved in H_2O	

Phosphate buffered saline (PBS), pH 7.4	
NaCl	24.00 mM
KCl	0.27 mM
Na_2HPO_4 x $7H_2O$	0.81 mM
KH_2PO_4	0.15 mM
dissolved in H_2O	

Western blot washing buffer (PBST)	
NaCl	24.00 mM
KCl	0.27 mM
Na_2HPO_4 x $7H_2O$	0.81 mM
KH_2PO_4	0.15 mM
Tween-20	0,10%
dissolved in H_2O	

qPCR reaction buffer, 10x	
Tris (pH 8.8)	750 mM
$(NH_4)_2SO_4$	200 mM
Tween 20	0.1%
dissolved in H_2O	

qPCR reaction mix, 25x	
10x qPCR reaction buffer	1x
SybrGreen	0,001620
$MgCl_2$	3.0 mM
Trehalose in 10 mM Tris (pH 8.5)	300.0 mM
dNTPs	0.2 mM
Triton X-100	0.25%
Taq polymerase	20 U/mL
dissolved in H_2O	

Western blot blocking solution	
milk powder	5%
dissolved in PBS	

Western blot buffer, for proteins < 130kDa	
Tris	25 mM
Glycin	192 mM
Methanol	20%
dissolved in H_2O	

Western blot buffer, for proteins > 130kDa	
Tris	25 mM
Glycin	192 mM
Methanol	10%
SDS	0,01%

Cell lysis buffer	
TRIS-HCl (pH 7.5)	20 mM
NaCl	150 mM
Na2EDTA	1 mM
EGTA	1 mM
Triton-X 100	1%
ß-glycerophosphate	1 mM
Urea	2 M
Protease Inhibitor Cocktail (PIC)	1x

SDS running buffer	
Tris	25.0 mM
Glycin	86.1 mM
SDS	3.5 mM
dissolved in H_2O	

NET buffer (IP lysis buffer)	
NaCl	150 mM
TRIS-HCl (pH 8.0)	50 mM
EDTA	1 mM
NP-40	1%
Protease Inhibitor Cocktail (PIC)	1x

Buffer B for chromatin fractionation	
EDTA, pH 8.0	3 mM
EGTA, pH 8.0	0.2 mM
DTT	1 mM
Protease Inhibitor Cocktail (PIC)	1x
dissolved in H_2O	

Buffer B for chromatin harvest (for ChIP)	
Triton X-100	0.25%
EDTA, pH 8.0	10 mM
EGTA, pH 8.0	0.5 mM
HEPES pH 7.6	20 mM
dissolved in H_2O	

Washbuffer 1 for ChIP	
SDS	0.1%
NaDOC	0.1%
Triton-X-100	1%
NaCl	0.15 M
EDTA, pH 8.0	1 mM
EGTA, pH 8.0	0.5 mM
HEPES pH 7.6	20 mM
dissolved in H_2O	

Buffer A for chromatin fractionation	
HEPES pH 7.9	10 mM
KCl	10 mM
MgCl2	1.5 mM
Sucrose	0.34 M
Glycerol	10%
DTT	1 mM
Protease Inhibitor Cocktail (PIC)	1x
dissolved in H_2O	

Buffer A for chromatin harvest (for ChIP)	
NaCl	0.1 M
EDTA, pH 8.0	1 mM
EGTA, pH 8.0	0.5 mM
HEPES pH 7.6	50 mM
dissolved in H_2O	

Buffer C for chromatin harvest (for ChIP)	
NaCl	0.15 M
EDTA, pH 8.0	1 mM
EGTA, pH 8.0	0.5 mM
HEPES pH 7.6	50 mM
dissolved in H_2O	

Washbuffer 2 for ChIP	
SDS	0.1%
NaDOC	0.1%
Triton-X-100	1%
NaCl	0.5 M
EDTA, pH 8.0	1 mM
EGTA, pH 8.0	0.5 mM
HEPES pH 7.6	20 mM
dissolved in H_2O	

Incubationbuffer stock for ChIP, 5x	
SDS	0.75%
Triton-X-100	5%
NaCl	0.75 M
EDTA, pH 8.0	5 mM
dissolved in H_2O	

Washbuffer 3 for ChIP	
LiCl	0.25 M
NaDOC	0.5%
NP-40	0.5%
EDTA, pH 8.0	1 mM
EGTA, pH 8.0	0.5 mM
HEPES pH 7.6	20 mM
dissolved in H_2O	

Washbuffer 4 for ChIP	
EDTA, pH 8.0	10 mM
EGTA, pH 8.0	5 mM
HEPES pH 7.6	200 mM
dissolved in H_2O	

Elutionbuffer for ChIP	
SDS	1%
$NaHCO_3$	0.1 M
dissolved in H_2O	

2.1.5 Enzymes and Kits

Table 2.6. Enzymes and Buffer

Reagent	Company
DNase I (50 u/µL)	Thermo Scientific fisher
DNase I buffer	Thermo Scientific fisher
RT Buffer, 5x	Thermo Scientific fisher
Revert Aid Reverse transcriptase (RT) (200 u/µL)	Thermo Scientific fisher
RiboLock RNAse Inhibitor (40 u/µL)	Thermo Scientific fisher

RNase A (100 mg/mL)	Qiagen, Venlo, Netherlands
Taq polymerase	Primetech

Table 2.7. Kits

Name	Company
Guava Check Kit	Millipore, Merck
Immobilon Western HRP Substrate Peroxide Solution	Millipore, Merck
Pierce BCA Protein assay kit	Thermo Scientific fisher
PureYield Plasmid Midiprep System	Promega
SuperSignal West Femto Maximum Sensitivity Substrate	Thermo Scientific fisher

2.1.6 Antibodies

Table 2.8. Primary antibodies

target	Clone, ID	Source organism	Dilution for immunoblotting (WB), ChIP or Co-IP	Company
actin	ab8227	rabbit	WB: 1/20000	Abcam, Cambridge, UK
BRMS1 (MO-1)	2D4-2G11	mouse	WB: 1/500	Abnova GmbH
CBP (A-22)	sc-369	rabbit	WB: 1/500	Santa Cruz Biotechnology
cleaved Caspase 3 (Asp175)	9664	rabbit	WB: 1/500	Cell Signaling Technology
GAPDH	ab8245	mouse	WB: 1/20000	Abcam, Cambridge, UK
Hsc70	B-6	mouse	WB: 1/2000	Santa Cruz Biotechnology,

iASPP	A4605	mouse	WB: 1/1000	Sigma-Aldrich
IgG, ChIP grade	ab46540	rabbit	ChIP: 2 µg	Abcam, Cambridge, UK
Lamin B1	ab16048	rabbit	WB: 1/2000	Abcam, Cambridge, UK
p21 WAFI AB (Ab-1,EA10)	OP64	mouse	WB: 1/500	Calbiochem
p300 (N-15)	sc-584	rabbit	WB: 1/500, Co-IP: 1 µg	Santa Cruz Biotechnology
p300 (N-15X)	sc-584X	rabbit	ChIP: 5µg	Santa Cruz Biotechnology,
p38	9212	rabbit	WB: 1/1000	Cell Signaling Technology
p53 (DO-1)	554293	mouse	WB: 1/1000	BD Pharmingen
p73	ab14430	rabbit	WB: 1/1000, ChIP: 2 µg	Abcam, Cambridge, UK
PARP	9542	rabbit	WB: 1/2000	Cell Signaling Technology
Phospho-HSP27 (Ser82)	2401	rabbit	WB:1:1000	Cell Signaling Technology
Phosho p38 MAPK (Thr180/ tyr 182)	9215	rabbit	WB: 1/1000	Cell Signaling Technology
Puma/bbc3 C-Term	P4618	rabbit	WB: 1/500	Sigma-Aldrich Germany
TBP	SL30	mouse	WB: 1/250	self-made

Table 2.9. Secondary antibodies

Antibody	Cat. Number	Company
HRP-coupled AffiniPure F(ab')2 fragment, anti mouse IgG (H+L)	711-036-152	Jackson Immunoresearch,
HRP-coupled AffiniPure F(ab')2 fragment, anti rabbit IgG (H+L)	715-036-150	Jackson, Immunoresearch

2.1.7 Eukaryotic cell culture

Table 2.10. Cell lines

cell lines	origin
A375	malignant melanoma
Brown	malignant melanoma
GH	testicular carcinoma
HCT116	colon adenocarcinoma
HCT116 -/-p53	colon adenocarcinoma, isogenic p53 knockout
HEK293T	human embryonic kidney cells, harbouring SV40 antigen
HMB-2	malignant melanoma
Lox	malignant melanoma
MEF	mouse embryonic fibroblasts, BALB/C background gifted by Yvonne Begus-Nahrmann
Mel2a	malignant melanoma
Mewo	malignant melanoma
MSM	malignant melanoma
MV3	malignant melanoma
U2OS	osteosarcoma

Table 2.11. Media and reagents for eukaryotic cell culture

Reagent	Company
Dulbecco's Modified Eagle Medium (DMEM), powder	Gibco, Life Technologies
Fetal Calf Serum (FCS)	Gibco, Life Technologies
L-Glutamine	Gibco, Life Technologies
PBS (tablets)	Gibco, Life Technologies
Penicillin/Streptomycin	Gibco, Life Technologies
Trypsin/EDTA	Gibco, Life Technologies

Table 2.12. Culture medium for eukaryotic cells

DMEM (dissolved in H_2O)	
DMEM, powder	10.0 g
$NaHCO_3$	3.7 g
HEPES	5.96 g

2.1.8 Bacteria

Table 2.13. Bacteria strains

Strain	Description	Company
TOP10	competent *E.coli*	Invitrogen, Life Technologies

Table 2.14. Bacteria culture media

2YT medium	
Tryptone	1.6%
Yeast extract	1.0%
NaCl	0.5%

2YT agar	
YT agar	15%
2YT medium	100%

2.1.9 Oligonucleotides and plasmids

Table 2.15. Primer for human gene expression studies

Primer	Sequence 5`-3`	target gene
BAX_ forward	CCGGGTTGTCGCCCTT	Bax
BAX_reverse	AGGGCCTTGAGCACCAGTT	Bax
BRMS1_forward	GGCAGCTCTCAGGGAATCTC	BRMS1
BRMS1_reverse	TCTTTGCTTGGAGGCTGGAC	BRMS1
CBP_forward	CATTGTCAGGCTGGGAAAGC	CBP

CBP_reverse	CAGGATGGTTTGTTGGTTTCG	CBP
cyclinE_forward	GACGGGGAGCTCAAAACTGA	CyclinE
cyclinE_reverse	CATGGCTTTCTTTGCTCGGG	CyclinE
Fas_forward	AGGAATGCACACTCACCAGC	Fas (CD95)
Fas_reverse	TGGAGATTCATGAGAACCTTGG	Fas (CD95)
HPRT1_forward	ATGCTGAGGATTTGGAAAGG	HPRT1
HPRT1_reverse	TCATCACATCTCGAGCAAGAC	HPRT1
IASPP_forward	ACAGCGAGGCATTCCAGAG	iASPP (PPP1R13L)
IASPP_reverse	TGCTTGGTCAGTTCATCCAC	iASPP (PPP1R13L)
Noxa_forward	GCCGCGGGTCGGGAGCGTGT	Noxa (PMAIP1)
Noxa_reverse	GCCCCTGTCCCCGCCCCTGT	Noxa (PMAIP1)
P21_forward	CTTTCTGGCCGTCAGGAACA	P21 (CDKN1A)
P21_reverse	CTTCTATGCCAGAGCTCAACATGT	P21 (CDKN1A)
P300_forward	GCGGCCTAAACTCTCATCTC	P300 (EP300)
P300_reverse	TGGTAAGTCGTGCTCCAAGTC	P300 (EP300)
PIG3_forward	ATGTTAGCCGTGCACTTTGACA	PIG3 (TP53I3)
PIG3_reverse	CACGTAGAGGTTTTCCGGTCC	PIG3 (TP53I3)
Pml_forward	CCGCAAGACCAACAACAT	PML
Pml_reverse	ACTGTGGCTGCTGTCAAG	PML
PUMA_forward	GAAACGGAATGGAAAGCTATGAGA	Puma (bbc3)
PUMA_reverse	GCAGACCCCATGCCAAATT	Puma (bbc3)
rad51_forward	GAGAAGTGGAGCGTAAGCCA	Rad51
rad51_reverse	GCTGCATCTGCATTGCCATT	Rad51

Table 2.16. Primer for mouse gene expression studies

Primer	**Sequence 5`-3`**	**target gene**
mHPRT1_forward	CGTCGTGATTAGCGATGATGAAC	HPRT1
mHPRT1_reverse	CATCTCGAGCAAGTCTTTCAGTC	HPRT1
miASPP_forward	ATCTTCGCCACCACTCTCAG	iASPP (ppp1r13l)
miASPP_reverse	ACAACGCCATTGTGCATCAG	iASPP (ppp1r13l)
mNoxa_forward	GCGAAAGCTAACACGCAGAG	Noxa (PMAIP1)
mNoxa_reverse	GGAGTGGGACAGCTGGATTT	Noxa (PMAIP1)
mP300_forward	CCTCGGTTGTATCTCCGAAAG	P300
mP300_reverse	TCCAGGTCAAACAGTGAACC	P300
mPuma_forward	TTCTCCGGAGTGTTCATGCC	Puma (bbc3)
mPuma_reverse	ATACAGCGGAGGGCATCAGG	Puma (bbc3)

Table 2.17. Primer for ChIP analysis

Primer	**Sequence 5`-3`**	**target gene**
ChIPpuma_forward	CTTGCTAACTGGCCCACTG	BBC3
ChiIPpuma_reverse	CGGAATGGAAAGCTATGAGAC	BBC3
ChIPFas_forward	AGGGCTTGTCCAGGAGTTC	CD95

ChIPFas_reverse	ACAGGAATTGAAGCGGAAGT	CD95
ChIPmyo_forward	CTCATGATGCCCCTTCTTCT	MB
ChIPmyo_reverse	GAAGGCGTCTGAGGACTTAAA	MB
ChIPp21_forward	GCAGATGTGGCATGTGTCC	CDKN1A
ChIPp21R_reverse	AGTGACTGCACGACCTTGG	CDKN1A
ChIPPIG3_forward	CCCTGGGTACCTGCATTAAG	TP53I3
ChIPPIG3_reverse	TAGCCGTGCACTTTGACAAG	TP53I3

Table 2.18. siRNA

All siRNA samples were purchased from Ambion (Silencer Select).

Target (No.)	ID	sequence
BRMS1 (kd1)	S24632	Sense: GGAAUAAGUACGAAUGUGAtt Antisense: UCACAUUCGUACUUAUUCCtg
BRMS2 (kd2)	S24633	Sense: GAUCAGGAAUAAGUACGAAtt Antisense: UUCGUACUUAUUCCUGAUCac
CBP	S3496	Sense: GGAUAUUGCUGUGGACGCAtt Antisense: UGCGUCCACAGCAAUAUCCaa
siRNA negative control 1	Cat.4390843	undisclosed
EP300	S4696	Sense: CCACUACUGGAAUUCGGAAtt Antisense: UUCCGAAUUCCAGUAGUGGat
iASPP (kd1)	S21296	Sense: GCCUUAAAUUUAGUAAUCUtt Antisense: AGAUUACUAAAUUUAAGGCtg
iASPP (kd2)	S195072	Sense: GGAGUAAAGUCUAGCAGGAtt Antisense: UCCUGCUAGACUUUACUCCtt

Table 2.19. shRNA

All shRNA constructs were purchased from Sigma Aldrich.

ID	Target	Sequence
PLKO.1-luc/ SHC007 (control kd)	luciferase	undisclosed

PLKO.1-TRCN0000022209	iASPP (kd1)	CCGGCCAACTACTCTATCGTGGATTCTCGAGAATCCACGATAGAGTAGTTGGTTTTT
PLKO.1-TRCN0000022210	iASPP (kd3)	CCGGGCCTCAAAGGAGTAAAGTCTACTCGAGTAGACTTTACTCCTTTGAGGCTTTTT
PLKO.1-TRCN0000022212	iASPP (kd2)	CCGGCCCTACCCACAAGAAACAGTACTCGAGTACTGTTTCTTGTGGGTAGGGTTTTT
PLKO.1-TRCN0000006507	P73 (kd1)	CCGGCTCTCCTTCCTGTGTGTCCAACTCGAGTTGGACACACAGGAAGGAGAGTTTTT
PLKO.1-TRCN0000006508	P73 (kd2)	CCGGCCCGCTCTTGAAGAAACTCTACTCGAGTAGAGTTTCTTCAAGAGCGGGTTTTT
PLKO.1-TRCN0000006511	P73 (kd3)	CCGGCCAAGGGTTACAGAGCATTTACTCGAGTAAATGCTCTGTAACCCTTGGTTTTT

Table 2.20. Plasmids

Name	Source	Description
pcDNA3.1	Invitrogen, Life Technologies	Expression vector for the exogenous expression of proteins under the control of a CMV promoter in eukaryotic cells; harbours ampicillin resistance cassette for amplification in E.coli.
pcDNA3.1-iASPPV5	from Xin Lu, Oxford	pcDNA3.1 vector with open reading frame coding for iASPP. C-terminal tagged with V5. Extra neomycin resistance for generation of stable cell lines; harbours ampicillin resistance cassette for amplification in E.coli.
pMD2.G (VSV-G)	Addgene Plasmid (12259)	Lentiviral vector encoding for viral envelop proteins; ORF is under the control of a CMV promoter. Contains ampicillin resistance.
pCMVΔR 8.91 (8.91)	Plasmidfactory Bielefeld	Viral vector for the production of lentivirus. Encodes for gag, pol and rev genes under the control of a CMV promoter. Contains ampicillin resistance.
M420	from AG Dietrich, GSH Frankfurt	Vector with coding sequence for GFP under the control of a CMV promoter. Contains a RNA packaging signal, LTR sequences for genomic insertion of the target sequences and a 3`SIN/LTR for production of replication deficient virus. Harbours an ampicillin resistance cassette for amplification in E.coli.

PLKO.1-luc (control vector)	from Sigma Aldrich	Vector with coding sequence for luciferase gene under the control of a CMV promoter. Contains a RNA packaging signal, LTR sequences for genomic insertion of the target sequences and a 3`SIN/LTR for production of replication deficient virus. Harbours an ampicillin resistance cassette for amplification in E.coli and a puromycin resistance gene for generation of stable cell lines.
PLKO.1-TRC	from Sigma Aldrich	Vector with coding sequence for iASPP or p73 gene under the control of a CMV promoter (see Table 2.19. for clones). Contains a RNA packaging signal, LTR sequences for genomic insertion of the target sequences and a 3`SIN/LTR for production of replication deficient virus. Harbours an ampicillin resistance cassette for amplification in E.coli and a puromycin resistance gene for generation of stable cell lines.

2.1.10 Software

Table 2.21. Software

Name	Company
Adobe Photoshop CS5	Adobe Systems, San Jose, CA, United States
AxioVision 3.0	Zeiss
CFX Manager Software for qPCR cycler	Bio-Rad
Excel	Microsoft, Redmond, WA, United States
Guava Express Software	Millipore, Merck
INTAS lab ID	Intas Science Imaging Instruments
NanoDrop Software	Peqlab

2.2 Methods

Cell biology

2.2.1 Cultivation of adherent cells

All cell lines were cultured in full DMEM medium (supplemented with 10% FCS, 50 U/mL penicillin/streptomycin and 200 µM L-glutamine) at 37°C and 5% CO_2 in a moistly incubator. For stable knockdown cell lines, full DMEM medium was freshly supplemented with 0.1% puromycin solution.

Cells were regularly split for 2-3 times per week. Hence, old medium was sucked off the plates, cells were gently washed with pre-warmed PBS (with $MgCl_2$) and finally detached by incubation with 0.1% pre-warmed trypsin/ EDTA solution. Trypsination was stopped by adding new, pre-warmed, medium. Finally, a portion of trypsinized cells was transferred to a new petridish and supplemented with fresh pre-warmed medium.

2.2.2 Freezing/Thawing of adherent cells

To secure low passage cultivation of the cell lines, cells were regularly frozen and kept at -80°C or in liquid nitrogen. For freezing, cells were trypsinized, centrifuged (5 min, 1000 rpm at RT) and subsequently dissolved in freezing medium containing 90% FCS and 10% DMSO. One full 10 cm plate was normally resuspended in 2 mL freezing medium and divided into 2 aliquots. The aliquots were placed in a freezing unit containing isopropanol, and placed for 24 h at -80°C, before the tubes were transferred to a storage tank containing liquid nitrogen.

For thawing of the cells, frozen aliquots were quickly warmed up and cells were added to a 10 cm dish containing 18 mL pre-warmed medium. 24 h after thawing, medium was changed to remove the toxic DMSO from growing cells.

2.2.3 Treatment of the cells with chemotherapeutic drugs and inhibitors

Cells were mostly treated with the chemotherapeutic drug cisplatin or Etoposide. Cisplatin solution was applied as an aqueous solution of 1 mg/mL. Final concentration of cisplatin ranged from 10-40 µM depending on the cell line and experiment. Etoposide, that had been

dissolved in DMSO before was applied in a concentration of 30 µM. All other chemicals and inhibitors that were used for treatment of the cells as well as the solvent and final concentration are listed in table 2.22.

Table 2.22. Concentrations of chemicals used for the treatment of cells

Chemical	Final concentration	Stock	Solvent
Cisplatin (CDDP)	10-40 µM	1 mg/mL	water
Etoposide	30 µM	10 mM	DMSO
zVad	40 µM	40 mM	DMSO
MG132	20 mM	10 mM	DMSO
CTB	10 µM, 20 µM	100 mM	DMSO
BCI	10 µM	10 mM	DMSO
SB203580	10 µM, 20 µM	10 mM	DMSO
CHX	100 µg/mL	100 mg/mL	Ethanol

For the control reactions, cells were always treated with the same concentration of the solvent as used for the treatment with the respective drug. Generally, for treatment of the cells, medium was removed and substituted by a master mix of the drug or chemicals pre-dissolved in fresh pre-warmed medium.

2.2.4 Transfection of cells using Calcium-phosphate

Transient over-expression of iASPP as well as the transfection of HEK293T cells for the production of lentivirus was conducted using Calcium-phosphate (Graham and van der Eb 1973). Therefore an appropriate amount of cells was seeded 24 h before transfection. For transient over-expression of iASPP, cells of a 10 cm plate were transfected with 10 µg plasmid. DNA, 500 µL 2x HBS buffer and 440 µL sterile water were mixed. Then 60 µL 2 M $CaCl_2$ solution was quickly added to the mix, followed by virtuously shaking and incubation for 30 min at 37°C. Finally the transfection mix was drop-wise pipetted on the cells and

incubated with the cells over night or at least for 8 h at 37°C. The next day, the medium of the transfected cells was exchanged. 48 h post transfection, cells were harvested or treated with chemotherapeutic drugs. For generation of control cells, same amount of cells were transfected with 5 µg pcDNA (empty vector) and 5 µg GFP-plasmid.

For the transfection and therefore production of lentivirus in HEK293T cells, $1x10^6$ cells were seeded 24h before and subsequently transfected with 2.5 µg shRNA construct for the respective gene, 1.6 µg 8.91 plasmid and 1 µg VSV-G plasmid (Naldini, Blomer et al. 1996; Stewart, Dykxhoorn et al. 2003). Concentration of $CaCl_2$ and 2x HBS buffer as well as the transfection protocol remained the same as for the transient over-expression of iASPP. For control, lentivirus with shRNA containing a siRNA sequence against the luciferase gene was generated as well as a virus expressing GFP.

2.2.5 siRNA mediated knockdown of cells

BRMS1, p300 and partially also iASPP were transiently knocked down in various cell lines using commercial available siRNA (Sequences see table 2.18). For transfection of a 6-well, 50pmol siRNA was added to 250 µL DMEM without FCS, Pen-Strep or glutamine (= DMEM (-)). In another tube 5 µL Lipofectamine 2000 (Invitrogen) was incubated with 250 µL DMEM (-) for 5 minutes at RT. Next DMEM with siRNA and DMEM with Lipofectamine were mixed and incubated for 20 minutes at RT. In the meantime, cells were trypsinated and counted. SiRNA/ Lipofectamine mix was spread on the dish and $20\text{-}40x10^5$ cells/ per 6-well were drop-wise added to the plate. The number of transfected cells depended on the cell line. Each well was filled up to 2.5 mL with full DMEM medium and incubated over night in the incubator at 37°C. Next day, medium was exchanged. 48 h-72 h post transfection, cells were treated and subsequently harvested for further analysis. For chromatin fractionation, 10 cm plates were transfected with 3 µL 50 pmol siRNA and 20 µL Lipofectamine 2000 in 2x 500 µL DMEM (-) medium.

2.2.6 Lentivirus mediated generation of stable knockdown cell lines

Stable knockdown cell lines were generated using lentivirus-mediated transduction, because lentivirus renders a high transfection efficiency and genomic integration rate of the constructs. As lentivirus belongs to the safety class 2 (S2) organisms, all following work was conducted under S2 safety rules. In general, lentivirus was produced in HEK293T cells, followed by transduction of the target cell lines with the virus containing supernatant

(modified after the protocol from www.sigma-aldrich.com). As the transduced shRNA-constructs contain a sequence encoding for a puromycin resistance gene, stably transduced cells were selected by cultivation of the cells with puromycin-containing medium. Once selected, cells were cultured with a medium containing low concentrated puromycin to maintain the knockdown.

For production of the lentivirus, HEK293T cells were transiently transfected with lentiviral packaging plasmids and the respective shRNA constructs using Calcium-phosphate (see table 2.19). Two control viruses were generated and transfected in parallel. One control represented a shRNA against the luciferase gene (= control knockdown cells) and the other control constituted a transducable GFP-plasmid that monitored the transduction efficiency.

48h post transfection, the supernatant including the lentivirus was collected and passed through a 0.45 µm filter. Polybrene (8 mg/ml) was added to the supernatant in a dilution of 1:1000 and the mix was finally placed on the target cells. Following, virus and target cells were incubated for 24 h in the incubator at 37°C. Virus incubation was stopped by sucking off the supernatant and supplementation of target cells with fresh full DMEM medium.

24 h-48 h post-transduction, transduction efficiency was controlled by detection of the green fluorescence of GFP-expressing control cells using the Zeiss fluorescence microscope. When GFP was broadly expressed, selection for stably knocked down cells was started by adding puromycin to a final concentration of 0.1%. In general, puromycin was always freshly supplemented to the medium as it is not stable for a longer time. When the cells stopped to die from incubation with puromycin, analysis of the cells was started and cells were frozen in parallel.

For transduction of MEFs, cells were not selected with puromycin but directly harvested after 4 days of transduction, as MEFs enter a senescence status if they are cultivated too long.

2.2.7 Cell cycle analysis of cells

Cell cycle analysis as well as the quantification of the apoptosis rate as the number of cells in subG1 phase was assessed by FACS (Tounekti, Belehradek et al. 1995). In general fixed cells were stained with Propidium iodide which specifically stains the DNA. Thus the DNA content and following also the number of cells in subG1, G1, S and G2/M are countable.

For preparation of the samples, cells were harvest by collection of the supernatant and trypsinized cells in 15 mL Falcon tubes. After centrifugation of the cells (5 min, 1500 rpm at RT) cell pellets were resuspended in 0.6mL 3% FCS/PBS. As the staining solution cannot

cross the cell membrane, cells had to be fixed. Therefore 1.4 mL 96% Ethanol was drop wise added to the resuspended cells by gentle agitation of the cells. Cells were fixed in Ethanol for at least 24 h at -20°C.

For subsequent analysis, fixed cells were centrifuged (5 min, 1500 rpm at RT) and washed with 5 mL PBS (with $MgCl_2$). After an additional centrifugation step (5 min, 1500 rpm at RT), cells were resuspended in 400-750 µL PBS (depending on the cell pellet) and 40 U RNAse A was added, followed by a brief incubation of the samples for 20 min at RT. Incubation with RNAse A is a crucial step, as FACS analysis with Propidium iodide-stained samples cannot discriminate between RNA and DNA.

Next, 200 µL sample was mixed with 6 µL Propidium iodide solution (Sigma) and cell number was assessed by FACS analysis using the Express Pro software (Guava System, Millipore). Of note, samples were pre-diluted with PBS to retrieve equal cell numbers between 300-500 cells/µL. For analysis, gates were set only once and same gate settings were applied for all samples of one series.

For assessment of the apoptosis rate, cells in subG1 phase were counted. As late apoptotic cells display fragmentation of the DNA, all signals that run lower than the G1 phase (after gating for whole cells not cell debris) can be stated as the population of dead cells.

Molecular biology

2.2.8 Transformation of E.coli

Plasmids used for over-expression experiments and lentivirus production were transformed and amplified in TOP10 E.coli cells (Invitrogen). Hence, 0.5 µg Plasmid DNA was incubated with 50 µL competent E.coli cells for 30 minutes on ice followed by a heat-shock transformation of the cells for 45 sec at 42°C. After heat-shock, cells were placed for 1.5min on ice followed by the addition of 950 µL pre-warmed YT medium. After another incubation time of the cells in a gently shaking thermoblock at 37°C for 1 h, cells were plated on YT plates containing 100 µg/mL ampicillin. E.coli cells were usually seeded in 1:100, 1:1000 and 1:10000 dilution to retain single colonies. Plates were subsequently incubated at 37°C over night. A single colony was picked and expanded by an overnight culture in 50 mL YT medium containing 100 µg/mL ampicillin. Finally, the plasmid DNA was extracted using the Midi-prep System (Promega).

2.2.9 Midi-preparation of plasmid DNA

Midi-preparation of plasmid DNA from a 50 mL over night culture was performed using the midi-prep kit from Promega. Plasmid DNA was extracted according to the manual. Of note, binding and washing of the columns was performed under vacuum. Finally, the plasmid DNA was eluted with 200 µL nuclease-free water. The concentration was measured with the Nanodrop (Peqlab). Plasmid DNA was then stored at -20°C until it was used for transfection of eukaryotic cells.

2.2.10 Primer design

ChIP-primers were designed with the Primer3 software (http://frodo.wi.mit.edu/primer3). Criteria for primer design were the following:

Template size: 50-150 bp, Primer size: 18-24, GC content: 40-60%, Melting temperature tm: 58.0-62.0°C, Max. Poly X: 5.00, Max. self complementary: 3.00, CG clamp: 1

As the basis for the design of ChIP primers served genomic DNA sequences that were retrieved from the UCSC genome browser (genome.ucsc.edu). For p73/p300 ChIP-Primer, self-made p73 ChIPseq tracks (Koeppel et al, 2011) were uploaded at the UCSC genome browser site. After zoom in to the respective p73 binding site, the corresponding genomic sequence was retrieved and served as the input sequence for the Primer3 software.

For gene expression primer, the Primer blast program of the NCBI website was used (*www.ncbi.nlm.nih.gov/tools/**primer-blast/***). Basis for this platform is the Primer3 software that was also used for the design of ChIP primer. The same criteria for primer design were applied as stated above. Additionally, primers were design as intron-spanning to avoid amplification of probably contaminating genomic DNA.

The resulting oligonucleotides were ordered at Biomers (www.biomers.net) and Metabion (www.metabion.com). Lyophilized primers were resuspended with nuclease-free water to a final concentration of 100 µM and stored at -20°C. For real-time PCR analysis, forward and reverse primer were mixed at a concentration of 10 µM and kept as working solutions.

2.2.11 Quality control of primer

Primers were validated for their efficiency and specificity prior to standard usage. Therefore dilution series of cDNA or genomic DNA (1:20, 1:40 and 1:80) served as templates for real-

time PCR analysis for each new primer pair. Composition of the real-time PCR reactions is depicted in Table 2.23. PCR was performed with the standard thermocycler program (table 2.24).

Table 2.23. Composition of real-time PCR reaction mixes

Compound	**Volume (per reaction: 25 µL)**
Sybr green mix (self-made, see table 2.5)	14 µL
Primer working solution (10 µM)	1 µL
Nuclease-free water	5 µL
cDNA (1:20 diluted)/ ChIP sample	5 µL

Table 2.24. Standard thermocycler program for real-time PCR

Temperature	**Time**	**Cycles**
95°C	3 min	
95°C	15 sec	40x
58°C	45 sec	
95°C	1 min	
Melting curve 65°C-95°C	0.5°C/ 10 sec	

From the resulting Ct values, the primer specificity as well as primer efficiency was calculated. Due to the theoretical basis that a 2-fold diluted cDNA (input) sample should give a 1.00 higher Ct value compared to the 2-fold higher concentrated cDNA (input) sample, a good primer efficiency was judged by plotting the log2 of the cDNA (input) dilutions (x-axis) against the Ct value (y-axis). A good primer pair should show a linear correlation between Ct values and dilution factor with an approximately slope of 1.00 and a regression higher than 0.95. Specificity of the primer was judged by looking at the respective melting curves of the primer pair. Specific primers always display one sharp melting curve of the PCR product;

unspecific primers result in multiple melting curve peaks or astringent curves. Nonspecific or inefficient primer were newly designed and replaced.

2.2.12 Isolation of total RNA

Basically RNA extraction was done according to the TRIZOL extraction protocol from Sigma-Aldrich.

Prior to RNA extraction, cells were harvested by trypsination and transferred to a 1.5 mL Eppendorf tube. After pelletation of the cells by centrifugation (1 min, 3800 rpm, at RT), cells were dissolved in 1mL TRIZOL and subsequently incubated for 2 minutes at RT. 200µL chloroform was added and the mix was virtuously shaked for 15 sec to separate the RNA from proteins and genomic DNA. After 2 minutes of additional incubation, the mix was centrifuged (for 5 min, 13000 rpm at 4°C) and the upper RNA-containing phase was transferred to a new 1.5 mL Eppendorf tube.

Next 0.5 mL Isopropanol was added and the mix was thoroughly vortexed. For precipitation of the RNA, the RNA-Isopropanol mix was incubated for 10 minutes on ice and afterwards centrifuged again (for 30 min, 13000 rpm at 4°C). After removal of the supernatant, the pellet was washed one time with 150 µL 70% EtOH (short vortexing and centrifugation for 1 min, 13000 rpm at 4°C) followed by removal of all liquid and short air drying of the RNA. Finally, the pellet was resuspended in 100 µl nuclease free water.

2.2.13 DNAse I digest of RNA samples

To ensure the total removal of any possible contaminating genomic DNA, a DNAse I digest was subsequently performed. Therefore the RNA was mixed with 20 µL DNAse I mix (table 2.25) and incubated at 37°C for 30 minutes, shaking.

Table 2.25. Composition of DNAse I mix (per reaction)

Compound	Volume
10x DNAse I Buffer	12 µL
DNAse I, hc	0.25 µL
RNAse inhibitor	1 µL
Nuclease-free water	6.75 µL

After incubation, samples were purified by Phenol-chloroform extraction. Therefore 120 µL Phenol-chloroform mix (5:1; pH 4.3) was added to each RNA sample and vortexed for 10 seconds. After short centrifugation of the tubes (for 1 min, 13000 rpm at 4°C) the upper aqueous phase was transferred to a new tube and the Phenol-chloroform extraction was repeated once. Following the Phenol-chloroform purification, the RNA-containing, upper phase was transferred to a new tube and mixed with 375 µL 96% EtOH and 17 µL NaAc for precipitation of the RNA. Next, the samples were either incubated over night at -20°C or for 1 h at -80°C followed by centrifugation of the samples for 30 minutes, 13000 rpm at 4°C. After removal of the supernatant, the resulting RNA pellet was washed again with 150 µL 70% EtOH (short vortexing and centrifugation for 1 min, 13000 rpm at 4°C). Following, the pellet was shortly air dried again and resuspended in 10-30 µL nuclease free water.

RNA samples were stored at -80°C or directly used for cDNA synthesis. Prior to reverse transcription the concentration of the RNA was determined with the Nanodrop (Peqlab). Therefore 2 µL RNA was measured at a wavelength of 260 nm and subsequently diluted to 400 ng RNA/µL.

2.2.14 cDNA synthesis

cDNA synthesis was principally done according to the manual of MMulV reverse transcription kit (Thermo Scientific Fisher). 2.5 µL (1 µg) of total RNA was incubated with 2 µL random hexamer primers (Thermo Scientific fisher) and 7.5 µL nuclease-free water for 5 min at 70°C. After short centrifugation of the samples, 8 µL of master mix (table 2.26) was added and reverse transcription was performed for 1 h at 42°C, followed by 10 minutes of heat inactivation at 65°C.

Following cDNA samples were 1:20 diluted with nuclease-free water and stored at -20°C.

Table 2.26. Master mix for cDNA synthesis

Compounds	Volume
5x RT Buffer	4 µL
20 mM dNTPs	1 µL
RNAse inhibitor (40 u/µL)	1 µL
MMulV RT enzyme	1 µL

2.2.15 Quantification of relative gene expression

For determination of the relative gene expression, real-time PCR was performed using the C1000 CFX96 real-time PCR thermocycler (Biorad). Low-profile PCR plates in 96-well format with an optical covering were used (4-titude).

Generally, gene expression values were obtained from three independently extracted RNA/ cDNA samples (biological replicas). Technical replicas were included in the biological replicas. Reactions were pipetted according to table 2.23. After sealing of the plate with optical foil, the whole plate was vortexed and shortly centrifuged (1 min, 1400 rpm, RT). All PCR plates were freshly prepared and directly analysed. The same thermocycler program as used for primer validation was applied (table 2.24).

For calculation of the relative gene expression the ΔΔCt method was applied. Therefore the threshold was manually set and the relative Ct values for target and reference genes were obtained. To account for variation of pipetting and independent runs, a reference gene (*HPRT1*) was always analysed in parallel to the target genes.

For calculation of the ΔCt value, Ct values of the target gene were normalized against the Ct values of the reference gene via subtraction. Next the ΔΔCt value was calculated by subtraction of the Ct value of the control knockdown or untreated sample from treated or iASPP, BRMS1 or p73 knockdown samples. Hence the ΔΔCt value of the control sample was set as 0 (= fold change). As Ct values resemble logarithmic values to the basis of 2, the mean log ratio was calculated with the following formula: $\mathbf{- 2^{(-\Delta\Delta Ct)}}$. Control or untreated samples are therefore set as 1 whereas up-regulation is represented by a mean log ratio >1 and a down-regulation is depicted as a mean log ratio ranging between 0 and 1.

Proteinbiochemistry

2.2.16 Protein harvest

For preparation of total cell lysates, cells were scraped with medium. Scraped cells and medium were collected in 15 mL Falcon tubes and centrifuged for 5 minutes, 1500 rpm at RT. Following the cell pellet was washed with 1 mL PBS, centrifuged again (3800 rpm, 5 minutes, RT) and dissolved in cell lysis buffer, containing ¼ volume 8 M Urea and 1x protease inhibitor complete (PIC). Cells from one 6-well were usually lysed in 100-200 µL buffer volume depending on the cell line.

Subsequently cell lysates were kept on ice. After virtuous pipetting, all samples were shortly sonicated to disrupt bulky genomic DNA. Sonication was performed with the Bioruptor (Diagenode) for 10 minutes at high power (30 sec on/off interval) in ice cold water. After sonication, the concentration of the cell lysates was determined using the BCA method.

2.2.17 Determination of the protein concentration- BCA assay

To ensure equal loading amounts of the protein samples, the concentration of the cell lysates was assessed using a BCA assay kit (Thermo Scientific Fisher). Basically 5 µL of each sample was incubated with 100 µL BCA-buffer at 37°C, 30 minutes, shaking. Afterwards relative protein concentration was determined using the Nanodrop (Peqlab). For calculation of the absolute protein concentration, a standard curve with defined standard concentrations of Albumin was measured in parallel.

Next, cell lysates were denatured by boiling of the samples with ¼ volume Laemmli buffer for 5 minutes at 95°C. For subsequent analysis of the protein samples, SDS-PAGE combined with Immunoblotting was performed. Therefore 20-40 µg of protein was loaded on SDS-PAGE gels, depending on the abundance of the proteins that had to be detected.

2.2.18 SDS-PAGE

For separation of proteins according to their size, denatured samples were analysed using SDS-PAGE gels. SDS is masking the charges of proteins thereby allowing the separation of cell lysates according to their size. Basically, SDS-PAGE is performed by two layers of gels: a stacking and a running gel (Table 2.27). The stacking gel (5% acrylamide at pH 6.8) is concentrating the samples leading to sharpened protein bands whereas the separation of proteins is performed by varying concentrations of the running gel (6-12% acrylamide at pH 8.8). For analysis of small proteins, small pore-gels were generated (12%) thereby allowing the standard detection of proteins ranging from 10-100 kDa, whereas 6% polyacrylamide gels were applied for separation of relatively big proteins (e.g. p300 and CBP, migrating at around 270 kDa). In general, for separation of the protein mixtures, the pre-casted gels were placed in a tank with 1x running buffer and samples were loaded in the pre-formed gel pockets together with a pre-stained protein marker. Next, power (constant voltage of 90-140 Volt) was applied which led to a separation of the samples by migration of the proteins from the cathode towards the anode.

Table 2.27. Composition of gels for SDS-PAGE

Compound	**Stacking gel**	**Running gel**
Acrylamide-bisacrylamide	5%	6-12%
Tris-HCl, pH 6.8 (0.5 M)	126 mM	-
Tris-HCl, pH 8.8 (1.5 M)	-	375 mM
SDS (10%)	0.1%	0.1%
APS (10%)	0.05%	0.05%
TEMED	0.1%	0.4%
Glycerol	-	10%

After appropriate separation of the samples, the proteins in the gels were transferred on nitrocellulose membranes by applying the Immunoblotting technique.

2.2.19 Immunoblotting

Proteins in polyacrylamide-gels are difficult to assess for any antibody staining. Therefore proteins are usually transferred to a nitrocellulose membrane and stained with a primary antibody against the desired protein. To visualize the protein of interested, staining with a secondary horse radish peroxidase (HRP)-conjugated antibody is performed that recognizes the first bound antibody (Renart et al., 1979, Towbin et al., 1979). Of note, sequential incubation and detection using two antibodies leads to an amplification of the signal, thereby allowing the detection of low protein amounts.

Finally the membrane is incubated with a chemiluminoscence reagent that is only activated at the sites of pre-antibody bound HRP enzyme. The emitted light of the bands can then be detected using the *Chemocam HR 16 3200 imager* (Intas).

Starting, the proteins that were previously separated by SDS-PAGE were transferred to nitrocellulose membranes by application of a transfer buffer (Table 2.5)) and power. For 10-100 kDa proteins a transfer buffer with 20% Methanol was used, for bigger proteins (>100 kDa) a transfer buffer with only 10% Methanol and 0.01% SDS was applied, as big proteins are difficult to extract from the gels.

The transfer was accomplished in a cassette composed of two outer layers of sponges, two layers of Whatman-paper (that keeps gel and membrane wet) and an inner layer of membrane and the gel itself. The gel was placed at the site of the cathode and the membrane was placed at the site of the anode. Positively charged proteins were transferred then to the membrane by applying a constant voltage (2 h 100 V for 10-100 kDa proteins; over night at 25 V for proteins >100 kDa). As the blotting generates a lot of heat, the tank containing blots and transfer buffer, was put on ice in the cold room for the duration of the transfer.

After finishing of the transfer, the membrane (or so called blot) was blocked in 5% milk/PBS, 1 h at RT, rotating, to avoid any unspecific background staining. Next, the blot was incubated with dilutions of primary antibody (in 5% milk/PBS) either over night at 4°C or at least 4 h at RT. After extensive washing (3x for 10 minutes with PBST), the blot was incubated with secondary antibody (in 5% milk/ PBS) for 1 h at RT, rotating. Finally, after additional washing for 3x 10 minutes with PBST, the membrane was stained with Millipore staining solution and analyzed using the chemiluminoscence detection machine *Chemocam HR 16 3200 imager* (Intas). For proteins that were weakly expressed, Femto staining solution from Thermo Scientific Fisher was applied.

2.2.20 Co-Immunoprecipitation (Co-IP)

To validate the direct interaction of two proteins, co-immunoprecipitation was performed. In principle total cell lysates are incubated with an antibody against the protein of interest or IgG as a control. To precipitate antibody-protein complexes, protein G coupled Sepharose beads are added to the mix, followed by intensive washing of the beads and elution of the bound protein-antibody complexes. These precipitated protein-protein complexes are then denatured by short boiling with Laemmli buffer and finally analyzed by Immunoblotting.

For precipitation of endogenous proteins, a relatively large amount of cells was needed as starting material. Therefore cells from one 15 cm petridish were used for 1 Co-IP reaction. Supernatant was sucked off and the plates were washed with 5 mL PBS by gently moving of the plate. After the liquid was sucked off again, cells were lysed with 750 µL NET lysis buffer + 1x PIC for 30 minutes at 4°C. Next the cell lysates were scraped from the plates and passed 5 times through a 23G syringe to ensure total cell lysis. Of note, all following steps were conducted on ice to avoid any protein degradation. After 5 minutes of sonication with the Bioruptor (30 sec on/off, high power), cell lysates were shortly centrifuged (13000 rpm, 1 min at 4°C).

After preparation of the cell lysates, the resulting supernatants were further pre-cleared by adding 30 µL Sepharose G beads (50% slurry in PBS) per 750 µL cell lysate and subsequent rotation of the reaction mix at 4°C for 1 h on a rotating wheel. This pre-clearing reaction is important as it reduces unspecific binding of proteins to the beads. Before Sepharose beads were added, storage buffer was removed from the beads by washing of the beads for 3 times with 800 µL PBS (inverting and 2 min centrifugation at 4000 rpm and 4°C).

An additional batch of Sepharose G beads, which were later used for the IP reaction, were washed in parallel and finally supplemented with blocking solution (Blocking solution from Roth, 1:10 in PBS). Blocking of the beads was performed on a rotating wheel at 4°C for 1 h together with the pre-clearing reaction. After the incubation time, blocked beads were shortly centrifuged (4000 rpm, 2 min, 4°C) and supernatant was removed. Finally beads were resolved in appropriate amounts of NET buffer to retrieve a 50% bead slurry.

After incubation of the cell lysates with beads, the pre-cleared samples were shortly centrifuged (4000 rpm, 2 min, 4°C) and the supernatants were united in a falcon tube. For the input sample, 100 µL of the pre-cleared cell lysate was mixed with ¼ volume Laemmli buffer and boiled for 5 minutes at 95°C.

For the IP reaction 30 µL of pre-blocked Sepharose G beads was added to 750 µL pre-cleared cell lysate together with 2 µg antibody against iASPP or p73. For the control reaction 2 µg of ß-Galactosidase antibody was applied with the same amount of cell lysate and beads. Next, all IP reactions were incubated on a rotating wheel at 4°C over night. The next day, the IP reactions were shortly centrifuged (4000 rpm, 2 min at 4°C) and supernatant was removed. Following the remaining beads with captured protein-antibody complexes were washed 4 times with NET buffer. Therefore 1 mL NET buffer was added to the beads, the mix was 4 times inverted, centrifuged (4000 rpm, 2 min at 4°C) and the supernatant discarded. After the last washing round, the beads were mixed with 25 µL Laemmli buffer and boiled for 5 minutes at 95°C. After short centrifugation, the resulting supernatants were transferred to a new tube and subsequently analyzed by SDS-PAGE/ Immunoblotting.

2.2.21 Chromatin fractionation

Basically chromatin fractionation was done after the protocol from Mendez and Stillman (Méndez and Stillman 2000).

Starting, approximately $1x10^7$ cells (one 10 cm plate, 60-70% confluence) were used for one chromatin fractionation. Medium was sucked off and cells were washed with 5 mL PBS. After

removal of the PBS, cells were scraped with the remaining liquid and transferred to an Eppendorf tube. After short centrifugation (1000 rpm, 2 min at RT) supernatant was discarded and cell pellet was washed again with 1 mL PBS (resuspension and centrifugation for 1000 rpm, 2 min at RT). From here on all steps were performed on ice and with pre-cooled buffers. After removal of the PBS, the cell pellet was thoroughly resuspended in 200 µL Buffer A. Next 1 µL 20% Triton-X 100 solution was added to start the lysis of the cell. After 8min of incubation on ice, cells were centrifuged for 5 min, 2000 rpm at 4°C to separate supernatant (S1) from Pellet (P1). The supernatant (S1) was transferred to a new tube and clarified by centrifugation on maximal speed (13000 rpm, 5 min at 4°C). The resulting clear supernatant (S2) constituted the cytosolic, non-chromatin bound fraction.

The Pellet (P1) was washed once with 200 µL Buffer A to remove rests of contaminating non-chromatin bound proteins. Therefore cells were resuspended and centrifuged (2000 rpm, 5 min at 4°C). The supernatant was discarded. Afterwards the pellet (P1) was lysed by resuspension in 100 µL Buffer B and subsequently incubated for 30 minutes on ice. After additional centrifugation (3000 rpm, 5 min at 4°C), the resulting supernatant (S3) was added to the supernatant (S2) as this liquid contains proteins that are localized in the nucleus but do not bind on the chromatin (nuclear, non-chromatin bound fraction). S2 + S3 (approx. 300 µL) were mixed with 100 µL Laemmli buffer and finally boiled for 5min at 95°C.

The resulting pellet (P3) was resuspended in 100 µL Buffer B and 100 µL Laemmli buffer and boiled for 20 minutes at 95°C. This fraction P3 constituted the triton-insoluble, chromatin bound protein fraction. From both fractions 20 µL was loaded on SDS-PAGE gels and analysed by Immunoblotting.

2.2.22 Chromatin harvest for chromatin-immunoprecipitation (ChIP)

For ChIP, chromatin was harvested from 10 cm plates. After removal of the medium and washing with 5 mL PBS, all liquid was removed from the plates. Next crosslinking was performed by gently adding 1mL formaldehyde-Buffer A-PBS solution (0.5 mL 37% formaldehyde + 1.18 mL Buffer A + 15 mL PBS) to the cells. After 30 minutes of incubation at RT, crosslinking reaction was stopped by adding 100 µL 1.25 M Glycine. Glycine solution was distributed by gently shaking of the dish and following incubation for 5 min at RT.

Next all liquid was sucked off and the fixed cells on the dish were carefully washed 2 times with 5 mL PBS. After removal of all remaining liquid, cell lysis was performed by adding 1 mL of Buffer B (virtuous distribution and incubation for 10 min at 4°C). Following the cells were scraped from the dish and transferred to a 2 mL Eppendorf tube on ice. After centrifugation

for 5 minutes, 3000 rpm at 4°C, supernatant was discarded and the cell pellet was washed with 2 mL Buffer C. Therefore cells were thoroughly resuspended by pipetting up and down and subsequently centrifuged for 5 minutes, 3000 rpm at 4°C. Finally the resulting cell pellet was estimated by eye and resuspended in sufficient sonication buffer (1x incubation buffer + 0.23% SDS and 1x PIC). For ChIP using HCT116 cells, a cell pellet deriving from a 80% confluent 10 cm dish was usually resuspended in 750 µL sonication buffer. Then, chromatin was sonicated for 2x 10 min and 1x 5 min using the Bioruptor (30 sec on/off interval, high power in ice cold water) to shear the chromatin. Finally, the sheared chromatin was centrifuged for 5 min, 13000 rpm at 4°C to pellet remaining unsheared chromatin. The supernatant was transferred to a new tube and stored at -80°C until ChIP was performed.

For analysis of the chromatin by Immunoblotting, 100 µL chromatin together with 50 µL 6x Laemmli buffer was boiled for 20 minutes. Usually, 20 µL of the denatured chromatin samples was loaded on SDS-PAGE gels and immunoblotted with the same antibodies that were used for ChIP, in order to validate equal amounts of the different chromatin samples as well as the presence of iASPP knockdown.

2.2.23 Chromatin immunoprecipitation

Chromatin immunoprecipitation detects the relative binding of a protein to a specific genomic site. The protein of interest can either bind to DNA itself (like p73) or localizes in a multi-protein complex that binds to DNA then (like p300). The specific binding of a protein to a single genomic locus can be detected by combining ChIP with real-time PCR analysis of the precipitated DNA. In principle a previously published protocol was applied and modified for the respective cell lines and antibodies (Denissov, van Driel et al. 2007).

Starting, 50 µL/ reaction protein A/G plus beads were washed 2 times with 100 µL/reaction beads washing buffer (1x incubation buffer with 0.2% BSA). Washing was performed by inversion and centrifugation of the beads for 2 min, 4000 rpm at 4°C. Finally, the washed beads were dissolved in 25 µL/ reaction beads wash buffer and stored on ice.

Next ChIP reaction was set up according to table 2.28.

Antibodies were pipetted as the last step (p73-ChIP: ab14430, abcam; p300-ChIP: N-15X, Santa Cruz; control ChIP: polyclonal rabbit IgG, ab46540, abcam). ChIP reactions were incubated on a rotating wheel at 4°C over night. In parallel 12 µL of chromatin was kept at 4°C as the input sample.

Table 2.28. Set-up of ChIP reactions

Compound	Volume
BSA (5%)	6 µL
25x PIC	12 µL
5x Incubation buffer (without SDS)	36 µL
Chromatin	120 µL
Protein A/G beads	25 µL
Antibody	2 µg
Water (for total volume of 300 µL)	99 µL

The next day ChIP reactions were washed with a series of washing buffers. Each washing step comprised centrifugation of the samples for 2 min, 4000 rpm at 4°C, removal of the supernatant and finally addition of 400 µL of the respective washing buffer. Then tubes were 4x4 times inverted on ice and centrifuged again. Washing was performed for 2 times with cold washbuffer 1, 1x with cold washbuffer 2, 1x time with cold washbuffer 3 and 2x with cold washbuffer 4. After the last washing step, the supernatant was completely removed and beads were supplemented with 400 µL elution buffer.

From this point on the input samples were included. 12 µL input sample was mixed with 388 µL elution buffer as well. For elution of the Protein-DNA complexes all samples, ChIP and input reactions, were incubated on a rotating wheel for 20 minutes at RT. Next samples were shortly centrifuged and supernatant was transferred to a new eppendorf tube. Subsequently de-crosslinking was performed by adding of 16 µL 5 M sodium chloride and shaking of the samples in a heating block for 4 h at 65°C and 1300 rpm.

After the de-crosslinking step, the DNA was purified using Phenol-Chloroform. First 400 µL Phenol-Chloroform (pH 8.0; 5:1 dilution) was added, samples were vortexed and afterwards centrifuged for 1 min, 13000 rpm at 4°C. The upper, aqueous phase was transferred to a new tube and supplemented with 400 µL Chloroform. After vortexing and centrifugation (1min, 13000 rpm at 4°C), the resulting upper phase was transferred again to another new tube. For precipitation of the DNA, 20 µg glycogen together with 1 mL 96% Ethanol and 44

µL 3 M Sodium acetate was added, samples were mixed and finally incubated over night at -20°C.

Final purification of the samples was conducted by centrifugation (30 min, 13000 rpm, 4°C) followed by removal of all liquid and subsequent washing of the pellet with 400 µL 70% Ethanol (vortexing and centrifugation for 1 min, 13000 rpm at 4°C). All liquid was sucked off and the DNA pellets were shortly air dried before they were resuspended in 100 µL nuclease-free water. Afterwards, to secure a homogenous resuspension of the DNA, samples were incubated in a heating block (30 min at 50°C, 1000 rpm shaking). Importantly, ChIP samples were always stored at 4°C and shortly pre-warmed before real-time PCR analysis was conducted.

2.2.24 Analysis of ChIP samples

ChIP samples were analyzed with the real-time PCR, using the thermocycler program and master mix as described for the analysis of RNA/ cDNA (Table 2.23 and Table 2.24). Instead of gene expression primers, specific ChIP-primers were used that anneal to genomic DNA fragments. 5 µL of each ChIP sample and 5 µL of 1:10 diluted input sample were mixed with 20 µL of master mix for one reaction. Input, IgG-ChIP and p73/p300-ChIP reactions were always analysed in parallel on one plate, to exclude analysis errors due to varying real-time PCR conditions.

After finishing of the real-time PCR analysis, the recovery as the percentage of input was calculated. Therefore the Ct value of the ChIP sample was subtracted from the input sample for each primer pair and ChIP reaction, followed by the calculation of the logarithm to the basis of 2 (as Ct values represent logarithmic values) and the dilution factor of the input (normally 100). The following formula was applied for the calculation of the recovery:

Recovery (% of input) = log2 (Ct value input-Ct value sample)/100*100

Partially, the relative binding was calculated. As ChIPs of biological replicas can vary in their absolute percentages of input (due to the different chromatin preparations), the calculation of the relative binding ensures the correct calculation of the p-value. Therefore, the fold enrichment of each ChIP was calculated (recovery p73/ p300-ChIP vs. recovery IgG-ChIP) followed by the comparison of the fold enrichment of ChIP with control knockdown cells to the fold enrichment of ChIP with iASPP knockdown cells. ChIP of control knockdown cells was set to 100%, and the relative loss of binding in iASPP knockdown cells (compared to the control cells) was calculated.

3. Results

3.1. P300 can directly interact with iASPP and p73 in cisplatin-treated cells.

It is well known that iASPP represents a crucial inhibitor of p53-dependent apoptosis induction as it directly binds to p53 and blocks its transcriptional regulation of pro-apoptotic target genes (Bergamaschi, Samuels et al. 2006). The currently prevalent view is, that iASPP is also capable of forming complexes with the p53-family member TAp73 and with the histone acetyltransferase p300, although functional consequences of both interactions remain elusive (Robinson, Lu et al. 2008). Therefore, we wanted to find out, which impact endogenous expression of iASPP will have on p300 and TAp73 function.

The functional interaction of TAp73 and p300 in cisplatin-mediated apoptosis has been intensively investigated before, especially in the adenocoloncarcinoma cell line HCT116 (Mantovani, Piazza et al. 2004; Levy, Adamovich et al. 2008). Due to the fact that this cell line expresses relatively high amounts of endogenous TAp73 and p300, we decided to use HCT116 cells for our analysis. Moreover, an isogenic p53 knockout cell line of HCT116 was investigated (HCT-/-p53 cells), which offered the possibility to confirm our findings to be independent from the expression of p53. Of note, we analysed the expression levels of TAp73 and ΔNp73 isoforms in HCT116 cells by using isoform-specific primers and real-time PCR. As we could not detect any expression of ΔNp73, we can state that our results are TAp73-specific.

We started to validate the interaction of iASPP with p300 and TAp73 in untreated as well as cisplatin-treated HCT116 cells. Under normal growing conditions of tumourigenic cells, we failed to detect any direct interaction of iASPP with p300 or TAp73 (Figure 3.1A). However, we could clearly validate the presence of iASPP-p300 as well as p300-TAp73 protein complexes in cisplatin-treated cells (Figure 3.1B). Of note, in both tested conditions, we could not detect an interaction between iASPP and TAp73, which might have been due to sub-optimal co-immunoprecipitation conditions though.

As we could show that p300 and iASPP form a protein complex with each other in cisplatin-treated HCT116 cells, we were interested in the functional consequences of iASPP depletion on p300 expression levels. Therefore, we generated stable iASPP knockdown cells by using two different shRNAs against iASPP. To exclude any off-target effects due to lentivirus-mediated knockdown or due to the selection of the transduced cells with the antibiotic puromycin, we generated a control knockdown cell line in parallel. For control knockdown,

shRNA targeting the luciferase gene was utilized. Following, lentiviral transduced cells were cultured under the same conditions.

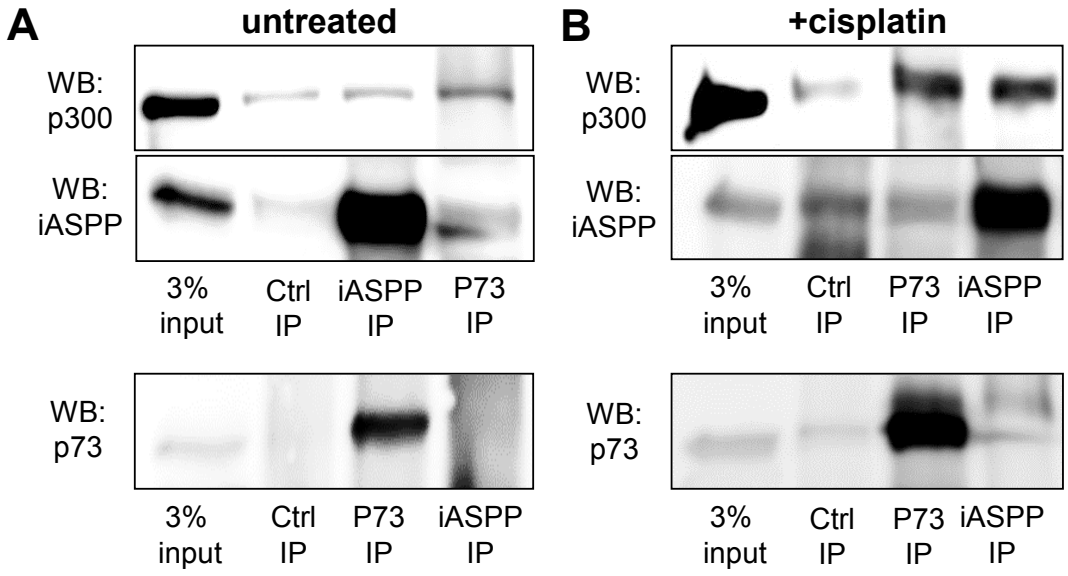

Figure 3.1. P300 directly interacts with TAp73 and iASPP in cisplatin-treated HCT116 cells.
For co-immunoprecipitation experiments, total cell lysates were prepared from untreated (A.) and cisplatin-treated (20 µM, 16 h) (B.) HCT116 cells. Immunoprecipitation was performed using an iASPP- or p73-specific antibody. As control, an independent immunoprecipitation reaction was performed using a ß-galactosidase antibody. After extensive washing, precipitated were extracted from the beads, and co-bound p300, p73 or iASPP was detected by immunoblotting. (Ctrl = control)

3.2. IASPP expression augments the protein levels of p300 and TAp73 after cisplatin treatment.

After establishment of HCT116 and HCT-/-p53 cells with stable iASPP knockdown, protein levels of p300 and its closely related homologue CBP were detected in total cell lysates from untreated as well as cisplatin-treated cells. CBP staining was included, as it was shown before, that p300 and CBP exert overlapping functions in various cellular responses. Thus, p300 and CBP could be similarly affected by iASPP depletion.

Interestingly, as untreated cells remain unaffected, cisplatin-treated iASPP knockdown cells displayed reduced protein levels of p300 (Figure 3.2A). Moreover, we obtained similar results from cisplatin-treated HCT-/-p53 cells, thereby excluding any influence of p53 on the observed effects (Figure 3.2B). Of note, protein levels of CBP were also decreased, although we could detect this effect in cisplatin-treated and untreated, iASPP-depleted HCT116 cells (Figure 3.2A). Furthermore, analysis of the mRNA levels of p300 and CBP in iASPP-depleted

cells confirmed that the decreased protein amounts of p300 and CBP derived from changes on protein level rather than from changes on mRNA level (Figure 3.2C).

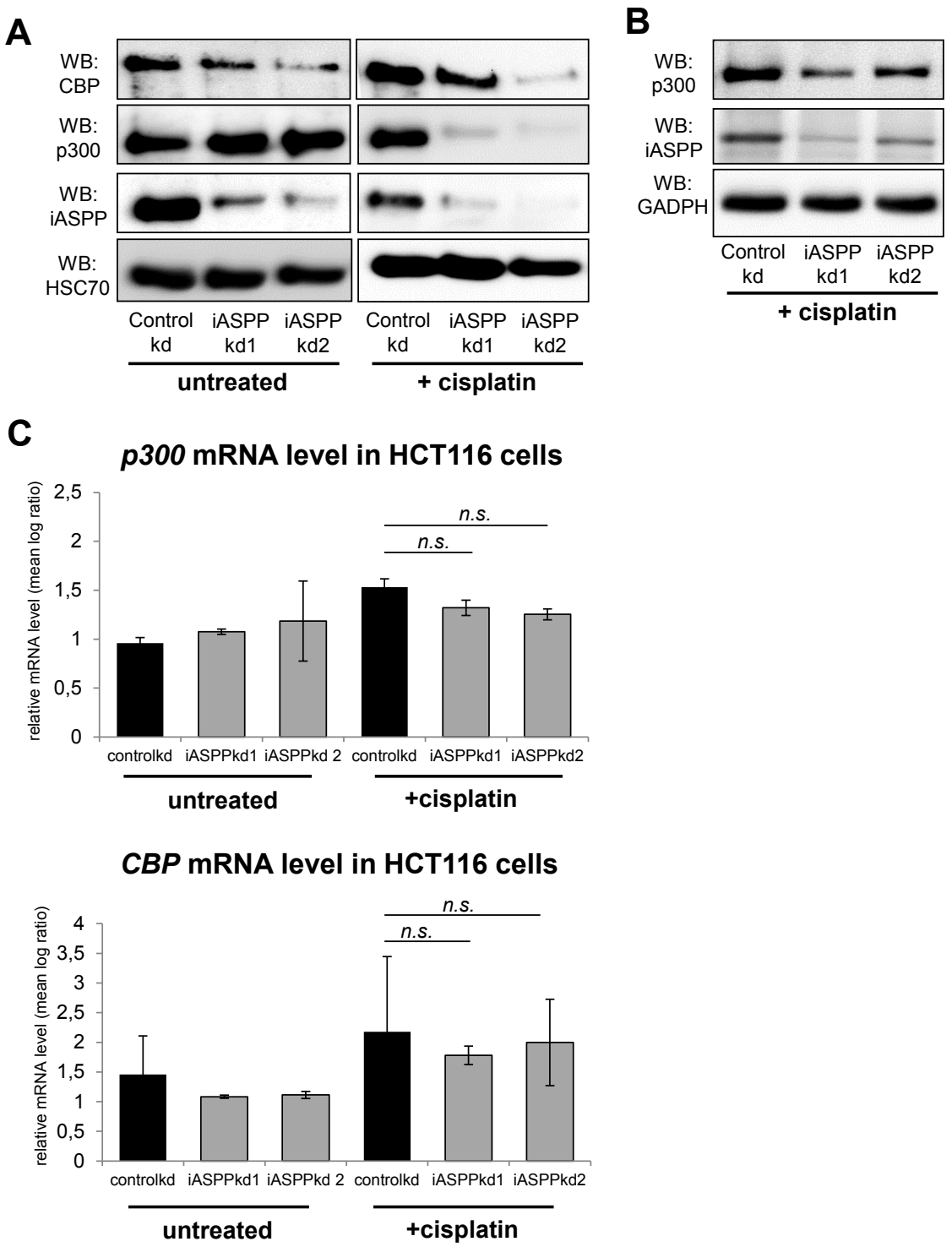

Figure 3.2. iASPP depletion leads to a decrease in p300 and CBP protein levels.
Stable iASPP knockdowns of HCT116 and HCT-/-p53 cells were generated using 2 independent shRNA constructs against iASPP. To exclude off target effects, control cells were stable transduced with shRNA against luciferase. (kd = knockdown).

A. iASPP depletion leads to a decrease in p300 and CBP protein level in cisplatin-treated HCT116 cells. *Cells were treated for 24 h with 20 µM cisplatin prior to preparation of total cell lysates. P300 and iASPP levels were detected by immunoblotting. HSC70 staining served as loading control.*
B. Decrease of p300 protein level in iASPP knockdown cells is independent of the presence of p53. *P300 protein level were analysed in cisplatin-treated, knockdown HCT-/-p53 cells. Cells were treated for 24 h with 20 µM cisplatin prior to preparation of protein lysates. P300 and iASPP level were detected by immunoblotting. GAPDH staining served as the loading control.*
C. iASPP knockdown does not affect the mRNA levels of p300 and CBP. *Total RNA was extracted from HCT116 knockdown cells. For cisplatin treatment, cells were incubated with 20 µM cisplatin for 12 h. Ct values were normalized to the reference gene HPRT1. To calculate the relative mRNA level (mean log ratio), untreated control knockdown cells were set to 1. (n.s. = not significant)*

3.3. iASPP regulates the protein stability of p300 and TAp73.

Concluding, we hypothesized that iASPP depletion seemed to reduce the protein stability of p300 and CBP. To validate our hypothesis, we performed a cycloheximide pulse chase experiment in cisplatin-treated HCT116 cells (Figure 3.3A). Cycloheximide inhibits protein de-novo synthesis, thereby displaying a tool for the analysis of protein turn over. Actually, we could observe a faster degradation of p300 in cisplatin-treated, iASPP knockdown cells compared to control knockdowns. Therefore, we conclude that iASPP enhances the protein stability of p300 in cisplatin-treated cells.

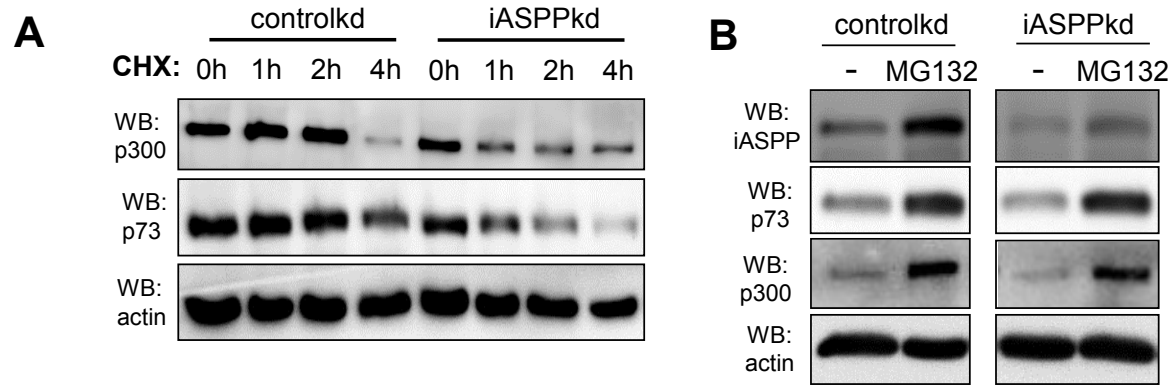

Figure 3.3. IASPP depletion decreases the protein stability of p300 and TAp73 in cisplatin-treated cells.
HCT116 knockdown cells were treated with 20µM cisplatin, prior to preparation of total cell lysates. Protein levels were detected by immunoblotting. Actin staining controlled equal loading of the samples. (CHX = cycloheximide, MG132 = proteasome inhibitor, kd = knockdown)
A. Cycloheximide pulse chase reveals faster degradation of p300 and TAp73 in iASPP knockdown cells. *HCT116 cells were treated for 20 h with 20 µM cisplatin followed by*

incubation with 100 µg/mL cycloheximide (CHX) for 1 h, 2 h or 4 h. As a control the 0 h sample was treated with the CHX solvent Ethanol.
B. Low protein levels of p300 and TAp73 can be rescued by treatment with the proteasome inhibitor MG132. *Cells were treated for 20 h with cisplatin followed by 4 h of treatment with 20 µM MG132 or DMSO as control.*

As it is well known that p300 can acetylate TAp73 after exposure of cells to cisplatin, which in turn enhances the protein stability of TAp73 (Costanzo, Merlo et al. 2002; Mantovani, Piazza et al. 2004), we included TAp73 staining of cycloheximide-treated samples. Similar to the effects of iASPP depletion on p300 protein stability, iASPP knockdown resulted in a faster degradation of TAp73 in cisplatin-treated cells (Figure 3.3A). However, we could not detect a direct interaction of iASPP and TAp73 in untreated or cisplatin-treated HCT116 cells. Hence, we suggest that the diminished stability of TAp73 protein results from the decreased protein levels of p300 and CBP.

Apart from proteasomal degradation processes, proteins can be degraded by alternative pathways. To prove the influence of iASPP on the proteasomal degradation process of p300 and TAp73, we investigated the level of both proteins in cells that were treated with the proteasome inhibitor MG132 (Figure 3.3B). Actually, MG132 treatment re-established the protein levels of p300 and TAp73 in cisplatin-treated iASPP knockdown cells. Concluding, iASPP expression is likely to inhibit the proteasomal degradation process of p300, TAp73, and probably also CBP after treatment of the cells with cisplatin.

3.4. iASPP depletion affects the chromatin localization of p300 and TAp73.

Next, we were interested in further consequences of iASPP depletion on p300 function. As p300 is mainly involved in the acetylation of histones, we performed chromatin fractionation as well as chromatin immunoprecipitation (ChIP) of p300 in HCT116 cells. In fact, less p300 protein localized to the chromatin fraction in cisplatin-treated, iASPP knockdown cells (Figure 3.4A). Consequently, ChIP experiments using a p300-specific antibody revealed diminished binding of p300 to known p300 target sites (e.g. *puma* and *pig3* promoter), again in cisplatin-treated HCT116 cells (Figure 3.4B).

As we detected reduced protein stability of TAp73 in iASPP-depleted cells as well (Figure 3.3A), we were also interested in functional consequences on TAp73 as a downstream target of p300. We hypothesized that the impaired chromatin localization of p300 in cisplatin-treated, iASPP-depleted cells should also affect the localization and DNA-binding affinities of TAp73. Indeed, chromatin fractionation of cisplatin-treated, iASPP-depleted HCT116 cells

proved a diminished recruitment of TAp73 protein to the chromatin (Figure 3.4C). Moreover, ChIP experiments using a TAp73-specific antibody validated a strong reduction of TAp73 binding to its target gene promoters in cisplatin-treated, iASPP-depleted cells (Figure 3.4D).

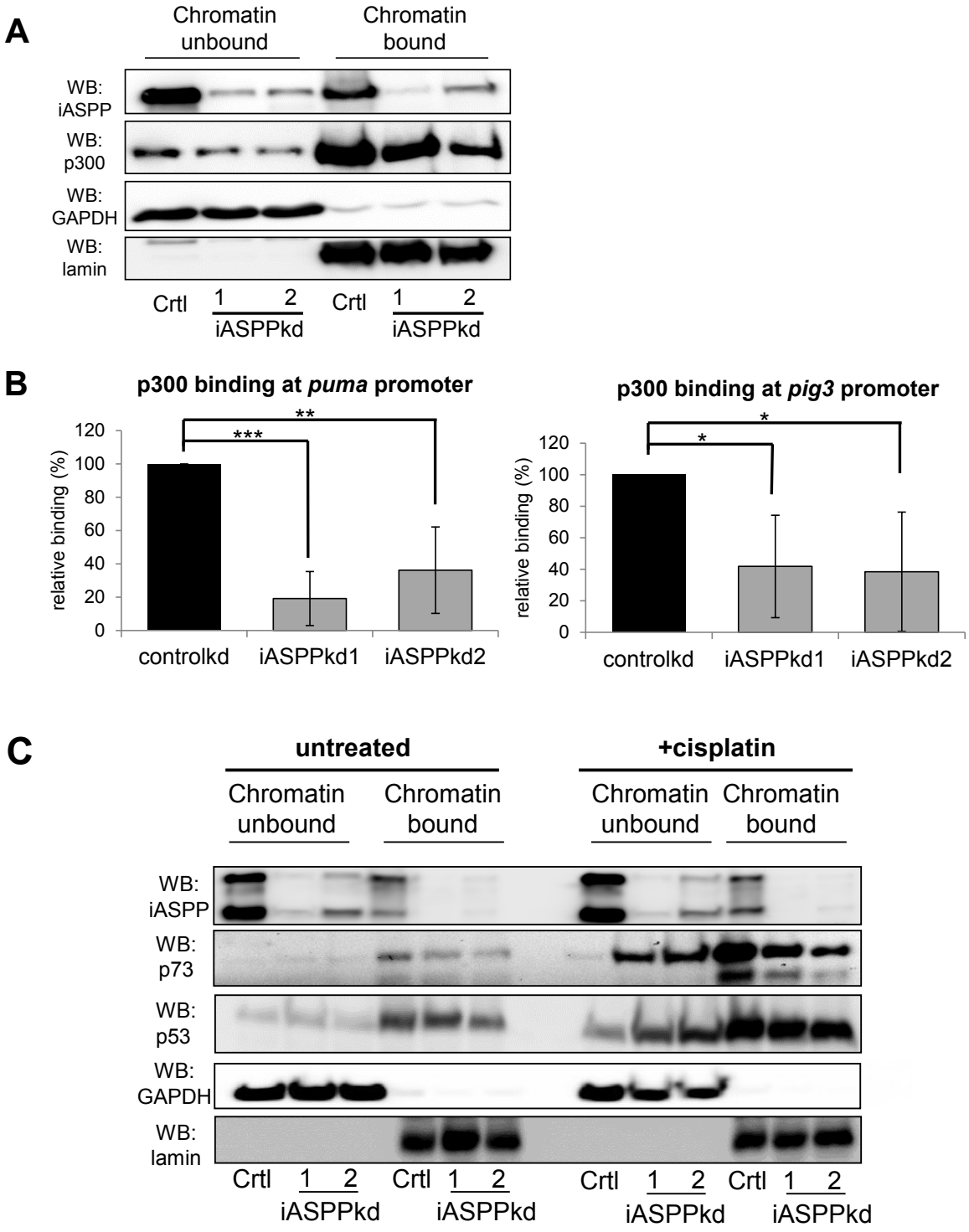

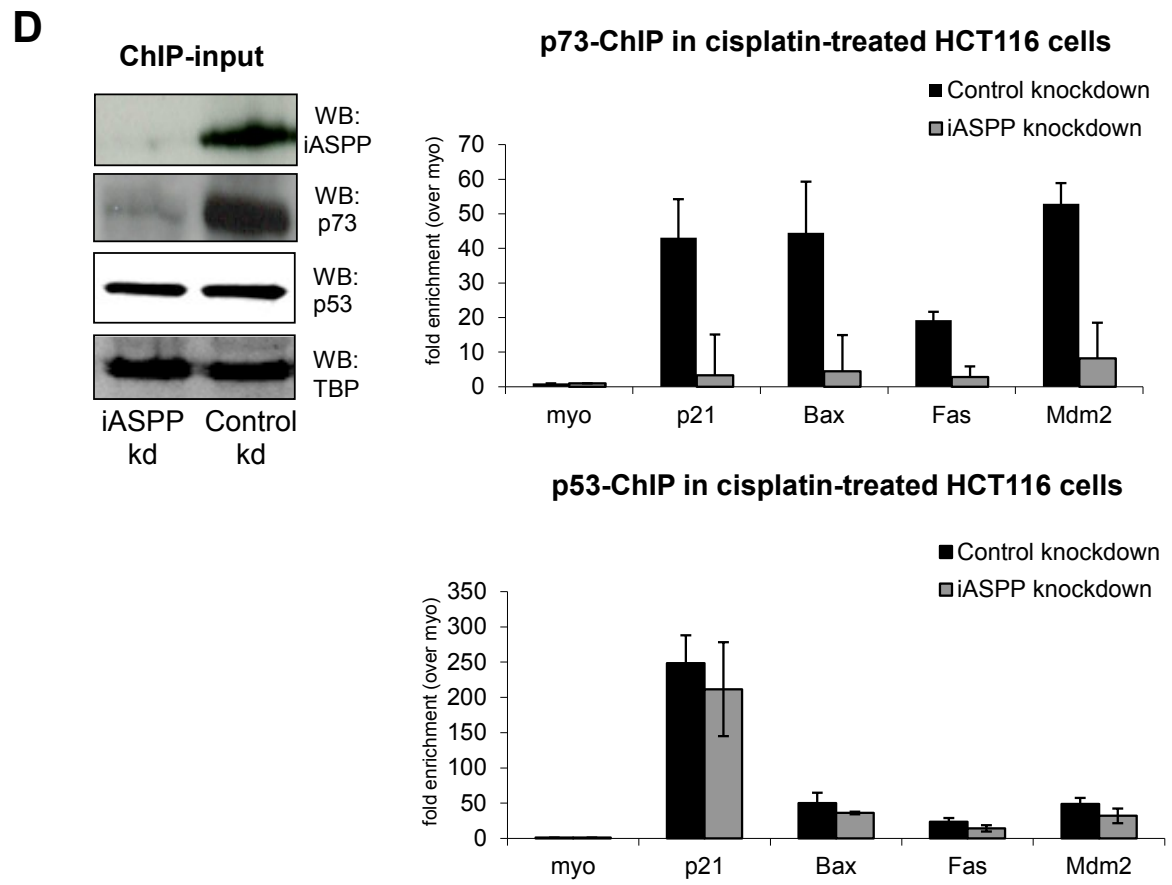

Figure 3.4. iASPP modulates the DNA-binding affinities of p300 and TAp73 in cisplatin-treated HCT116 cells.

A. Lower amounts of p300 protein localizes to the chromatin fraction. *Cells were treated for 16 h with cisplatin prior to chromatin fractionation of cells (separation of cells into triton-soluble and triton-insoluble fractions). GAPDH staining served as control for unbound chromatin, lamin B1 staining controls the purity of the chromatin fraction.*

B. Diminished localization of p300 to genomic target sites in iASPP-depleted HCT116 cells. *For analysis of p300 level, that are bound to genomic target sites (puma, pig3), cells were treated for 8 h with cisplatin prior to chromatin preparation. Following, chromatin immunoprecipitation was performed using an IgG- or p300-specific antibody. To reveal the % of bound p300 protein on single target sites, real-time PCR was performed using specific primers. The relative binding was calculated by setting the fold enrichment (of p300 over IgG) to 100% in control knockdown cells. The significance was calculated by using the student`s t-test.*

C. In iASPP-depleted cells, less TAp73 is recruited to the chromatin fraction. *Cells were left untreated or incubated for 16 h with 20 μM cisplatin prior to separation of the cells in triton-soluble and triton-insoluble fractions. Similar controls were used as described under A.*

D. IASPP knockdown results in diminished DNA-binding of TAp73 while p53 remains unaffected. *HCT116 control and iASPP knockdown cells were treated for 24 h with 10 μM cisplatin prior to chromatin harvest. Chromatin immunoprecipitation was performed using a p73- or p53-specific antibody. For both ChIPs, the same primer pairs were utilized in real-*

time PCR analysis. Myo primers detect a region in the heterochromatin thereby serving as an internal negative control. To visualize protein levels in ChIP inputs, a fraction of chromatin was denatured with Laemmli buffer, boiled and analysed by immunoblotting. TBP staining served as loading control.

Besides TAp73, p300 is also known to elevate the DNA-binding properties of p53 as well. Therefore, we included p53 in our analysis. Interestingly, we did not observe diminished recruitment of p53 to the chromatin in iASPP-depleted HCT116 cells, as seen for TAp73 (Figure 3.4C). In line, we also failed to detect a similar loss of p53 binding to common p53 and p73 target sites in ChIP experiments using a p53-specific antibody (Figure 3.4D).

Therefore we state, that iASPP depletion mainly affects the function of p300 and CBP. Following, the consequences of diminished protein levels of p300 (and CBP) on TAp73 or p53 function might then be dependent on the cellular context and treatment of the cells. In HCT116 cells though, TAp73 seems to be mainly affected by the diminished p300 protein level after iASPP knockdown

3.5. iASPP depletion leads to an overlapping loss of p300 and TAp73 to promoters of pro-apoptotic TAp73 target genes.

Next, additional p73- and p300-ChIPs were repeated in parallel using the same chromatin batches of cisplatin-treated HCT116 knockdown cells. As shown for the *puma* promoter (Figure 3.5), as well as for the *fas* and *p21* gene locus (Appendix Sup-1), we could validate an overlapping loss of p300- and p73-binding to specific p73 target gene promoters.

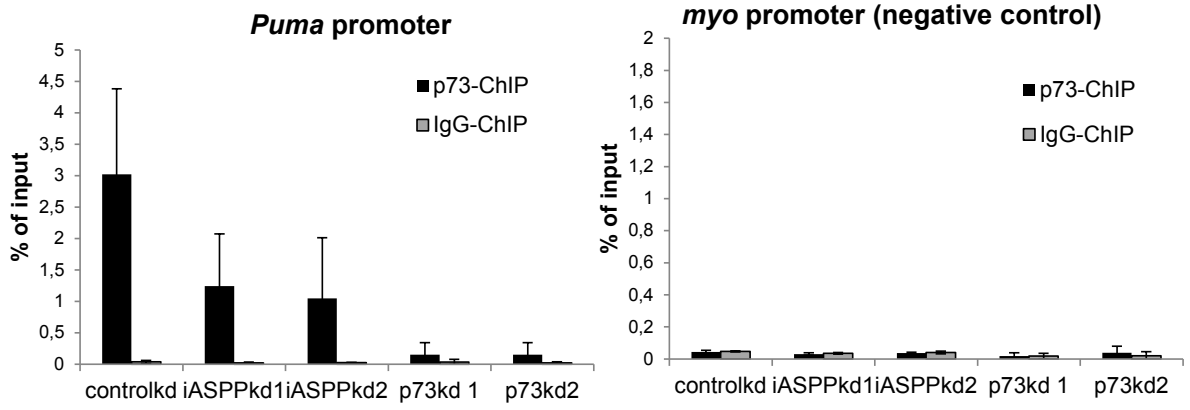

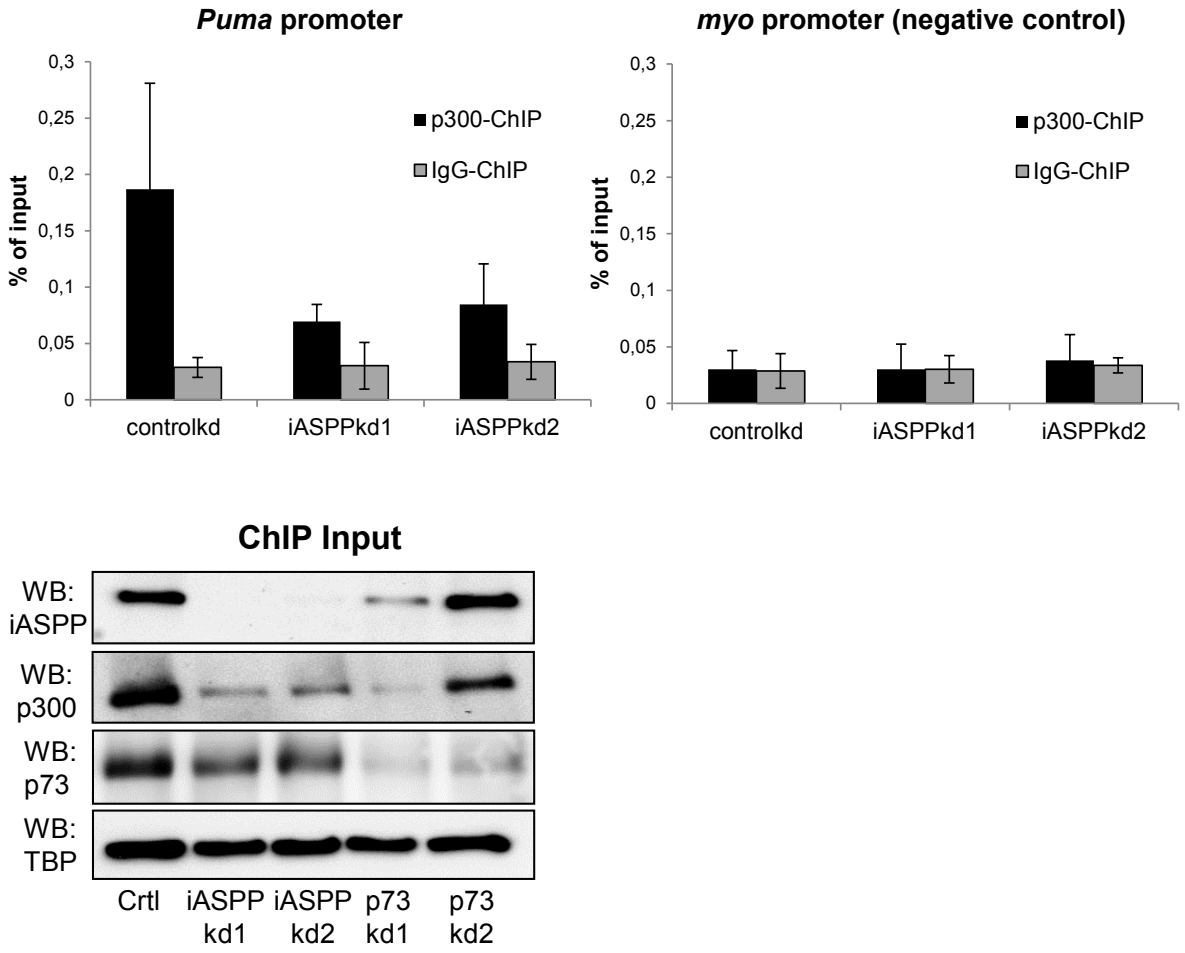

Figure 3.5. After cisplatin treatment, iASPP depletion leads to an overlapping loss of p300 and p73 binding to promoters of p73 target genes.
For chromatin immunoprecipitation HCT116 knockdown cells were treated for 8 h with 20 μM cisplatin prior to chromatin harvest. ChIP input derived from an aliquot of chromatin that was denatured with Laemmli buffer, boiled and analysed by immunoblotting. TBP staining served as a loading control. Chromatin immunoprecipitations (ChIP) were performed using a p73- as well as p300-specific antibody. For control, an IgG reaction was performed in parallel. The data is represented as the % of input sample of the respective target site. Puma is presented as an example of a co-bound promoter region of p73 and p300. The promoter region of myoglobulin (myo) served as an internal negative control to exclude any unspecific binding of the antibodies to DNA.

3.6. IASPP depletion counteracts the accumulation of pro-apoptotic p73 target genes in DNA-damaged cells.

TAp73 constitutes a transcription factor that is known to induce the gene expression of pro-apoptotic target genes after cisplatin treatment (Irwin, Kondo et al. 2003; Strano, Monti et al. 2005). Thus, we were interested in the functional consequences of iASPP depletion on the expression of p73 target genes. We analysed the gene expression of a panel of known p73

target genes in iASPP-depleted HCT116 and HCT-/-p53 cells. As shown by the analysis of the mRNA levels of *puma* and *pig3,* pro-apoptotic target genes were significantly less induced in DNA-damaged, iASPP-depleted HCT116 cells compared to control knockdown cells (Figure 3.6A and Appendix Sup-2A). These effects were reproducible in HCT-/-p53 cells, thereby confirming that the observed effects were independently of the presence of p53 (Figure 3.6B). Moreover, we could confirm the role of TAp73 in the transcriptional up-regulation of the analysed target genes analysis, by gene expression studies of TAp73 knockdown cells (Appendix Sup-2B).

Furthermore, we investigated the total protein levels of the p73 targets puma and p21. Immunoblot detection of both proteins revealed that a diminished induction of p73 target genes also resulted in an impaired accumulation of these effector proteins in cisplatin-treated iASPP and TAp73 knockdown cells (Figure 3.6C).

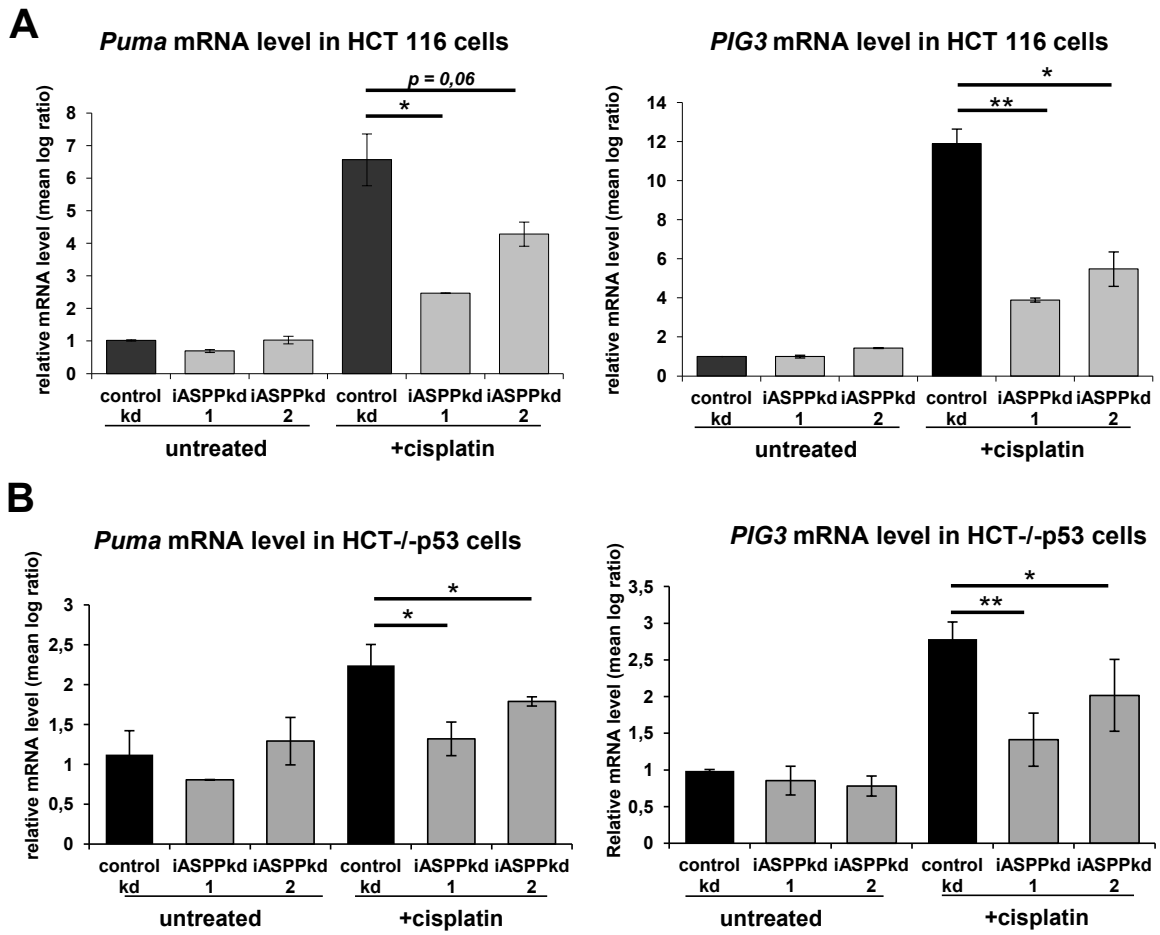

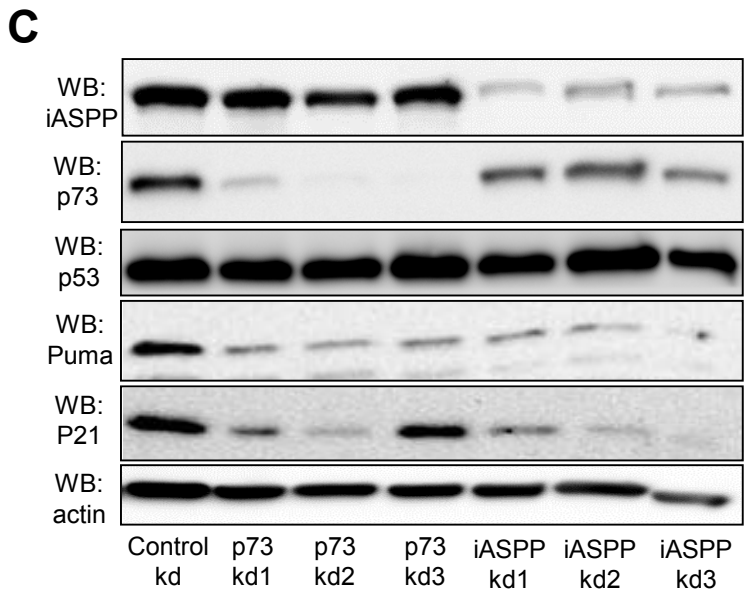

Figure 3.6. iASPP knockdown leads to a decreased induction of pro-apoptotic p73 target genes in cisplatin-treated cells.
For RNA extraction, cells were treated for 8 h (pig3) or 12 h (puma) with 20 µM cisplatin. For immunoblotting, 24 h of treatment with 20 µM cisplatin was applied. Significance was calculated using student`s t-test.
A.+B. Relative gene expression of puma and pig3 in stable iASPP and control knockdown cells. A. *Analysis of untreated and cisplatin-treated HCT116 cells.* ***B.*** *Analysis of untreated and cisplatin-treated HCT-/-p53 cells.*
C. iASPP or p73 depletion leads to diminished puma and p21 protein level in cisplatin-treated cells. *Total cell lysates of HCT116 knockdown cells were immunoblotted. Actin staining controlled equal loading of the samples.*

As we were only able to detect any effects of iASPP knockdown after treatment of the cells with cisplatin, we were interested if cisplatin treatment is a pre-requisite for the observed effects. Therefore we repeated gene expression analysis of the same pro-apoptotic target genes in Etoposide-treated HCT116 knockdown cells (Appendix Sup-3A). Etoposide is a topoisomerase II inhibitor that is known to activate the p53-family and therefore triggering p53-family dependent apoptosis induction (Irwin, Kondo et al. 2003; Codelia, Cisterna et al. 2010). Indeed, Etoposide treatment of iASPP knockdown and TAp73 knockdown HCT116 cells resulted in a similar impaired induction of pro-apoptotic p73 target genes as shown for cisplatin treatment before. Concluding, as cisplatin and Etoposide treatment resulted in the same diminished induction of p73 target genes in iASPP-depleted cells, we suggest that the observed effects are dependent on the activation of DNA damaging pathways rather than being specific for cisplatin treatment.

3.7. iASPP depletion counteracts p300- and p73-mediated apoptosis.

Subsequently, we wanted to investigate which consequences iASPP knockdown and following diminished induction of p73 target genes would have on apoptosis induction. It have been revealed that *puma* among other pro-apoptotic p73 target genes plays a crucial role in the induction of apoptosis after cisplatin treatment (Melino, Bernassola et al. 2004). Therefore, we studied the effects of iASPP depletion on the level of apoptosis induction after cisplatin (Figure 3.7) or Etoposide (Appendix Sup-3B) treatment.

Detection of cleaved caspase 3 fragments using a specific cleaved caspase 3 antibody represents a reliable marker for the level of apoptosis induction (Fernandes-Alnemri, Litwack et al. 1994; Nicholson, Ali et al. 1995). Therefore we investigated the level of cleaved caspase 3 in cisplatin-treated HCT116 knockdown cells (Figure 3.7A). As expected, cisplatin-treated, iASPP knockdown HCT116 cells displayed lower levels of cleaved caspase 3 than control knockdown cells. In parallel, we performed transient knockdown of p300 and CBP to validate the pro-apoptotic role of both proteins in cisplatin treatment-induced apoptosis in HCT116 cells. Interestingly, transient knockdown of p300 (but not of CBP) resulted in a similar reduction of cleaved caspase 3 levels compared to control knockdown cells, thereby confirming the crucial pro-apoptotic role of p300 in cisplatin-mediated apoptosis induction.

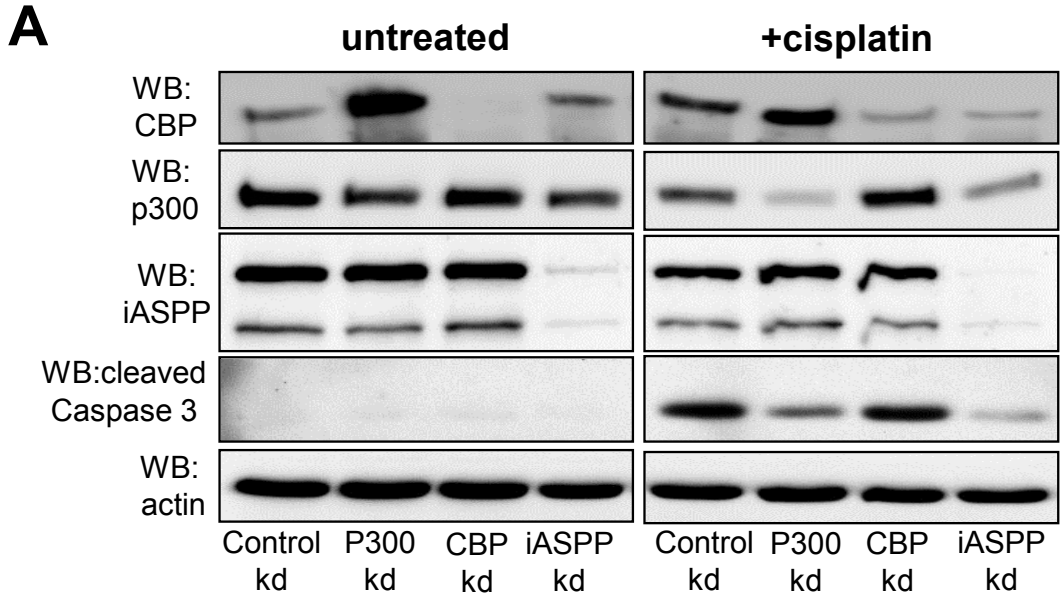

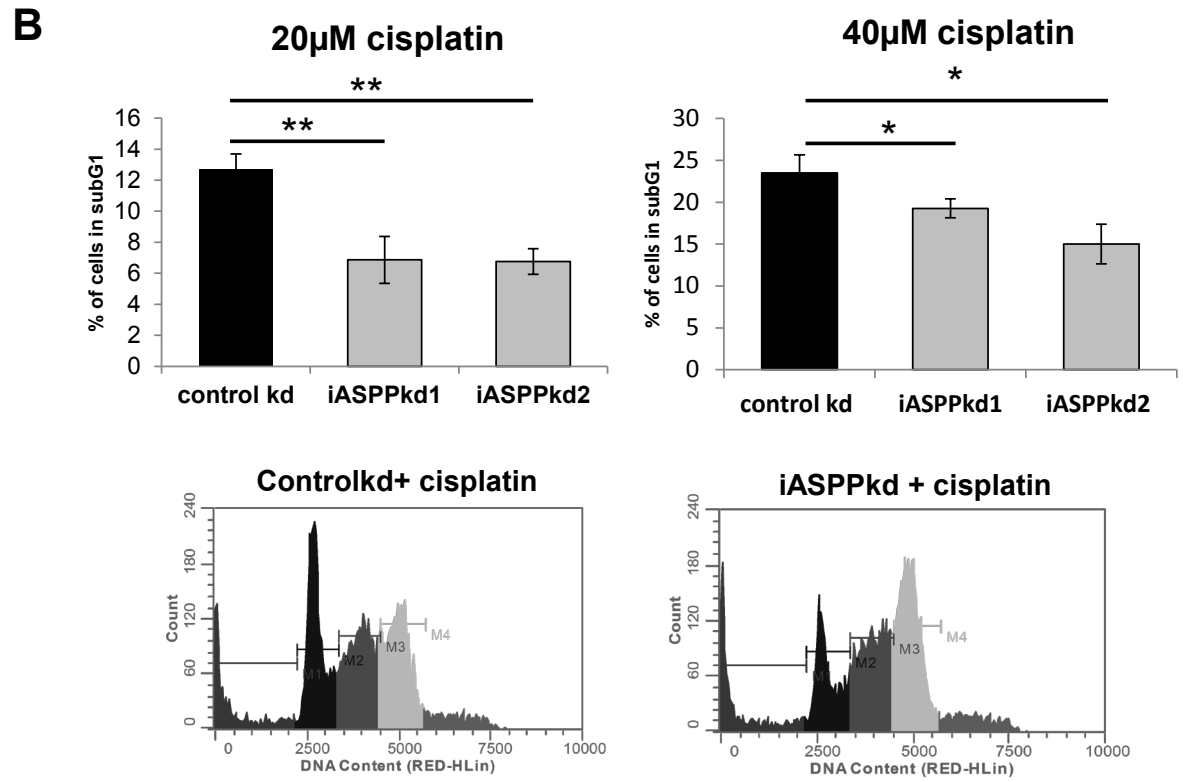

Figure 3.7. iASPP knockdown in HCT116 cells leads to diminished apoptosis induction after cisplatin treatment.

A. Lower levels of cleaved caspase 3 accumulate in cisplatin-treated iASPP and p300 knockdown cells. *P300 and CBP were transiently knocked down in control knockdown cells using siRNA. As control, stable, shRNA-transduced control and iASPP knockdown cells were transfected with scrambled siRNA. 48 h post-transfection, cells were treated with 40 µM cisplatin for 24 h prior to protein harvest. Knockdown efficiency was validated by immunoblotting. As a marker for apoptosis induction, cleaved caspase 3 levels were detected using a specific antibody.*

B. Cell cycle profiles of cisplatin-treated iASPP knockdown cells reveal a lower portion of cells in subG1 phase. *Control and iASPP knockdowns were treated for 24 h with 20 µM or 40 µM cisplatin. Cells were harvested, fixed with Ethanol and stained with propidium iodide. Cell cycle profiles were generated by FACS analysis. Same gate settings were applied for all samples. As an example of the analysed cell cycle profiles, one example for cisplatin-treated control knockdown cells and one example for cisplatin-treated, iASPP knockdown cells are shown. The significance of the FACS analysis was calculated using the student`s t-test.*

In addition, we performed cell cycle analysis of HCT116 cells by applying propidium iodide staining of previously fixed cells. As apoptotic cells display DNA fragmentation, quantification of the number of cells in subG1 phase can be used as an indicator for the percentage of dead cells in a cell population (Tounekti, Belehradek et al. 1995). Quantification of the subG1 phase in cisplatin-treated HCT116 knockdown cells, revealed significant lower levels of

apoptosis in iASPP-depleted cells compared to control knockdowns (Figure 3.7B). Moreover we could confirm a similar, pro-apoptotic role for iASPP after Etoposide treatment by similar FACS analysis of HCT116 knockdown cells (Appendix Sup-3B).

3.8. iASPP regulates the protein levels of p300 in mouse embryonic fibroblasts.

To generalize our findings, we tested the effects of iASPP depletion in several cell lines including non-tumourigenic mouse embryo fibroblasts (MEFs). Indeed stable knockdown of iASPP in wild-type MEF cells led to a reduction of p300 protein levels (Figure 3.8A). Interestingly, we could observe this effect in untreated as well as cisplatin-treated cells, thereby indicating that primary cells might display a slight different mechanism of iASPP-mediated regulation of p300 levels.

Moreover, we analysed the mRNA levels of p300 in iASPP-depleted MEF cells (Figure 3.8B). Actually, gene expression analysis of p300 revealed, that the decreased p300 protein levels in untreated MEF cells seemed to partially result from a transcriptional repression of p300. In cisplatin-treated MEF cells though, we could not detect any transcriptional changes in the gene expression of p300. Thus, we suggest that iASPP regulates the protein stability of p300 in cisplatin-treated MEF cells, similar to the findings we obtained for HCT116 cells.

Furthermore, we analysed the expression of pro-apoptotic target genes in iASPP-depleted MEF cells to validate a pro-apoptotic role of iASPP and subsequently also p300 in primary cells (Figure 3.8C). However, we failed to detect any significant changes in the expression of several pro-apoptotic genes (like *Puma* and *Noxa*) due to iASPP depletion. Therefore, iASPP does not seem to contribute to cisplatin-mediated apoptosis induction in MEF cells.

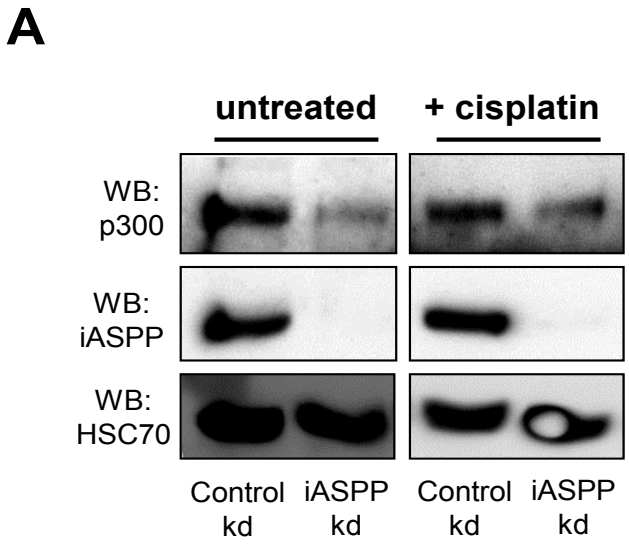

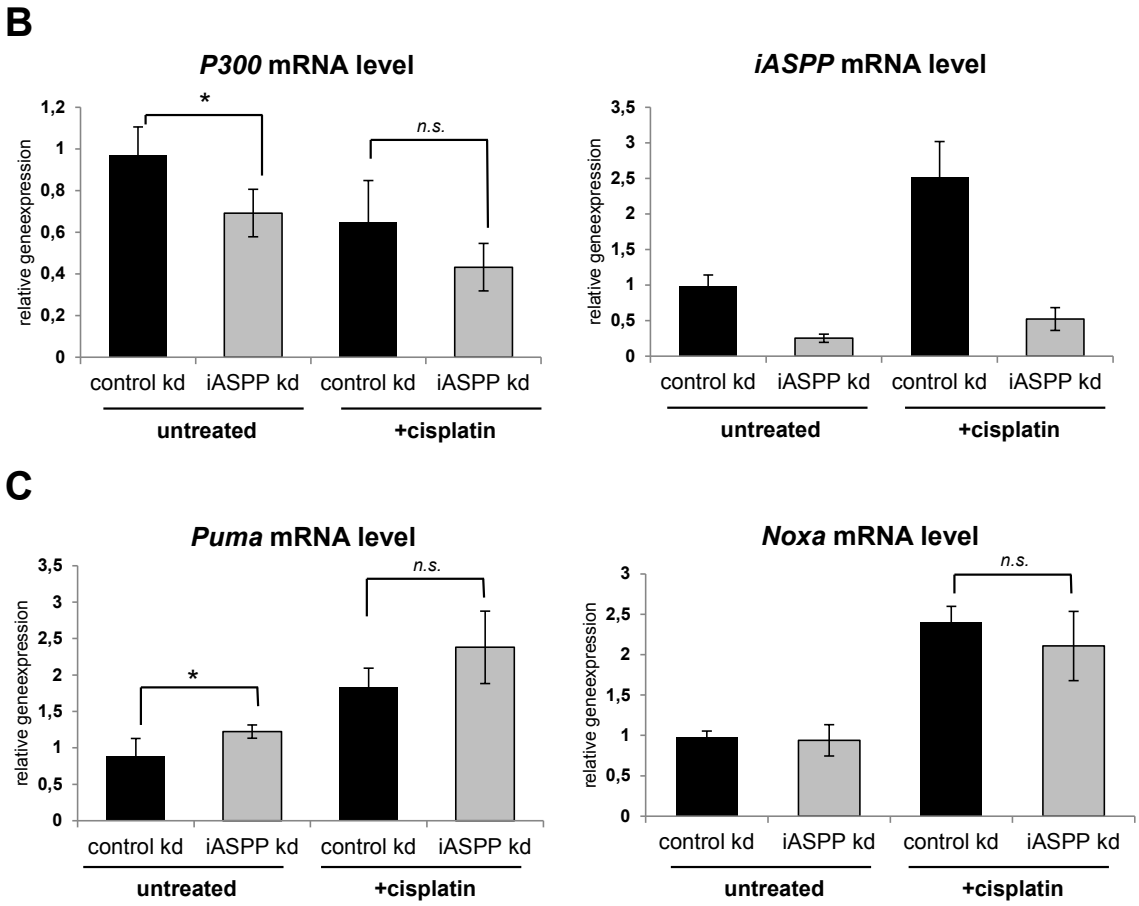

Figure 3.8. iASPP depletion in mouse embryonic fibroblasts results in reduced p300 levels.

Mouse embryonic fibroblasts (MEF) were transduced with shRNA against iASPP. For control cells, MEFs were transduced in parallel with shRNA against luciferase. Four days after transduction cells were treated with 20 µM cisplatin. Significance was calculated using the student`s t-test.

A. P300 levels decrease in iASPP-depleted MEFs. *For immunoblotting, MEF cells were treated for 12 h with 20 µM cisplatin prior to cell lysate preparation. P300 protein levels were detected by immunoblotting. Knockdown efficiency was controlled by staining for iASPP. HSC70 staining served as loading control.*

B. P300 mRNA levels are repressed in untreated, iASPP-depleted cells. *MEF cells were treated for 8 h with 20 µM cisplatin prior to RNA extraction. Relative gene expression was analysed by real-time PCR. Ct values were normalized to HPRT1. Depicted is the mean log ratio as the relative gene expression (untreated control knockdown cells are set to 1).*

C. iASPP depletion does not alter the transcription of pro-apoptotic target genes. *To monitor any changes in the expression of pro-apoptotic genes, Puma and Noxa mRNA levels were analysed in control and iASPP knockdown cells. (n.s. = not significant)*

This might be caused by differential protein expression patterns of MEF cells compared to HCT116 cells, or iASPP function might not be conserved between mouse and human.

Nevertheless, iASPP is likely to regulate the protein levels of p300 in cisplatin-treated primary cells.

3.9. P300 levels are regulated by iASPP in cisplatin-treated melanoma cell lines.

Apart from analysis of MEF cells, we investigated the effects of transient iASPP knockdown in 4 different tumourigenic melanoma cell lines (Figure 3.9A). In fact, all cell lines displayed a similar reduction of p300 protein levels in iASPP-depleted, cisplatin-treated cells compared to control knockdowns.

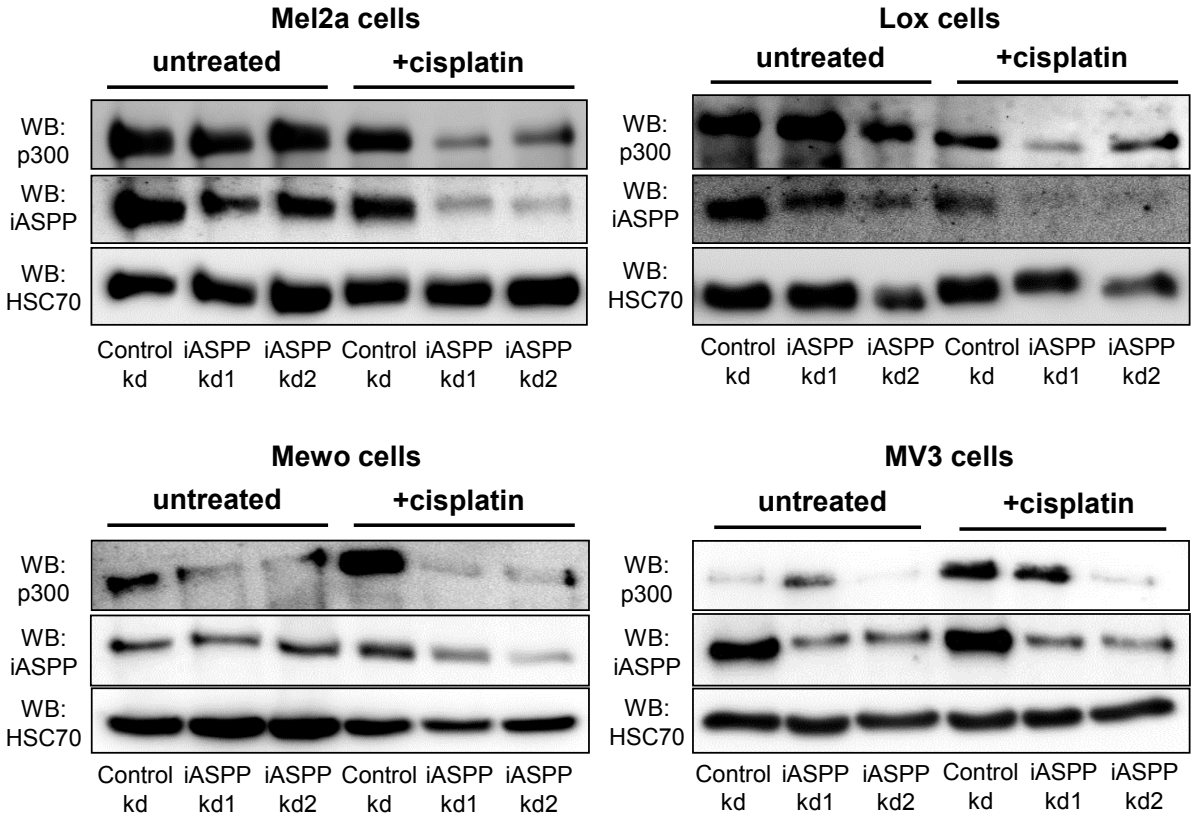

Figure 3.9. Melanoma cell lines show a decrease in p300 levels in cisplatin-treated, iASPP knockdown cells.
IASPP was transiently depleted in 4 different melanoma cell lines (Mel2a, Mewo, Lox and MV3 cells) using 2 different siRNA and a scrambled siRNA as control. 48 h after transfection, cells were treated for 24 h with 20 μM cisplatin. Total cell lysates were prepared and immunoblotted. HSC70 staining served as a loading control.

Probably due to a long half-life of iASPP protein, siRNA-mediated, transient knockdown of iASPP was difficult to apply in untreated cells. Thus, iASPP protein levels did not significantly decreased in untreated, iASPP knockdown cells (Figure 3.9). However, we also failed to

detect any effects on p300 protein levels in untreated iASPP knockdown cells. We cannot exclude though, that iASPP knockdown affects p300 levels in untreated cells as well, due to this problems with siRNA-mediated knockdown of iASPP. We will have to repeat this experiment using stable shRNA-mediated iASPP knockdowns of melanoma cell lines.

In summary, iASPP depletion affected p300 protein levels in cisplatin-treated melanoma cell lines as well. Therefore, iASPP represents a common regulator for p300 protein stability in several tumourigenic cell lines.

3.10. BRMS1 is required for p300 degradation in HCT116 cells.

As we already proved, that iASPP depletion leads to an accelerated proteasomal degradation of p300 in HCT116 cells (Figure 3.3A and Figure 3.3B), we were interested in the responsible E3 ubiquitin ligase mediating this effects. Up to now, little is known about p300- and CBP-specific ubiquitin ligases. Recently Liu and colleagues discovered that the breast metastasis suppressor 1 (BRMS1) protein can poly-ubiquitinate and therefore degrade p300 in lung cancer cell lines (Liu, Mayo et al. 2013). Therefore, we decided to test if BRMS1 is also involved in the proteasomal degradation of p300 and CBP in untreated as well as cisplatin-treated HCT116 cells. BRMS1 was transiently knocked down using two different siRNA against BRSM1 and a scrambled siRNA for generation of control knockdown cells (Figure 3.10). Indeed knockdown of BRMS1 resulted in an accumulation of p300 and CBP protein in untreated and cisplatin-treated HCT116 cells (Figure 3.10A).

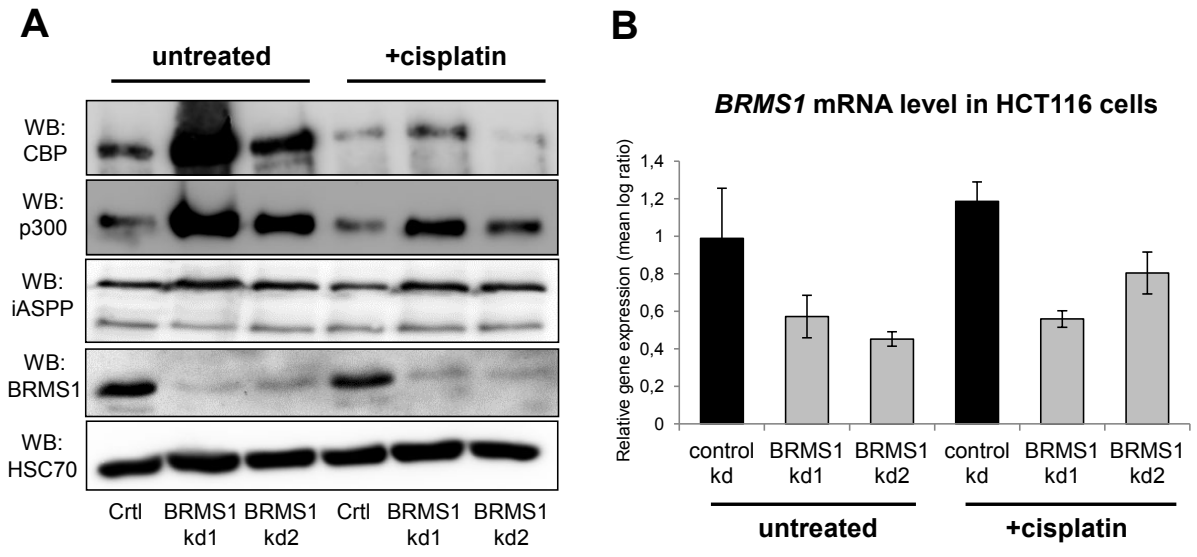

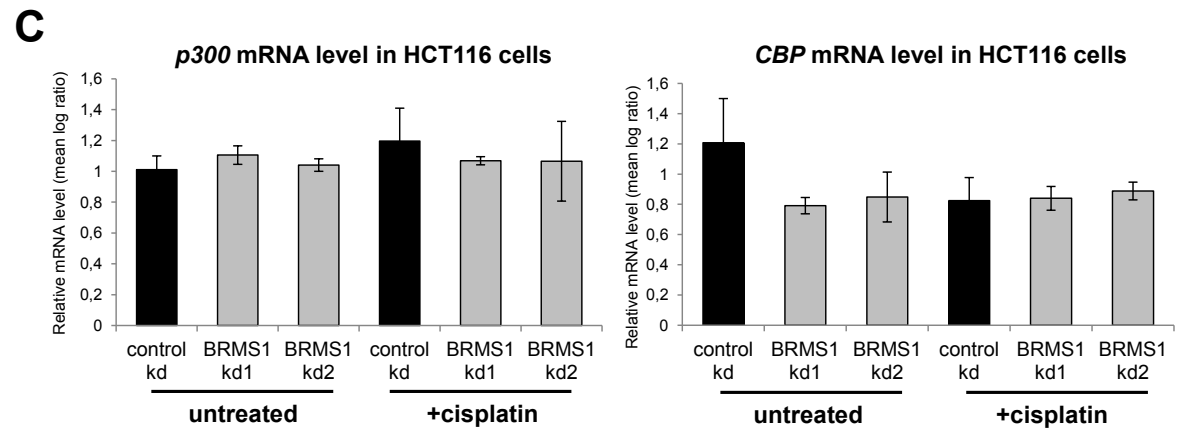

Figure 3.10. BRMS1 regulates the protein levels of p300 and CBP in untreated and cisplatin-treated HCT116 cells.
BRMS1 was transiently knocked down in HCT116 cells using two different siRNA against BRMS1 or scrambled siRNA as a control. 48 h post transfection cells were treated for 24 h (for protein) or 8 h (for RNA) with 20 µM cisplatin prior to cell harvest.
A. BRMS1 knockdown leads to an accumulation of p300 and CBP protein in HCT116 cells. *Protein levels of p300 and CBP were detected via immunoblotting. HSC70 served as the loading control.*
B.+C. BRMS1 knockdown does not affect the mRNA levels of p300 and CBP. *Efficiency of BRMS1 knockdown* ***(B.)*** *as well as mRNA levels of p300 and CBP* ***(C.)*** *were analysed by real-time PCR using gene-specific primer. All Ct values were normalized to HPRT1 and untreated control knockdown cells were set to 1 (calculation of the mean log ratio).*

Analysis of the mRNA levels of p300 and CBP in BRMS1-depleted cells proved that the observed effects were not deriving from transcriptional changes in p300 and CBP levels (Figure 3.10B and Figure 3.10C). Thus, BRMS1 can proteasomally degrade p300 and CBP in HCT116 cells.

3.11. BRMS1 knockdown compensates for diminished p300 level in cisplatin-treated iASPP knockdown cells.

Next we transiently knocked down BRMS1 in control as well as iASPP knockdown HCT116 cells (Figure 3.11). If BRMS1 is mediating the proteasomal degradation of p300 and CBP in iASPP-depleted cells, additional knockdown of BRMS1 should re-establish the protein levels of p300 and CBP.

We already showed that iASPP does not have an effect on p300 level in untreated cells. Thus, as expected, additional knockdown of BRMS1 in untreated control and iASPP knockdown HCT116 cells did not differentially influence the protein levels of p300 and CBP.

However, knockdown of BRMS1 in cisplatin-treated iASPP knockdown cells was able to abrogate the diminished protein levels of p300 and CBP. Concluding we claim, that iASPP, maybe due to its direct interaction with p300, seems to inhibit the BRMS1-mediated proteasomal degradation of p300 and CBP in cisplatin-treated HCT116 cells.

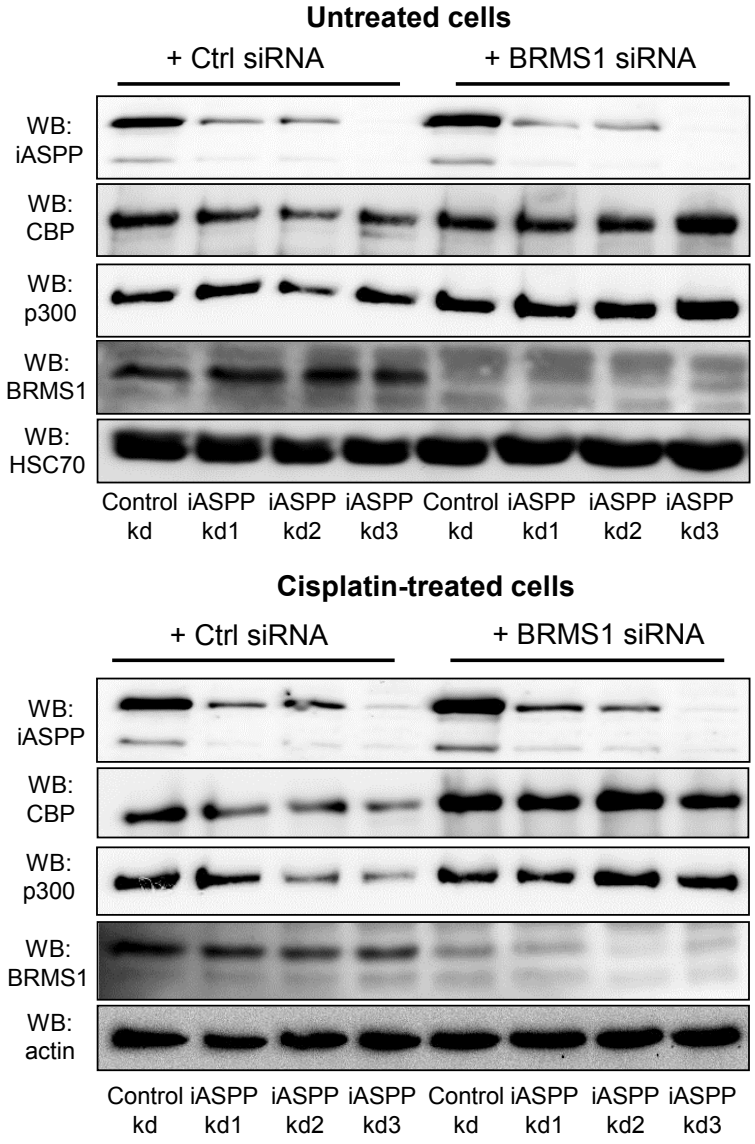

Figure 3.11. Effects of iASPP knockdown on p300 and CBP protein levels depend on the presence of BRMS1.

BRMS1 was transiently knocked down in HCT116 control and iASPP knockdown cells using a BRMS1-specific siRNA or scrambled siRNA as a control. 48 h post transfection cells were treated for 24 h with 20 µM cisplatin prior to harvest of the cells. Protein levels of p300 and CBP were detected via immunoblotting. The presence of iASPP knockdown was controlled by detection of iASPP. Knockdown efficiency of BRMS1 knockdown was determined by BRMS1 staining. Actin staining controlled equal loading of the samples.

Following, we also analysed the effects of BRMS1 knockdown on p73 and p300 target genes (Appendix Sup-4). If BRMS1 degrades p300, we hypothesized that BRMS1 depletion should indirectly elevate the expression of the previously described p73/ p300 target genes (for example *puma*, *fas* or *pig3*) due to increased p300 protein level. Nevertheless, we could only detect an increase in the mRNA levels of some p73 and/or p300 target genes in untreated as well as cisplatin-treated HCT116 cells. Therefore, we hypothesize that iASPP does not only affect p300 and TAp73 protein levels by inhibition of BRMS1-mediated degradation of p300. Likely, yet unidentified post-translational modifications of p300 might be affected by iASPP knockdown as well, thus contributing to the observed, impaired function of p300 and TAp73 in iASPP-depleted cells.

3.12. Malignant melanoma are characterized by down-regulated iASPP expression.

iASPP-depleted HCT116 cells showed a significant reduction in the pro-apoptotic response to cisplatin and Etoposide. Therefore, we argued that there have to be tumour types that display low iASPP expression. Hence, down-regulation of iASPP might also correlate then with a down-regulation and therefore functional inactivation of the pro-apoptotic protein p300, thus promoting chemoresistance as well.

To address this question, we scanned the gene expression atlas of the EMBL institute (www.ebi.ac.uk/gxa/) for microarray data sets of various tumour types. Interestingly, a study in 2005 revealed a significant down-regulation of iASPP mRNA levels in a panel of 45 malignant melanoma samples compared to benign nevi and normal skin samples (Talantov, Mazumder et al. 2005). Statistical evaluation of this data set (Figure 3.12, conducted by Dr. Annalen Bleckmann and Michaela Bayerlova) confirmed a strong decrease of iASPP mRNA levels in tissue of malignant melanoma. Additionally, the same data set also revealed a statistical significant up-regulation of BRMS1 mRNA levels in the same set of malignant melanoma samples compared to benign nevus and normal skin cells.

Moreover, two other gene expression studies that analysed melanoma tissue, normal skin and benign nevi, validated a significant down-regulation of iASPP mRNA levels in malignant melanoma (Appendix Sup-5) (Haqq, Nosrati et al. 2005; Riker, Enkemann et al. 2008).

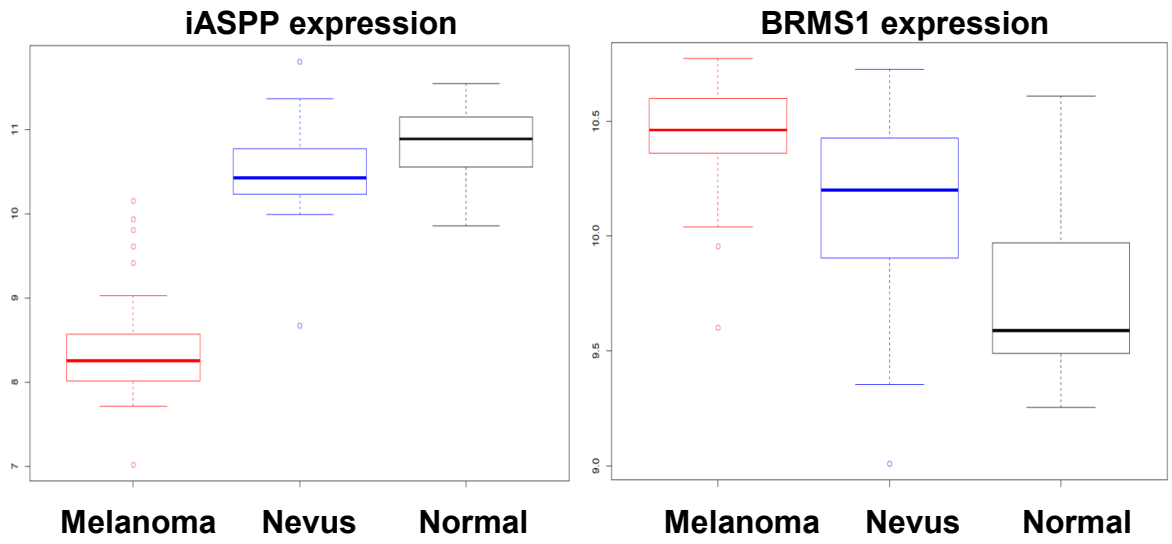

Figure 3.12. Microarray analysis reveals a down-regulation of iASPP and up-regulation of BRMS1 in malignant melanoma.
*Microarray data was retrieved from the gene expression atlas of the EMBL institute (www.ebi.ac.uk/gxa). The data set was published by Talantov and colleagues in 2005 (*Talantov, Mazumder et al. 2005*). In brief, 7 normal skin samples, 18 benign nevi and 45 melanoma samples were analysed using the Affymetrix Gene CHIP A-AFFY-33. Analysis of the gene expression study for iASPP expression and evaluation of the statistical significance was conducted by Dr. Annalen Bleckmann and Michaela Bayerlova*.

3.13. Cisplatin-treated melanoma cell lines are show low protein levels of iASPP,p300 and CBP

Based on these findings, we further investigated the role of iASPP, p300 and CBP in malignant melanoma. Analysis of 8 untreated melanoma cell lines (Figure 3.13A) confirmed low expression levels of iASPP in 6 out of 8 melanoma cell lines compared to HCT116 cells or the osteosarcoma cell line U2OS. However, we failed to detect a correlating down-regulation of p300/ CBP protein levels in the same, untreated melanoma cell lines.

Cisplatin and its derivatives are a commonly used for a variety of different tumour types (Basu and Krishnamurthy 2010). As we only revealed a significant role for iASPP (and BRMS1) in the regulation of p300 level after cisplatin treatment, we investigated the protein levels of iASPP, p300 and CBP in cisplatin-treated melanoma cell lines, as well (Figure 3.13B).

Surprisingly, in cisplatin-treated melanoma cell lines, we could detect correlating low expression levels of iASPP and p300 in at least 5 out of the 7 analysed cell lines (compared to HCT116 und U2OS cells). Therefore, we suggest that p300 protein is degraded in

cisplatin-treated melanoma cell lines, and this might be dependent on the low iASPP expression levels. Moreover, some of the melanoma cell lines also expressed BRMS1, thereby raising the possibility that BRMS1-mediated degradation could be responsible for the low protein levels of p300 in cisplatin-treated melanoma cell lines.

PARP1 is normally cleaved during the process of apoptosis induction. Hence, detection of PARP1 cleavage products serves as a marker for the level of apoptosis (Satoh and Lindahl 1992). We stained for PARP1 cleavage in cisplatin-treated melanoma cells (Figure 3.13B). However, we failed to reveal a correlation between the level of apoptosis induction and the expression levels of p300, iASPP and BRMS1. Thus, other factors might determine the sensitivity of melanoma cell lines to cisplatin-mediated apoptosis.

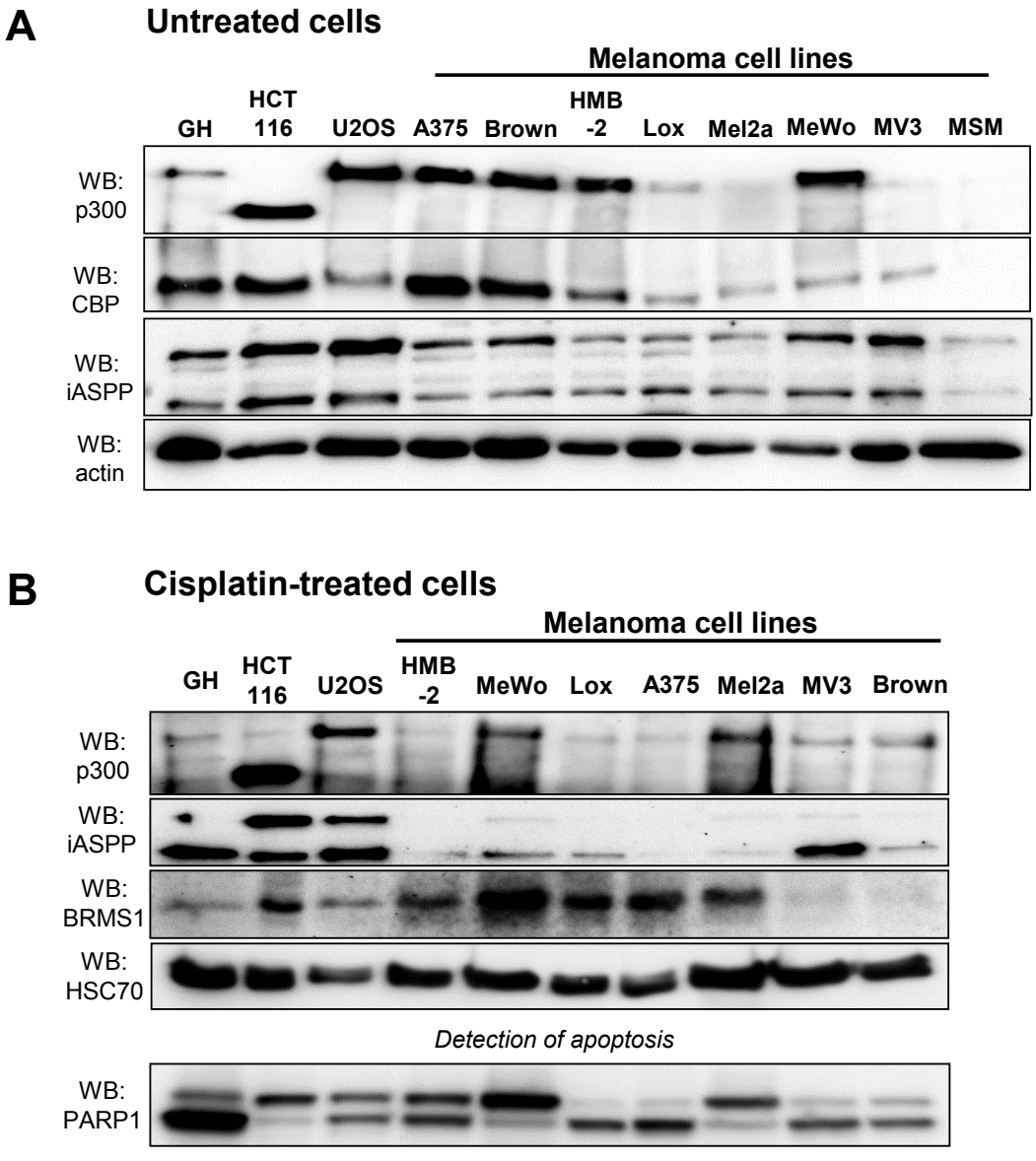

C

	p53 status	B-RAF status	N-RAS status	tumor/ metastasis	Reference
A375	wt	V600E	wt	Primary tumor	Giard et al 1973
HMB-2	mutant?	V600E		metastasis	Poser et al 2004
Lox	wt	V600E	wt	metastasis	Fodstad et al 1988
Mel2a	mutant	V600E		metastasis	Bruggen et al 1981
Mewo	wt	wt	wt	metastasis	Bean et al 1975
MV3	wt (but inactive)	wt	wt	metastasis	van Mujien 1991

Figure 3.13. Cisplatin-treated melanoma cells are characterized by low expression levels of iASPP and p300/CBP, independently of the mutation status of the cells.
A. Expression level of p300, CBP and iASPP in untreated cell lines. *Total protein lysates of 8 different melanoma cell lines as well as GH, HCT116 and U2OS cells were prepared. For immunoblotting, 30 µg protein of each sample was analysed. Actin staining served as a loading control.*
B. Expression level of p300, iASPP and BRMS1 in cisplatin-treated cell lines. *7 different melanoma cell lines as well as GH, HCT116 and U2OS cells were treated for 24 h with 20 µM cisplatin prior to preparation of total cell lysates. 30 µg protein of each sample was immunoblotted and stained for iASPP, p300 and BRMS1. Detection of PARP1 cleavage served as a control for the level of apoptosis induction. HSC70 staining controlled equal loading of the samples.*
C. Characteristics of melanoma cell lines (according to literature). *Shown is the mutational status of p53, B-RAF and N-RAS in the analysed melanoma cell lines. Information about Brown cells could not be retrieved (therefore not listed). The table also states the origin of the cells.*

Malignant melanoma are characterized by mutations that frequently occur during the process of melanocyte transformation. 50% of all melanoma display mutations in the kinase B-RAF. Other commonly observed mutations include activating mutations of N-RAS (~15%) or upstream mutations in the p53 signalling pathway, thus resulting in inactive p53 protein (Pollock and Meltzer 2002; Kelleher and McArthur 2012; Tsao, Chin et al. 2012). However, current melanoma therapies targeting B-RAF, N-RAS, or those therapy approaches that are aiming at a re-activation of p53, show a low response rate or a high rate of tumour re-occurrence due to acquired chemoresistance. Therefore, new candidates for melanoma therapy are urgently needed. Interestingly, low levels of iASPP or p300 expression did not correlate with any of these mutations, as revealed by the analysis of the mutation status of the investigated cell lines (Figure 3.13C). Our analysis indicates, that iASPP and p300 expression might constitute new biomarkers for certain therapy approaches of malignant

melanoma, as diminished expression of both proteins occurs independently of the most commonly found mutations.

3.14. BRMS1 mediates the degradation of p300 and CBP in a set of cisplatin-treated melanoma cell lines.

Subsequently, we investigated if BRMS1 is responsible for p300/CBP degradation in low iASPP-expressing melanoma cell lines. We performed transient knockdown of BRMS1 in those cell lines, in which we previously monitored a reduction of p300 levels after knockdown of iASPP (Figure 3.9). We hypothesized that BRMS1 knockdown should recover p300 and CBP protein levels in cisplatin-treated cells, at least to some extent. Truly, transient depletion of BRMS1 in A375, Lox and MV3 cells partially re-established p300 and CBP protein levels in cisplatin-treated cells (Figure 3.14). In line to our previous findings, BRMS1 knockdown did not significantly increased p300/ CBP level in untreated cells.

However, we failed to validate BRMS1-mediated degradation of p300/CBP in all of the analysed cell lines. In Mel2a and MeWo cells for example, BRMS1 knockdown did not elevate the protein levels of p300 or CBP (data not shown). Concluding, BRMS1-mediates the degradation of p300 and CBP in some of the analysed melanoma cell lines.

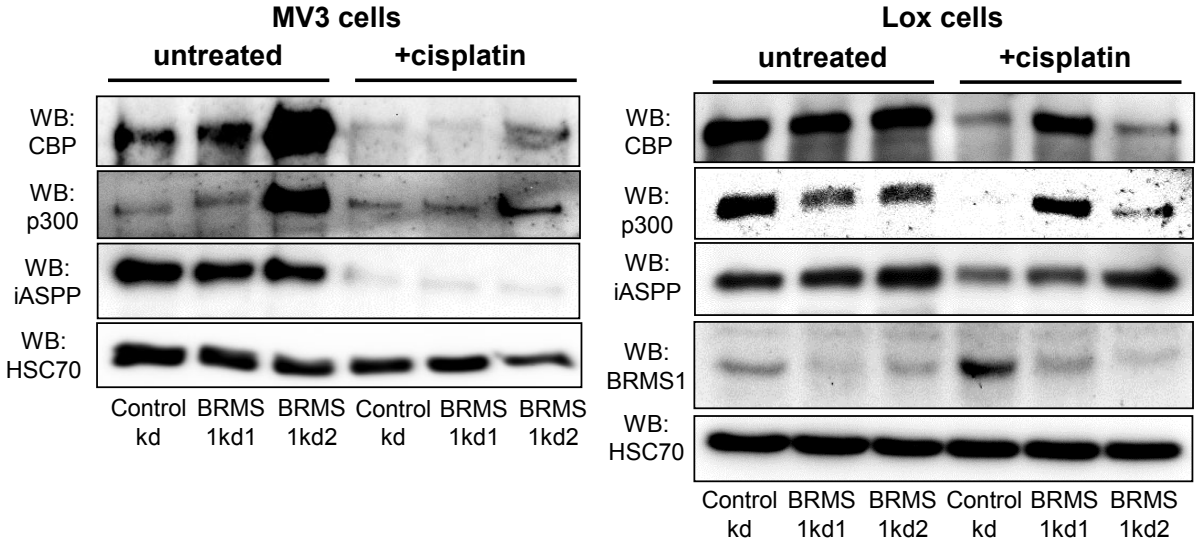

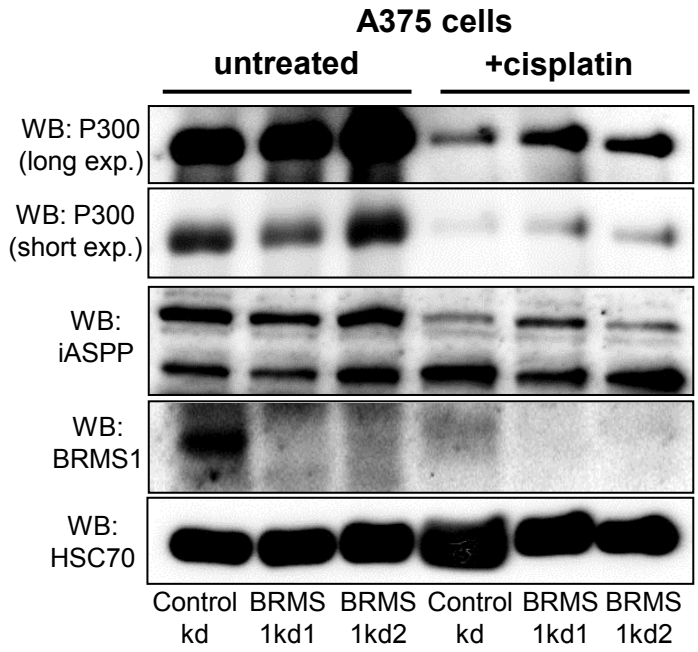

Figure 3.14. BRMS1 contributes to the proteasomal degradation of p300 and CBP in cisplatin-treated melanoma cell lines.
Lox, MV3 and A375 cells were transiently transfected with 2 different BRMS1 siRNA or a scrambled siRNA for the control knockdown. 48 h after transfection, cells were treated with 20 µM cisplatin, before total cell lysates were prepared. Knockdown efficiency was controlled by detection of BRMS1 protein level. Of note BRMS1 level in MV3 cells were not detectable. HSC70 staining controlled the equal loading of the samples (n = 1).

3.15. Treatment of MEF cells with the p300 activator CTB can re-establish the protein level and function of p300.

Recently a substance from the cashew nut shell liquid anacardic acid, called CTB, was extracted, that was shown to modulate p300 activity (Balasubramanyam, Swaminathan et al. 2003). CTB is a trifluoromethyl-phenyl-benzamide that binds to p300 and therefore enhances the HAT activity of p300. As this substance is commercially available, we tried to re-establish p300 levels in low iASPP-expressing cells by treatment of the cells with CTB. As a first experiment wild-type mouse embryonic fibroblasts were treated with CTB, cisplatin or a combination of CTB and cisplatin (Figure 3.15).

Indeed, incubation of cells with CTB alone or in combination with cisplatin resulted in a strong accumulation of p300 protein (Figure 3.15A). Interestingly, combinational treatment with CTB and cisplatin also led to an elevation of iASPP protein levels, though we do not have an explanation for this observation. Moreover combinational treatment of cells with CTB and cisplatin induced higher level of apoptosis, as shown by the different amounts of cleaved caspases 3 in the cells. Gene expression analysis of similar treated MEF cells revealed, that

CTB treatment did not only resulted in an accumulation of p300 protein, but also led to a slight induction of p300 mRNA levels. (Figure 3.15A, right site).

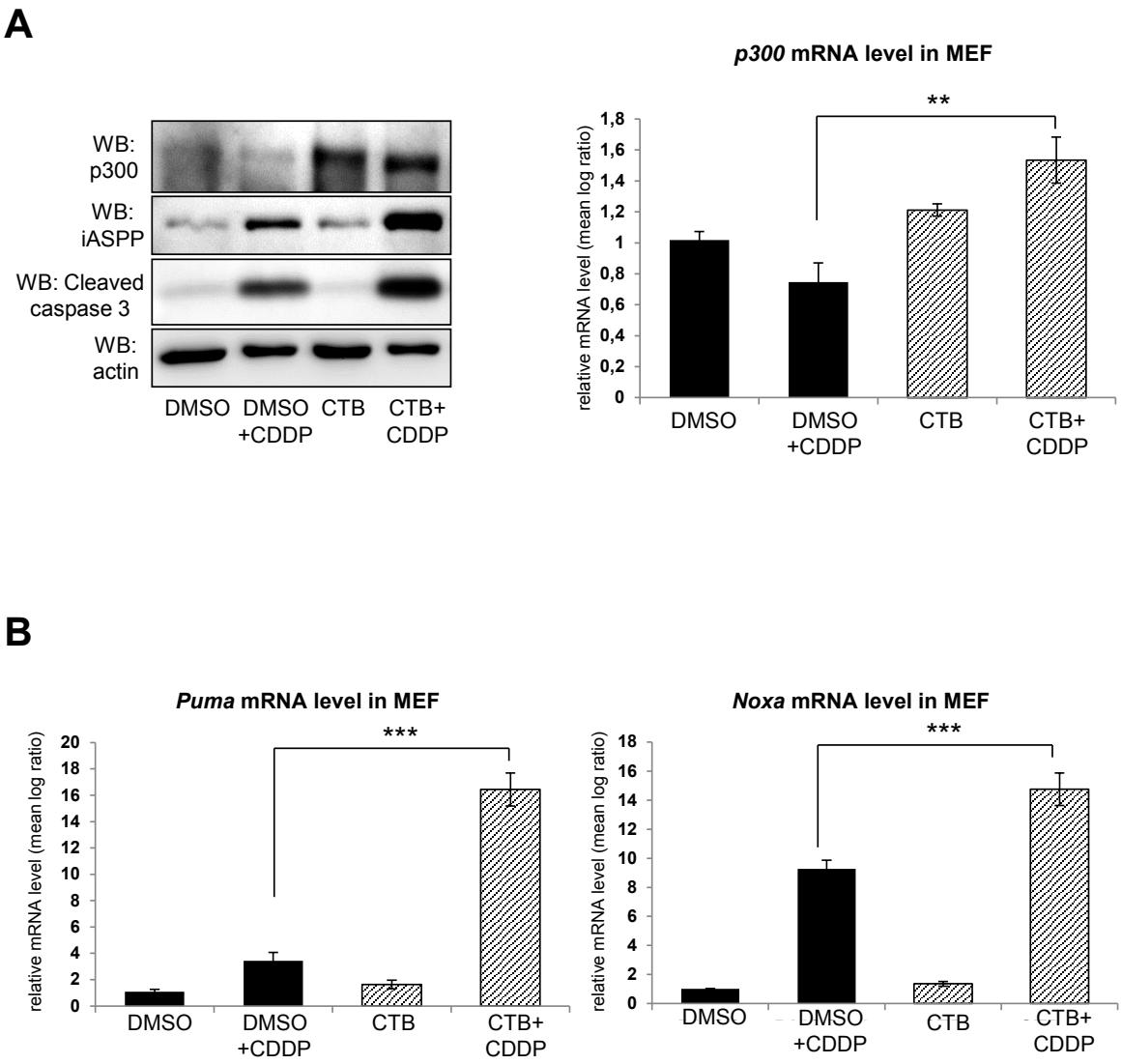

Figure 3.15. Treatment of mouse embryonic fibroblasts (MEF) with CTB leads to increased p300 levels and a stronger induction of apoptosis.

Wild-type MEFs were treated with DMSO, 10 µM CTB, 20 µM cisplatin or a combination of 10 µM CTB and 20 µM cisplatin. (CTB = p300-activating substance)

A. CTB treatment leads to a stabilisation of p300 protein levels and subsequently to a higher rate of apoptosis. *For immunoblotting, cells were treated for 16 h with CTB and cisplatin before cells were harvested and analysed. Total levels of p300, iASPP and cleaved caspase 3 were detected by immunoblotting. Actin staining served as loading control. Of note a slight but significant increase of p300 mRNA levels was detected in CTB and cisplatin-treated MEF cells.*

B. CTB treatment causes a transcriptional up-regulation of pro-apoptotic target genes. *For RNA extraction cells were harvested after 9 h of incubation with CTB and cisplatin. Gene expression analysis of Puma, Noxa and P300 were performed using gene-specific primers*

and real-time PCR. Ct values were normalized to HPRT1. The graphs display the mean log ratio as the relative mRNA levels. DMSO-treated samples were set to 1 (mean log ratio).

Moreover, we found a dramatic increase in the gene expression of pro-apoptotic p73 target genes, such as *Puma* and *Noxa,* in CTB and cisplatin-treated MEF cells. Thus, CTB does not only lead to an accumulation of p300 protein but also triggers its activation (Figure 3.15B). Following p300 is likely to mediate apoptosis by transcriptional up-regulation of pro-apoptotic target genes.

3.16. CTB treatment cannot re-establish the protein levels of p300 in low iASPP expressing melanoma cell lines or iASPP knockdown cells.

Due to these promising results we treated melanoma cell lines with CTB or a combination of CTB and cisplatin (Figure 3.16). As exemplarily shown for Lox and MV3 cells (Figure 3.16A), CTB treatment, alone or in combination with cisplatin, neither elevated p300 protein levels nor did it significantly increase the level of apoptosis induction, as shown by detection of PARP1 cleavage. We argue, that melanoma cells seem to have multi-facetted impairments in the regulation of p300 expression that cannot be rescued by sole re-activation of p300. In line with these findings, treatment of iASPP-depleted HCT116 cells with CTB and cisplatin could neither rescue the diminished p300 protein levels, nor overcome the observed defects in apoptosis induction (Figure 3.16B). Therefore, we state, that CTB does not represent a suitable drug for re-activation of p300 in low iASPP-expressing cells.

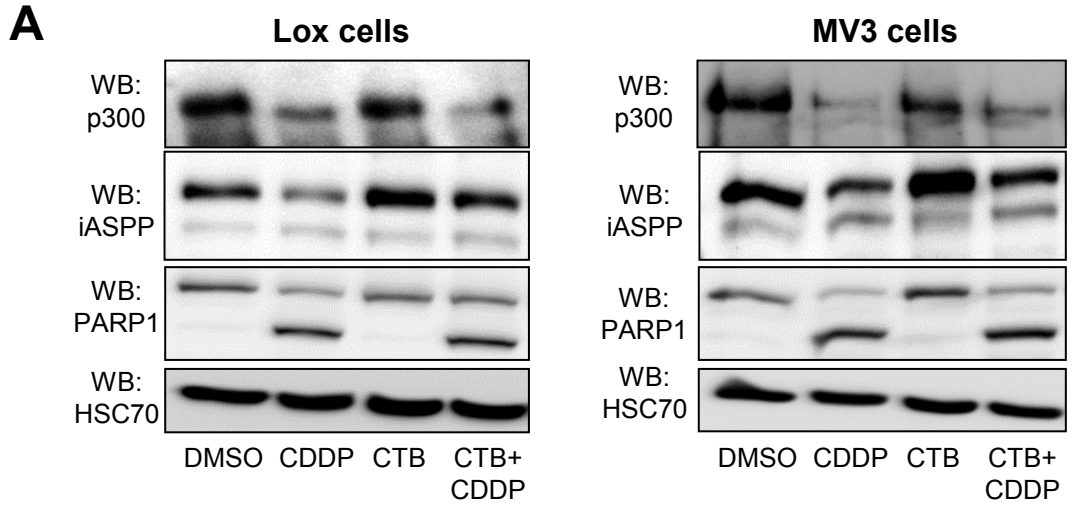

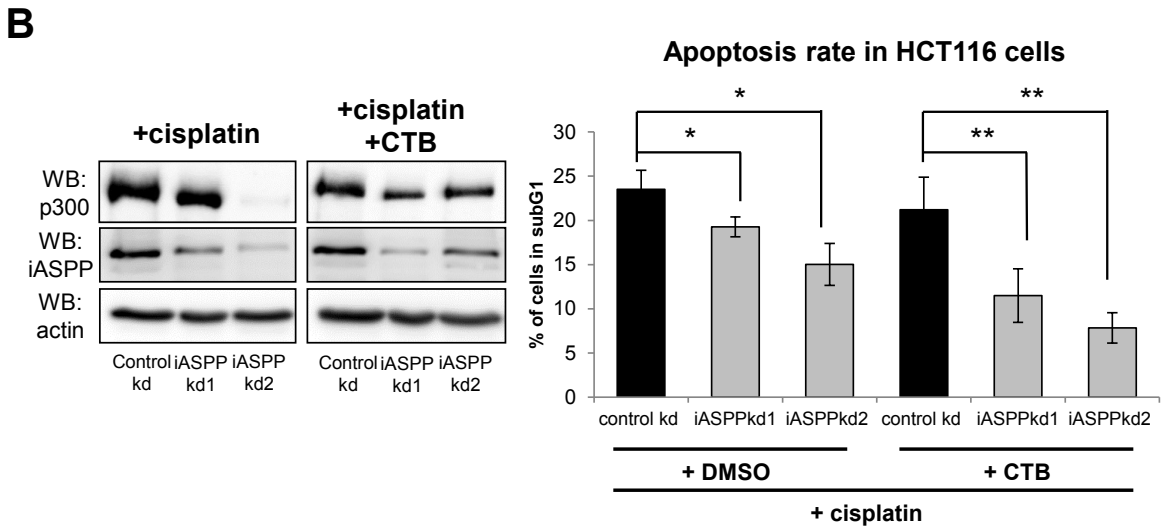

Figure 3.16. CTB treatment cannot re-establish the protein levels of p300 in low iASPP-expressing cells.

Lox, MV3 and HCT116 iASPP knockdown cells were treated for 24 h with DMSO, 20 µM CTB, 20 µM cisplatin (CDDP) or a combination of 20 µM CTB and 20 µM cisplatin (CDDP). (CTB = p300-activating substance, kd = knockdown)

A. CTB treatment of low iASPP-expressing cells does not recover the protein levels of p300. *Protein lysates were analysed by immunoblotting. Samples of treated Lox and MV3 cells were stained for p300 and iASPP. Detection of PARP1 cleavage served as an indicator for the level of apoptosis induction. HSC70 staining validated equal loading of all samples.*

B. CTB treatment of iASPP-depleted HCT116 cells can neither rescue the protein levels of p300 nor defects in apoptosis induction. *HCT116 control and iASPP knockdown cells were immunoblotted for p300 and iASPP. Actin staining was performed as a loading control. Detection of proteins in CTB and cisplatin-treated HCT116 control and iASPP knockdown cells was conducted by Viola Meyer-Pannwitt. To measure the level of apoptosis induction, cisplatin-treated or CTB and cisplatin-treated cells were Ethanol-fixed, stained with propidium iodide and assessed by FACS analysis. The graph displays the percentage of cells in subG1 phase. All samples were analysed using the same gate settings.*

3.17. P38 activity influences iASPP-mediated regulation of p300 level.

Following, we thought of analysing additional signalling pathways that might regulate the expression levels of p300. Therefore, we investigated protein levels and activity of known p300-modifying proteins (p38, c-abl and Akt), that had been previously described to contribute to cisplatin-dependent apoptosis induction (data not shown). We suggest that these proteins might be affected by iASPP knockdown, as well. As p300 cannot be directly re-activated through application of CTB, modulation or re-establishment of the activity of these p300-modifying proteins might result in an elevation of the protein levels and activity of p300 in melanoma cells.

Phosphorylation level at threonine residue 180 and tyrosine residue 182 of p38 is a marker for the activity of p38. Surprisingly, we found decreased phosphorylation level of p38 (p-p38) in untreated and cisplatin-treated, iASPP knockdown MV3 cells (Figure 3.17A). Thus, iASPP depletion is likely to decrease the activity of p38. Vice versa, transient over-expression of iASPP in MV3 cells resulted in increased p38 activity as detected by phosphorylation level of p38 again (Figure 3.17B).

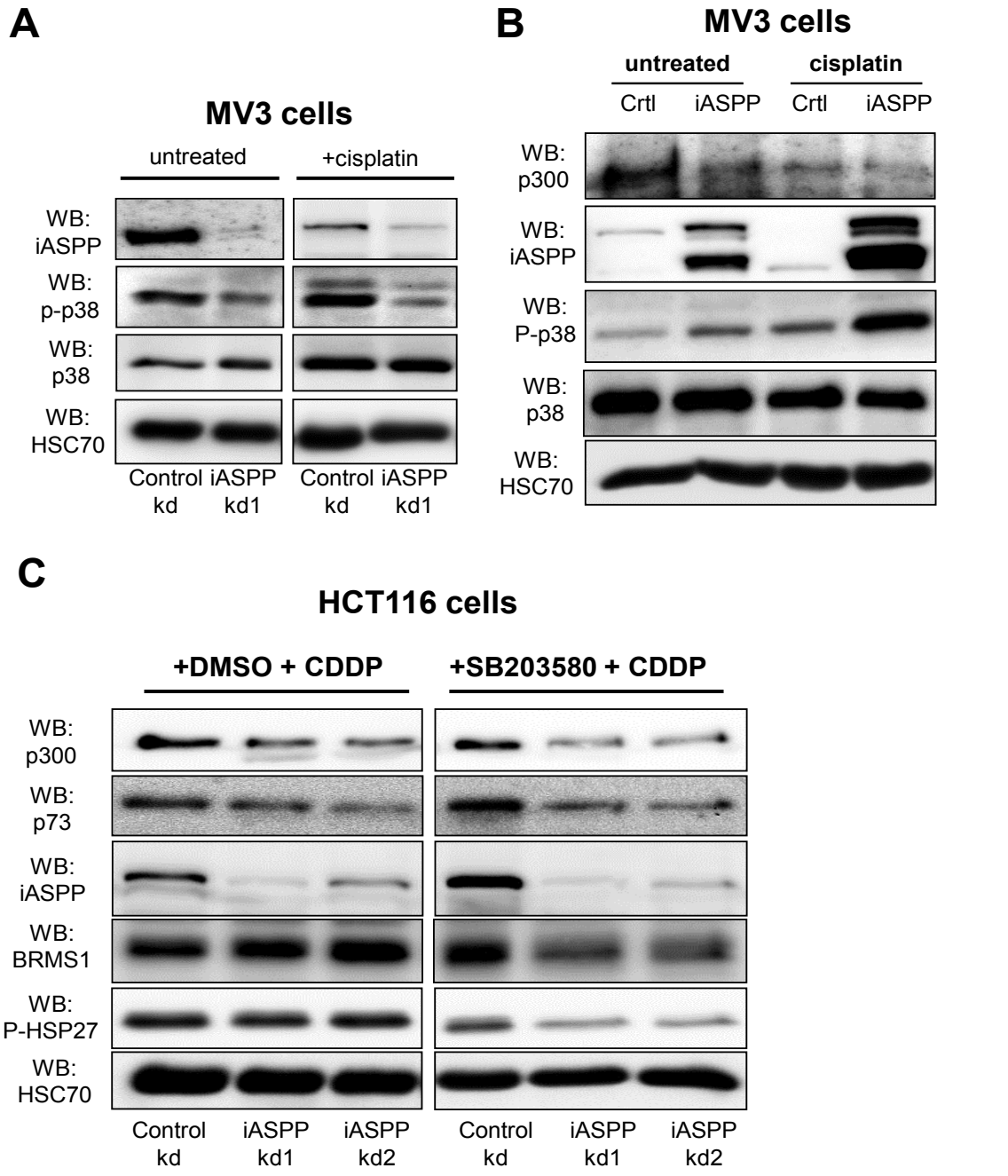

Figure 3.17. P38 activity is modified by iASPP expression, thus contributing to diminished level of p300 in cisplatin-treated, iASPP knockdown cells.

A. P38 activity is decreased in MV3 iASPP knockdown cells. *IASPP was stably knocked down in MV3 cells using shRNA. Control knockdown cells were generated using shRNA against the luciferase gene. Cells were treated for 24 h with 20 μM cisplatin prior to protein harvest and analysis by immunoblotting. IASPP knockdown efficiency was controlled by staining for iASPP. The level of p38 activity was detected by staining for phosphorylated p38 (p-p38). P38 staining controlled equal levels of the total protein; HSC70 staining served as a loading control.*
B. Transient over-expression of iASPP increases p38 activity in MV3 cells. *Cells were transiently transfected with equal amounts of empty vector or a plasmid encoding for iASPP. 48 h after transfection, cells were treated for 24 h with 20 μM cisplatin. Total cell lysates were prepared and immunoblotting. Protein detection was similar as for A.*
C. Inhibition of p38 in cisplatin-treated iASPP knockdown cells amplifies diminished protein levels of p300 and TAp73. *Stable HCT116 knockdown cells were treated for 24 h with 20 μM cisplatin and DMSO or 20 μM cisplatin and 10 μM SB203580. Total protein lysates were prepared and immunoblotted. Detection of phosphorylated HSP27 (P-HSP27) controlled effective p38 inhibition. IASPP staining validated the presence of iASPP knockdown. HSC70 staining served as a loading control (kd = knockdown; SB203580 = p38-specific inhibitor, CDDP = cisplatin)*

P38 is a MAPK kinase that is known to be activated by phosphorylation in response to DNA damage. Following, active p38 can phosphorylate and therefore activate the p53-family to induce apoptosis (Bulavin, Saito et al. 1999; Sanchez-Prieto, Sanchez-Arevalo et al. 2002).

Moreover, it had been recently found, that p38 can phosphorylate p300 at serine 1834, thereby contributing to the activation of p300 after DNA damage (Poizat, Puri et al. 2005; Wang, Han et al. 2013). Concluding, modulation of p38 activity in iASPP knockdown cells might indeed contribute to the observed decrease in p300 level and function. Thus, we tested the effects of the p38 inhibitor SB203580 on p300 level in cisplatin-treated HCT116 knockdown cells (Figure 3.17C).

Interestingly, inhibition of p38 slightly amplified the effects of iASPP knockdown in cisplatin-treated cells, thereby further decreasing p300 levels in iASPP knockdowns. We think, that this amplification is low but significant, as BRMS1, the ubiquitin ligase which mediates the reduction of p300 protein level, decreased in iASPP-depleted, SB203580-treated cells, as well. Thus, this decrease of BRMS1 partially compensated for diminished p300 level due to the inhibition of p38 in iASPP knockdown cells.

Moreover we obtained a more pronounced effect of iASPP knockdown on TAp73 level after additional treatment with SB203580. This result underscores, that the diminished activity of p38 in iASPP knockdown cells is contributing to the diminished protein stability and function of p300 and TAp73. However, it has to be noted, that these results are preliminary. In future

experiments, we will have to dissect the role of p38 in the functional interaction of iASPP, p300 and BRMS1 in more detail.

Of note, cisplatin treatment of MV3 and Brown cells resulted in an accumulation of a lower running, iASPP-specific band (at around 80kDa) (Appendix Sup-6A). We hypothesized that in these DNA-damaged cells, iASPP seems to be subjected to caspase-cleavage. Accordingly, we could inhibit the generation of an iASPP-cleavage product by simultaneous treatment of the cells with cisplatin and the caspase-inhibitor Z-VAD (Appendix Sup-6A). In-silico analysis of the iASPP protein sequence revealed a cleavage site for caspases at its N-terminus (Appendix Sup-6B). As the N-terminus of iASPP determines its cytoplasmic localization, N-terminal cleavage of iASPP might modulate its sub-cellular localization and therefore function. Hence, p300 might be differentially affected by full-length iASPP and N-terminal truncated iASPP. Concluding, we suggest that iASPP cleavage might represent another level of iASPP-mediated regulation of p300 protein level. However, we did not further analyse this mechanism.

3.18. Inhibition of MKP-1 can re-establish p300 level and apoptosis in low-iASPP expressing cell lines.

Phosphorylation of p38 is normally regulated by MKP-1 mediated de-phosphorylation (Franklin and Kraft 1997). Following, Wang and co-workers reported that MKP-1 is over-expressed in breast cancer and could be associated with increased chemoresistance (Wang, Cheng et al. 2003). Moreover, Kundu and colleagues elucidated an over-expression of MKP-1 in malignant melanoma tissue. Thus, treatment of melanoma cell lines with the MKP-1 inhibitor tyrosine phosphatase inhibitor-3 (TPI-3) was able to sensitize melanoma cells for chemotherapeutical treatment (Kundu, Fan et al. 2010).

We showed that modulation of p38 activity after knockdown of iASPP is likely to contribute to decreased stability and protein level of p300. Concluding, we hypothesized that inhibition of MKP-1 and therefore activation of p38 in low iASPP expressing melanoma cell lines could contribute to a re-establishment of p300 levels followed by enhanced chemosensitivity.

As TPI-3 is not commercially available, we utilized the MKP-1/ MKP-3 dual inhibitor BCI and treated various melanoma cell lines with BCI alone or in combination with cisplatin. Following, cell lysates were immunoblotted and stained for p300 (Figure 3.18A). Interestingly, BCI treatment alone was already sufficient to elevate p300 protein levels in MV3 and A375 cells. Furthermore, BCI treatment induced apoptosis in MV3 and A375 cells as detected by PARP1 cleavage (Figure 3.18A). Accordingly, propidium iodide staining of

previously BCI-treated melanoma cells validated a 2-6 times higher percentage of apoptotic cells as shown by analysis of the subG1 phase. (Figure 3.18B) Therefore, BCI treatment alone already constitutes a potent inducer of apoptosis in melanoma cell lines.

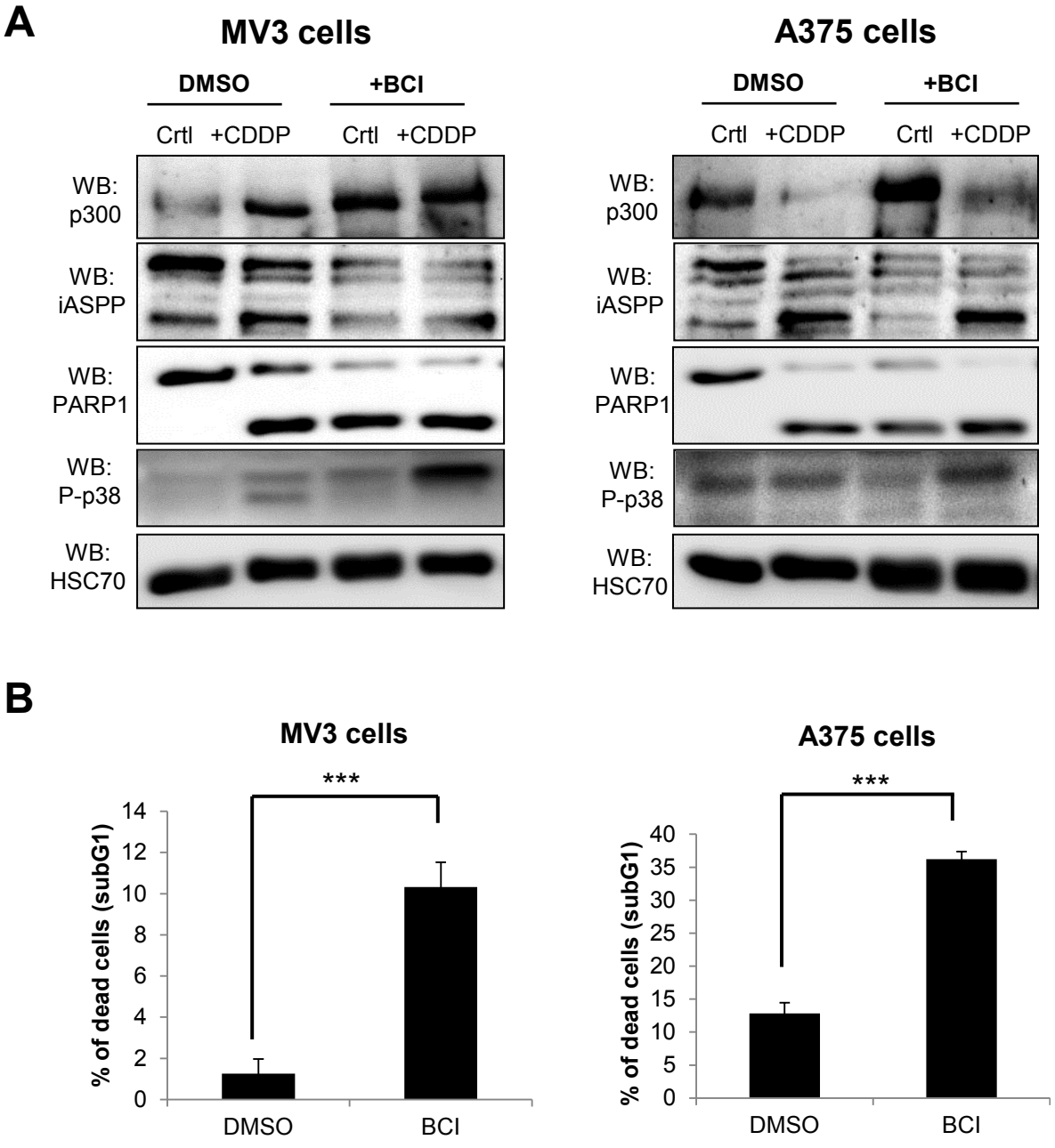

Figure 3.18. MKP-1 inhibition leads to a re-establishment of p300 level and induction of apoptosis.

A. BCI treatment elevates the level of p300 in MV3 and A375 cells. *MV3 and A375 cells were treated for 20 h with 10 µM BCI, 10 µM cisplatin or 10 µM BCI and 10 µM cisplatin. Total cell lysates were prepared and immunoblotted. Phosphorylated p38 was stained as a control for MKP-1 inhibition. Detection of PARP1 cleavage served as a marker for the level of apoptosis. (BCI = MKP-1 inhibitor, CDDP = cisplatin)*

B. MKP-1 inhibition triggers apoptosis in melanoma cell lines. *A375 and MV3 cells were treated for 24 h with DMSO or 10 μM BCI. Cells were fixed with Ethanol and subsequently stained with propidium iodide. Percentage of dead cells was assessed by FACS analysis and quantification of cells in subG1 phase. Same gate settings were applied for all analysed samples.*

3.19. P300 partially contributes to BCI- and cisplatin treatment-induced apoptosis in low iASPP-expressing melanoma cells.

We hypothesized that BCI treatment mediated apoptosis induction partially derived from re-establishment of p300 protein levels and activity. Therefore, we investigated the level of apoptosis induction after BCI and/or cisplatin treatment of control and p300 knockdown A375 cells (Figure 3.19).

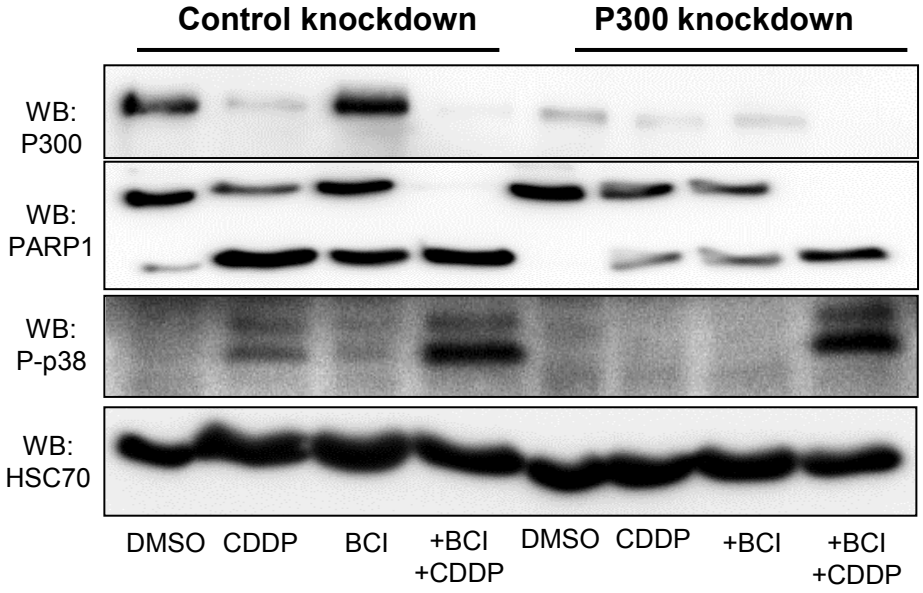

Figure 3.19. BCI treatment-mediated apoptosis is partially dependent on the re-stabilisation of p300 protein level.
P300 was transiently knocked down using specific siRNA. Control knockdown cells were transfected in parallel using scrambled siRNA. 48 h post-transfection, cells were treated for 20 h with 10 μM BCI, 10 μM cisplatin or 10 μM BCI and 10 μM cisplatin. Total cell lysates were prepared and immunoblotted. Phosphorylated p38 (p-p38) was stained as a control for MKP-1 inhibition. Detection of cleaved PARP1 served as a marker for the level of apoptosis. HSC70 staining served as a loading control. (BCI = MKP-1 inhibitor, CDDP = cisplatin)

As shown before, control knockdown cells displayed high levels of apoptosis induction after treatment with cisplatin, BCI or a combination of BCI and cisplatin. In contrast, p300 knockdown cells exhibited only low levels of PARP1 cleavage, especially in single treatments

of cisplatin and BCI. Thus, in A375 cells at least, apoptosis that is induced by BCI and cisplatin treatment is partially mediated by p300. Therefore, we claim that the MKP-1 inhibitor BCI can induce apoptosis in melanoma cells due to the re-establishment and re-activation of p300. It might be that MKP-1 inhibition does not only re-activate p38 but also re-constitute iASPP-p300 interaction or alternatively abolishes BRMS1-mediated degradation of p300. Future experiments will further investigate the molecular mechanism behind MKP-1 inhibitor-mediated apoptosis induction in melanoma cells.

4. Discussion

4.1. iASPP constitutes a new regulator for p300 and TAp73 function by control of p300 stability.

One of the molecular causes for cancer development results from functional inactivation of tumour suppressor proteins, thereby contributing to chemoresistance and tumour progression (Hanahan and Weinberg 2000; Röckmann and Schadendorf 2003). P300 and CBP represent two histone acetyltransferase proteins that have been described to participate in chemotherapy-induced tumour cell apoptosis (Goodman, 2000; Kitagawa et al, 2008). Following, inactivation of p300/CBP-dependent tumour suppressor functions are frequently detected in cancer due to mutations or genomic aberrations of both gene loci (Blobel et al, 2002; Chan et al, 2011; Gayther et al, 2000; Goodman 2000). Molecular basis of their tumour suppressor activities partially derives from their co-activator role for the tumour suppressor proteins p53 and TAp73 (Avantaggiati, Ogryzko et al. 1997; Zeng, Li et al. 2000; Costanzo, Merlo et al. 2002; Iyer, Chin et al. 2004). However, as p300 and CBP can mediate acetylation and therefore activation of oncogenic proteins as well, it still remains to be revealed, how p300/CBP activity is specifically regulated (Kalkhoven 2004; Bedford and Brindle 2012). Most importantly, modulation of these regulatory mechanisms of p300/CBP function might provide the basis for new anti-cancer therapy approaches.

Direct interaction of iASPP, another co-factor of the p53-family, with p300 as well as with its downstream target protein TAp73 has been reported before (Robinson, Lu et al. 2008; Gillotin and Lu 2011). Functional consequences of these interactions remain elusive though. Therefore, we investigated the consequences of iASPP depletion on p300 and TAp73 expression levels as well as on their function in chemotherapeutic drug-induced apoptosis.

Most of the previously assigned functions of iASPP revealed an inhibitory role of iASPP on the function of its interaction partner. Surprisingly, we found that iASPP enhances the protein stability of p300 as well as it promotes the co-activator function of p300 in TAp73-mediated apoptosis induction (Figure 3.2 and Figure 3.3). Interestingly, we could only validate the interaction between iASPP and p300, as well as the resulting stabilization of p300, after cisplatin treatment of the cells (Figure 3.1 and Figure 3.2). Hence, iASPP-p300 complex formation in cisplatin-treated cells represents the molecular basis for iASPP-mediated regulation of p300 level. This might be due to post-translational modifications of p300, such

as p38-mediated phosphorylation of p300, thus leading to conformational changes of p300 that enable the interaction with iASPP then (see also section 4.6).

Subsequently, we also found a new, though unexpected, pro-apoptotic role for iASPP in cisplatin- and Etoposide-treated HCT116 cells. In detail, iASPP depletion led to diminished recruitment of p300 and TAp73 to pro-apoptotic target gene promoters (Figure 3.4 and Figure 3.5). Consequently, we could detect diminished up-regulation of pro-apoptotic p73 target genes in cisplatin-treated cells (Figure 3.6) as well as impaired induction of cisplatin- or Etoposide-mediated apoptosis in tumourigenic cell lines (Figure 3.7 and Appendix Sup-3).

So far, the inhibitory role of iASPP in p53-mediated apoptosis induction has been implicated as its most important function (Bergamaschi, Samuels et al. 2003). However, endogenous iASPP expression in a variety of cell lines did not interfere with chemotherapy-induced, p53-mediated apoptosis (Mantovani, Tocco et al. 2007; Laska, Vogel et al. 2010). Moreover, a molecular mechanism has not been revealed yet, to explain how iASPP over-expression impairs p53-mediated up-regulation of pro-apoptotic target genes, while p53-dependent induction of cell cycle arrest genes remains unaffected (Trigiante and Lu 2006; Espinosa 2008). Hence, a role for iASPP in promotion or inhibition of apoptosis might be dependent on iASPP expression level and the cellular context.

Furthermore, we could validate that iASPP constitutes a regulator of p300 protein level in cisplatin-treated primary MEF cells as well as in melanoma cell lines, thereby validating our previous findings (Figure 3.8 and Figure 3.9). Accordingly, the functional interaction of iASPP and p300 represents a new aspect in the regulation of p300 level, which seems to account for both, primary and tumourigenic cell lines.

Interestingly, studies in iASPP knockout mice revealed a positive feedback-loop between p63 and iASPP, that regulates skin homeostasis (Chikh, Matin et al. 2011; Notari, Hu et al. 2011). In MEF cells and keratinocytes, iASPP was able to increase the protein levels of ΔNp63 and TAp63 without altering the corresponding mRNA levels of total p63 (Chikh, Matin et al. 2011). Follow-up studies discovered that two microRNAs are regulated by iASPP, thus controlling p63 protein levels. Nevertheless, repression of these microRNAs could not fully re-establish p63 level in iASPP-depleted keratinocytes. Concluding, these results show that iASPP can also enhance the protein stability of p63 in keratinocytes, similar to our findings that iASPP mediates increased protein stability of TAp73 in cisplatin-treated cells (Figure 3.3).

Moreover, p300 has been implicated as an important regulator of keratinocyte differentiation and cell cycle, although the underlying mechanism still needs to be elucidated (Wong,

Pickard et al. 2010). Therefore, it can be claimed that the functional interaction of iASPP and p300 might also contribute to iASPP-dependent regulation of p63 level in keratinocytes and MEF cells. Strikingly, iASPP depletion and the following decrease in p63 expression level caused an increase in differentiation as well as inhibition of keratinocyte proliferation (Chikh, Matin et al. 2011). In contrast, previous studies described a loss of keratinocyte differentiation after knockdown of total p63 protein (Truong, Kretz et al. 2006). Hence, Chikh and colleagues suggested that iASPP can also act upstream of p63; and due to our findings, it might be speculated that iASPP regulates p63 function through direct control of p300 levels in keratinocytes (Chikh, Matin et al. 2011).

A previous study of the cellular function of the ASPP-family member ASPP1 further underscores our findings (Vigneron, Ludwig et al. 2010). It was shown that in untreated as well as hydroxyurea-treated HCT116 und U2OS cells, ASPP1 increased the protein stability of YAP-1 and TAZ through direct interaction with the YAP-1/TAZ modifying kinase LATS1. However, the E3 ubiquitin ligase that mediated these effects remains elusive. Consequently, ASPP1 promoted the pro-survival role of nuclear YAP-1/TAZ complexes, thereby inhibiting apoptosis and senescence of the cells (Vigneron, Ludwig et al. 2010; Vigneron and Vousden 2012). Of note, this function of ASPP1 depended on its sub-cellular localization. Cytoplasmic ASPP1 led to YAP-1/TAZ-dependent inhibition of apoptosis, whereas nuclear localization of ASPP1 promoted its previously described co-activator role of p53-mediated apoptosis induction. Concluding, the sub-cellular localization of iASPP might influence the regulation of p300 and TAp73 function in cisplatin-mediated apoptosis, as well.

4.2. BRMS1 is required for p300 degradation in iASPP knockdown cells.

As proteasomal degradation of p300 is mediated by specific E3 ubiquitin ligases, and iASPP knockdown leads to accelerated degradation of p300, we investigated the responsible E3 ubiquitin ligase mediating these effects. We found that BRMS1, a recently identified E3 ubiquitin ligase for p300 in lung cancer cells (Liu, Mayo et al. 2013), could degrade p300 and CBP in HCT116 cells (Figure 3.10). Further analysis of BRMS1 and iASPP double knockdown cells elucidated, that BRMS1 expression was required for accelerated degradation of p300 and CBP in iASPP-depleted, cisplatin-treated cells (Figure 3.11). Therefore, iASPP is likely to inhibit BRMS1-mediated degradation of p300 and CBP in cisplatin-treated HCT116 cells.

We hypothesize, that iASPP-p300 interaction masks the interaction site for BRMS1, that is located at the C-terminus of the p300 protein (Liu, Mayo et al. 2013). Consequently, BRMS1

and p300 interaction is prevented and p300 protein is not degraded anymore. However, we still have to prove this hypothesis by investigating BRMS1 and p300 interaction in the presence and absence of iASPP and cisplatin treatment. This will be done in future co-immunoprecipitations. Figure 4.1 summarizes our present working hypothesis.

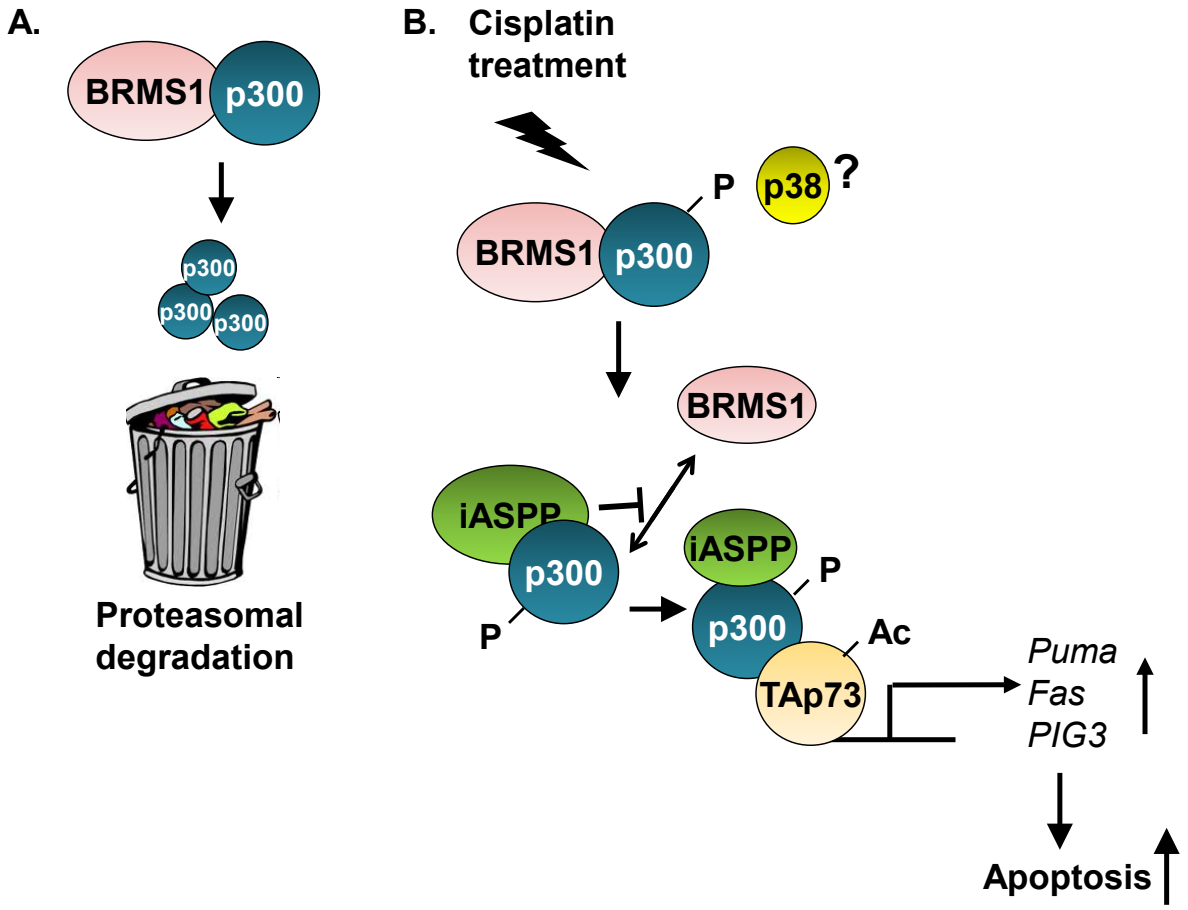

Figure 4.1. iASPP inhibits BRMS1-mediated degradation of p300.
A. BRMS1 is required for p300 degradation in untreated cells. *In normal proliferating cells, BRMS1 can interact with p300 (and CBP) followed by the proteasomal degradation of the proteins.*
B. iASPP-p300 interaction contributes to TAp73-mediated apoptosis induction after DNA damage. *After cisplatin treatment or severe DNA damage in general, iASPP starts to bind to p300, probably due to post-translational modifications of p300 (for example phosphorylation by p38). Hence, BRMS1 dissociates from p300 protein and subsequently enhances its protein stability. Next, p300 becomes associated with TAp73, which leads to the acetylation and therefore activation of TAp73 protein. Subsequently, TAp73-mediated transcription of pro-apoptotic p73 target genes such as puma or pig3 is induced, ultimately leading to apoptosis induction. In this hypothesis, iASPP contributes to cisplatin-induced apoptosis by positively regulating the co-activator function of p300 in TAp73-mediated apoptosis.*

4.3. Sub-cellular localization of iASPP, BRMS1 and p300 can determine their functional interaction.

Most studies showed a proteasomal degradation of p300 and CBP protein in the nucleus (Poizat, Sartorelli et al. 2000; Poizat, Puri et al. 2005; St-Germain, Chen et al. 2008). Moreover, as BRMS1 is mostly described as a nuclear protein as well (Hurst, Xie et al. 2013), BRMS1-mediated degradation of p300/CBP could take place in the nucleus as well (Figure 4.2A). In contrast, iASPP is likely to be predominantly localized in the cytoplasm of the cells, as the N-terminus of iASPP leads to complete cytoplasmic localization of full-length iASPP (Slee, Gillotin et al. 2004). Therefore, direct interaction of iASPP and p300 in cisplatin-treated cells might not fully explain, how iASPP can prevent the nuclear, BRMS1-mediated degradation of p300.

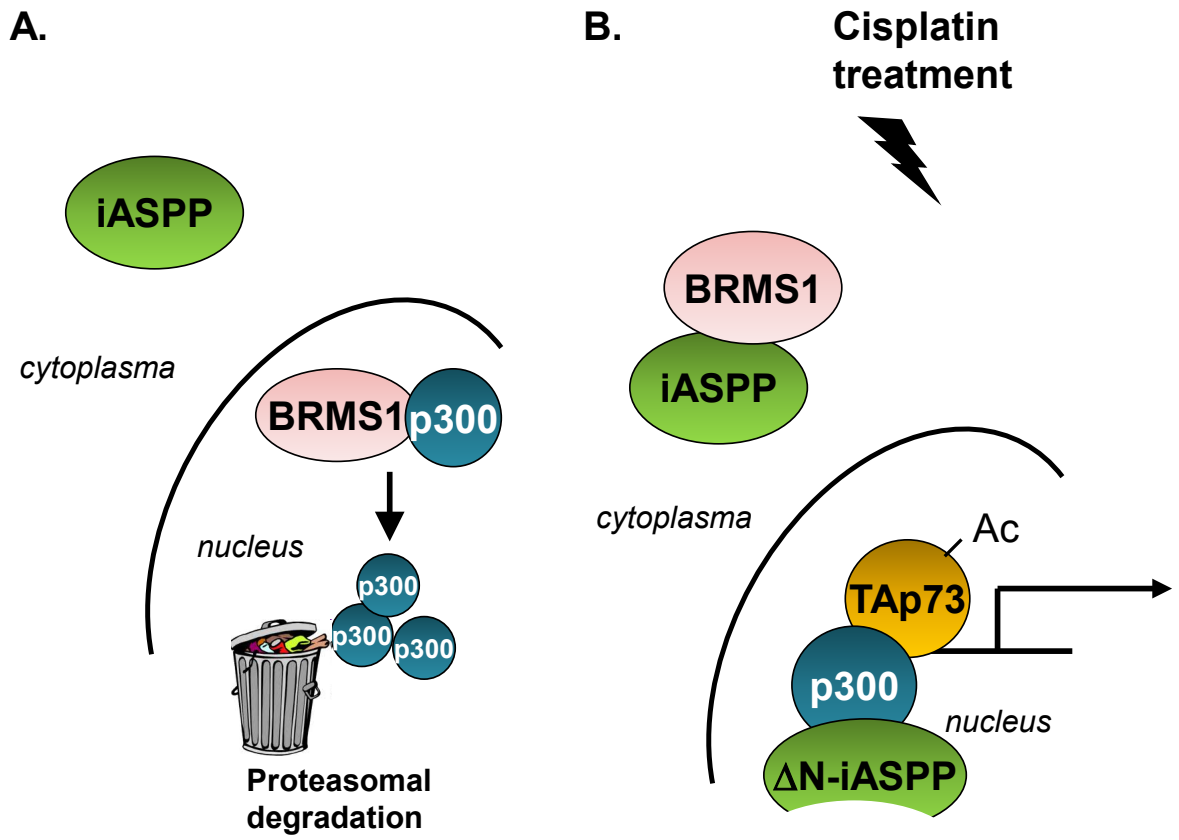

Figure 4.2. Subcellular localization as a possible determinant for the functional interaction of iASPP and p300.
A. BRMS1 mediates the degradation of p300 in the nucleus. *In untreated cells, p300 is degraded by BRMS1 in the nucleus. IASPP cannot inhibit this degradation as it localizes to the cytoplasm.*
B. iASPP enhances the protein stability of p300 by cytoplasmic sequestration of BRMS1. *After cisplatin treatment, BRMS1 is exported from the nucleus followed by its*

cytoplasmic sequestration though interaction with iASPP. Thus, p300 accumulates in the nucleus, probably due to its interaction with N-terminal, caspase-cleaved iASPP, and subsequently mediates the activation of TAp73 by acetylation. Finally, cisplatin treatment triggers p300-dependent apoptosis.

Nevertheless, a direct interaction of BRMS1 and iASPP in cisplatin-treated cells represents an alternative hypothesis that can explain iASPP-mediated inhibition of p300 degradation. Therefore, an interaction between cytoplasmic iASPP and BRMS1 in cisplatin-treated cells could induce a cytoplasmic sequestration of BRMS1, which then anticipates BRMS1-mediated, nuclear degradation of p300 (Figure 4.2B). Hence, we will have to elucidate if iASPP can directly interact with BRMS1 and if this interaction takes place in the nucleus or cytoplasm of the cell. Concluding, if cisplatin treatment does not alter the cytoplasmic localization of iASPP, we could explain the effects of iASPP knockdown on p300 protein stability by the fact that iASPP regulates the sub-cellular localization of BRMS1.

To test this, we could perform localization studies of BRMS1 in cisplatin-treated control and iASPP knockdown cells by applying immunofluorescence staining. However, we cannot exclude a BRMS1-mediated cytoplasmic degradation of p300 and CBP at the moment. Therefore, we will also have to perform co-immunoprecipitation experiments of BRMS1, p300 and iASPP using purified nuclear and cytoplasmic extracts of cisplatin-treated cells as input. This experiment will not only determine the localization of iASPP-p300 and BRMS1-p300 complexes, but also validate or reject our current working hypothesis (Figure 4.1). Figure 4.2 summarizes, how iASPP-mediated regulation of the sub-cellular localization of BRMS1 can control p300 level.

Interestingly, it has been shown before that the sub-cellular localization of BRMS1 modifies its function (Slipicevic, Holm et al. 2012). In melanoma, they discovered that cytoplasmic localization of BRMS1 was associated with disease-free survival of patients, whereas nuclear localization of BRMS1 correlated with metastasis and poor survival rate of the patients. Accordingly, we found that BRMS1 mediates the proteasomal degradation of p300 in some but not all cisplatin-treated melanoma cell lines (Figure 3.14). Therefore, iASPP-mediated cytoplasmic localization of BRMS1 could lead to the promotion of the anti-metastatic functions of BRMS1 that are likely to be independent of p300 and CBP. Hence, in low iASPP-expressing melanoma cells, BRMS1 could become localized to the nucleus, thereby probably mediating the proteasomal degradation of p300/CBP. Consequently, nuclear BRMS1 could be responsible for the frequently detected low levels of p300 and CBP in cisplatin-treated melanoma cell lines and could therefore contribute to chemoresistance (Figure 3.13).

However, another observation might also argue against an iASPP-mediated regulation of BRMS1 localization. In some of the analysed, cisplatin-treated melanoma cell lines we detected N-terminal truncated iASPP instead of the full-length protein (Appendix Sup-6A). The N-terminal truncation resulted from caspase cleavage of iASPP in the process of apoptosis induction (Appendix Sup-6A and Sup-6B). As the N-terminus of iASPP (consisting of amino acids 1-478) determines the cytoplasmic localization of full-length iASPP protein (Slee, Gillotin et al. 2004), N-terminal cleavage of iASPP at amino acid 296 might cut off a putative nuclear export signal. Thus, N-terminal truncated iASPP is getting localized to the nucleus. Similar results were obtained by Zhang and colleagues, who found a N-terminal truncated isoform of iASPP, called iASPP-SV, that predominantly localized to the nucleus (Zhang, Diao et al. 2007). Following, N-terminal cleavage of iASPP might induce its translocalization to the nucleus of cisplatin-treated cells, which then permits a complex formation between iASPP and nuclear p300 (Figure 4.2). Hence, nuclear localization of N-terminal cleaved iASPP would exclude an iASPP-mediated sequestration of BRMS1 in the cytoplasm of cisplatin-treated cells. We did not immunoprecipitate iASPP from p300-protein complexes (we only immunoprecipitated iASPP and detected co-bound p300; Figure 3.1). Therefore we cannot exclude that N-terminal truncated iASPP is binding to p300 instead of full-length iASPP. We will have to test this by further co-immunoprecipitation studies in cisplatin-treated melanoma cell lines, in which we will precipitate p300 and subsequently detect co-bound full length or N-terminal truncated iASPP by immunoblotting.

Nevertheless, sub-cellular localization of BRMS1 in melanoma cell lines has to be taken into consideration when describing BRMS1-mediated degradation of p300. We already showed that BRMS1 mediates the degradation of p300 and CBP in some of the analysed, cisplatin-treated melanoma cell lines (Figure 3.14). However, differential localization of BRMS1 might imply that not all melanoma cell lines will display BRMS1-mediated degradation of p300/CBP after cisplatin treatment of the cells. Concluding, it will be interesting to reveal if there is a correlation between BRMS1 localization and total protein level of iASPP. Therefore localization of p300, BRMS1 and iASPP in untreated and cisplatin-treated HCT116 and melanoma cell lines needs to be investigated in future experiments.

4.4. The pro- and anti-apoptotic function of iASPP depends on its interaction partners and external stimuli.

We did not find a direct interaction of TAp73 with iASPP in untreated or cisplatin-treated HCT116 cells. However, p300 becomes associated with TAp73 and iASPP in cisplatin-treated cells (Figure 3.1). Therefore p300 might mediate an indirect, functional interaction

between TAp73 and iASPP. Moreover we showed reduced protein stability of TAp73 in iASPP-depleted, cisplatin-treated HCT116 cells, similar to the effects of iASPP depletion on p300 level (Figure 3.2). As a consequence, we could show that iASPP depletion results in diminished recruitment of TAp73 to the chromatin, followed by overlapping loss of p300 and TAp73 binding to genomic p73 target gene promoters (Figure 3.3 and Figure 3.4). Therefore, we conclude that these effects on TAp73 function are likely to be the result of impaired p300 function in iASPP-depleted cells.

However, it has to be noted, that other reports depicted an inhibitory role for iASPP with respect to TAp73 function (Bell, Dufes et al. 2007; Cai, Qiu et al. 2012). Bell and colleagues showed that a fragment derived from the C-terminus of p53, called 37AA, can interfere with iASPP-p73 complex formation in the osteosarcoma cell line SaOS-2. Consequently, 37AA partially promoted TAp73-dependent apoptosis induction that is likely to be mediated through a transcriptionally independent, mitochondrial pathway (Bell et al, 2007). Though different from our results, these findings do not necessarily have to contradict ours, as we suggest a pro-apoptotic role for iASPP in chemotherapeutic drug-induced, TAp73-mediated apoptosis. Previous publications failed to analyse the effects of iASPP expression after chemotherapy leading to active TAp73 (Bell, Dufes et al. 2007; Cai, Qiu et al. 2012). Therefore, iASPP might inhibit TAp73 function in untreated cells; though after DNA damage, we found that iASPP helps to activate the pro-apoptotic function of TAp73.

4.5. iASPP specifically regulates the p300-specific function towards TAp73, while p53 remains unaffected.

Importantly, p300 can also function as a co-activator of p53 (Grossman 2001). Therefore, we also analysed p53 function in respect to its chromatin localization and DNA-binding affinities in iASPP-depleted, cisplatin-treated HCT116 cells (Figure 3.3). Surprisingly, p53 seemed to remain unaffected by the functional impairment of p300 that results from iASPP knockdown. This result is unexpected as it has been shown before that cisplatin treatment leads to p300-mediated acetylation of p53 at lysine residue 382 (Gu and Roeder 1997; Sakaguchi, Herrera et al. 1998). Consequently, cisplatin-induced acetylation of p53 promotes an increase in p53`s protein stability and DNA-binding affinity (Luo, Li et al. 2004). Thus, impaired p300 function should also affect the DNA-binding properties of p53.

The molecular basis of this differential, iASPP-mediated effect on p53-family function might consist in the different binding sites that mediate the interaction of p300 with TAp73 and p53. P53 mainly interacts with the C-terminal CH3 and IBID domains of p300, while binding of

p300 to TAp73 protein is mediated by its central located CH1 and CH2 regions (Zeng, Li et al. 2000; Burge, Teufel et al. 2009; Chen and Li 2011). Thus, iASPP may impede with only one of these interactions.

Moreover, p53-p300 interaction might interfere with BRMS1-mediated proteasomal degradation of p300, as BRMS1 binds to the C-terminal located IBID domain of p300, as well (Liu, Mayo et al. 2013). Concluding, p53-associated p300 is likely to be fully protected from BRMS1-dependent degradation, thus making an iASPP-dependent regulation of BRMS1-mediated degradation of p300 dispensable. In contrast, TAp73-associated p300 can be theoretically degraded by BRMS1. Therefore, iASPP-p300 interaction is likely to be indispensable for effective activation of TAp73 by p300.

The structure of iASPP comprises a SH3 domain that is located at the C-terminus of the protein. SH3 domains preferentially recognize proline-rich regions of target proteins, hence leading to the interaction of a SH3 domain containing protein with a proline-rich region containing target protein (Alexandropoulos, Cheng et al. 1995; Kay, Williamson et al. 2000). Therefore, although binding sites of an iASPP-p300 interaction are not discovered yet, iASPP is likely to bind to the C-terminal located proline-rich region of p300. As a consequence, iASPP-p300 interaction will exclude simultaneously binding of BRMS1 or p53 to p300 protein. This hypothesis would not only explain why iASPP depletion leads to impaired TAp73 function while p53 remains unaffected, it might also underscore our working hypothesis that BRMS1-p300 and iASPP-p300 interaction are mutually exclusive.

Of note, we cannot exclude that iASPP knockdown affects p53 function in other cell lines or after different stimuli as well, as we do not know yet which domains of p300 are binding to iASPP. Therefore, we will have to over-express different p300 fragments and co-immunoprecipitate these fragments with iASPP. Moreover, we will also have to detect acetylated p53 level, in different chemotherapeutic drug-treated cell lines, in the presence or absence of iASPP. Thus, we will elucidate if iASPP knockdown also affects the co-activator role of p300 in p53-mediated apoptosis in some cell lines.

4.6. DNA damage constitutes a pre-requisite for functional interaction of p300, TAp73 and iASPP.

We showed that iASPP can only regulate the function of p300 and TAp73 after DNA damage (Figure 3.1 and Figure 3.2). We propose that the complex formation between iASPP and p300 as well as the one between p300 and TAp73 in cisplatin-treated cells represents a pre-requisite for iASPP`s regulatory functions on p300. Concluding, cisplatin treatment might

activate enzymes that cause post-translational modifications of p300 or iASPP. Hence, this post-translational modification might represent a pre-requisite for interaction of iASPP and p300, either through conformational changes of the proteins or by recruitment of additional co-factors to iASPP-p300 complexes.

P38 constitutes one candidate protein that has been shown before to post-translationally modify p300 after DNA damage (Poizat, Puri et al. 2005; Ogiwara and Kohno 2012). Ogiwara and colleagues revealed that cisplatin treatment induced p38- and Akt-mediated phosphorylation of p300 at serine residue 1834, thus contributing to the activation of the protein (Ogiwara and Kohno 2012). Moreover, others have shown that p38 constitutes a protein that is getting activated by cisplatin-treatment, thus contributing to cisplatin-induced apoptosis induction (Sanchez-Prieto, Sanchez-Arevalo et al. 2002).

Interestingly, iASPP knockdown only affected p300 and TAp73 function after cisplatin treatment. Therefore, and also due to the fact that p38 can modify p300 function, we investigated if p38 contributes to the functional interaction of iASPP and p300.

Our preliminary data indicate, that over-expression of iASPP increases the level of phosphorylated p38 (Figure 3.17A), whereas iASPP knockdown decreases the activity of p38 in melanoma cells (Figure 3.17B). Thus, iASPP is likely to regulate the activity of p38. Following, additional treatment of iASPP-depleted, cisplatin-treated HCT116 cells with the p38 inhibitor SB203580 seems to intensify the diminished protein level of p300 (Figure 3.17C). In contrast, treatment with BCI, an inhibitor of the p38 dephosphatase MKP-1, could partially re-establish p300 protein level in low iASPP expressing melanoma cell lines. Concluding, we suggest that p38-mediated phosphorylation of p300 might contribute to the functional interaction of iASPP and p300. Additionally, it might also impede BRMS1-mediated degradation of p300. Following, we will have to analyse iASPP-p300 complex formation, in the presence or absence of p38 inhibitor. Moreover, BRMS1 knockdown in BCI-treated cells will elucidate if p38-mediated phosphorylation of p300 can modify BRMS1-p300 interaction. If so, it will be possible to equalize the p300 protein level in untreated cells to the protein level of p300 in BCI-treated cells by additional knockdown of BRMS1.

In line with our hypothesis, researchers detected an over-expression of MKP-1 in some melanoma cells. Hence, MKP-1 over-expressing melanoma cell lines displayed increased chemoresistance which was abolished by treatment of the cells with the MKP-1 inhibitor TPI-3 (Kundu, Fan et al. 2010). Thus, over-expression of MKP-1 or down-regulation of iASPP could be mutually exclusive in melanoma as both mechanisms contribute to the functional

inactivation of p300. Consequently, we will have to test if the expression of iASPP and MKP-1 activity is inversely correlating in melanoma tissue or not.

However, we should also keep in mind that other post-translational modifications of p300 might determine the functional interaction of p300 and iASPP. For example, it has been shown before, that ERK1 and ERK2 can phosphorylate p300. Moreover, the MKP-1 inhibitor BCI can inhibit the activity of the ERK1 and ERK2 dephosphatase MKP-3, as well (Molina, Vogt et al. 2009). Therefore, re-establishment of p300 level by BCI treatment can also derive from inhibition of MKP-3 rather than from inhibition of MKP-1 (Figure 3.18). Accordingly, MKP-3 over-expression has been detected in melanoma as well (Li et al, 2012). Following, we will have to dissect the molecular mechanism underlying BCI treatment-mediated re-establishment of p300 level in melanoma cells. Knockdown experiments of p38, ERK1 or ERK2, followed by BCI-treatment of melanoma cells, will reveal if re-establishment of p300 level depends on re-activation of p38, ERK1 or ERK2.

4.7. Malignant melanoma are characterized by down-regulated iASPP expression.

As iASPP enhances the co-activator function of p300 in cisplatin-induced, TAp73-mediated apoptosis induction, we concluded, that there have to exist tumours that display a down-regulation in iASPP expression. As a consequence, low expression of iASPP could lead to functional inactivation of p300 and therefore possibly to chemoresistance and tumourigenesis as well. We re-analysed multiple gene expression studies of various cancer types that have been published before. Hence, statistical evaluation of 3 independent gene expression studies displayed a significant down-regulation of iASPP mRNA levels in malignant melanoma compared to normal skin tissue and benign nevi (Figure 3.12 and Appendix Sup-5). Therefore, our findings describe for the first time a cancer type that is associated with decreased iASPP expression, whereas other researchers have only detected an over-expression of iASPP in various tumour types (Zhang, Wang et al. 2005; Jiang, Siu et al. 2011; Li, Wang et al. 2011; Cao, Huang et al. 2013). Of note, these studies elucidated an increase of iASPP on protein level rather than on mRNA level (Cao, Huang et al. 2013). Another study failed to show significant differences in iASPP mRNA level of cancer tissue compared to normal tissue samples (Li, Wang et al. 2011).

Protein level and mRNA level do not necessarily have to correlate. In order to validate our findings of down-regulated iASPP mRNA levels in malignant melanoma, we analysed the protein levels of iASPP in several untreated and cisplatin-treated melanoma cell lines (Figure 3.13). We were able to detect decreased iASPP protein level in untreated and cisplatin-

treated melanoma cells, compared to other, tumourigenic cell lines. However, we lack a comparative analysis with melanocytes, that represent the origin cell type from which melanoma evolve (Elder 1999). Therefore it is difficult to conclude if iASPP protein levels are decreased in the process of melanocyte transformation or not. Nevertheless, analysis of iASPP protein level in melanoma cell lines compared to other cancer cell lines could validate an overall down-regulation of iASPP at protein level.

Of note, Lu and colleagues reported that melanoma tissue and melanoma cell lines are characterized by high expression of nuclear cyclin B1/CDK1-phosphorylated iASPP (Lu, Breyssens et al. 2013). This hyperphosphorylated form could be detected as a slow-migrating isoform of iASPP in denaturating polyacrylamide gels. Following, they stated that cyclin B1/CDK1-phosphorylated iASPP contributes to the frequently observed inactivation of p53 in melanoma, thus promoting chemoresistance (Avery-Kiejda, Bowden et al. 2011). So far, we could not detect a slower migrating isoform of iASPP in the melanoma cell lines we analysed (data not shown). However, their findings do not necessarily have to contradict our results. It might be, that iASPP is down-regulated in the majority of melanoma tumours. However those melanoma that still display high iASPP expression might harbour constitutive expression of cyclin B1/CDK1 instead. Constitutively active cyclin B1/CDK1 might then lead to a change in iASPP function, which would also imply a loss of its co-activator function for p300. Accordingly, over-expression of cyclin B1/CDK1 can be frequently detected in melanoma (Georgieva, Sinha et al. 2001; Stefanaki, Stefanaki et al. 2007; Avery-Kiejda, Bowden et al. 2011). On the other hand, we suggest that low iASPP expressing melanoma should have normal cyclin B1/CDK1 activity. However, we have not yet analysed this possible correlation of iASPP expression level and cyclin B1/CDK1 activity.

4.8. Does cisplatin treatment of melanoma cell lines constitute a model for analysing chemoresistance in melanoma?

We suggest that low iASPP expression in melanoma contributes to a functional inactivation of p300 and therefore promotion of chemoresistance. Following, we could detect in some of the low iASPP-expressing melanoma cell lines down-regulated p300 protein level after treatment of the cells with cisplatin (Figure 3.13B). Nevertheless, protein level of p300 did not correlate with the overall induction of cisplatin-induced apoptosis as shown by detection of PARP1 cleavage (Figure 3.13B). Interestingly, clinical studies revealed that in-vivo, melanoma have a low response rate (~10%) to cisplatin (Bhatia, Tykodi et al. 2009). Therefore, cisplatin is only used in combination with other chemotherapeutic drugs for treatment of melanoma (Legha, Ring et al. 1996; Daponte, Ascierto et al. 2005). As we could

detect strong cisplatin-induced apoptosis in most of the melanoma cell lines, it might be that 2D cultures of melanoma cell lines do not correctly reflect the in-vivo situation of malignant melanoma. Therefore, we should investigate the function of iASPP and p300 in the development of chemoresistance in 3D cell culture or in xenograft mouse models using stable iASPP or p300 knockdown melanoma cell lines. These experiments would reflect the situation in melanoma patients more realistically.

Furthermore, we suggest to exchange cisplatin with dacarbazine, one of the few FDA-approved chemotherapeutical drugs for treatment of malignant melanoma (Serrone and Hersey 1999; Finn, Markovic et al. 2012). Dacarbazine represents an alkylating agent that triggers DNA damage by adding an alkyl group to DNA, hence inducing pro-apoptotic pathways that can be compared to those that are induced by cisplatin treatment (Bergamaschi, Gasco et al. 2003; Marchesini, Bono et al. 2007; Sanada, Hidaka et al. 2007). Therefore, it will be interesting to investigate the impact of iASPP, p300 and BRMS1 expression on dacarbazine-induced apoptosis in melanoma cell lines. It is not clear though, if dacarbazine can be applied in cell culture experiments or if it needs to be metabolised in the liver to become activated (Reid, Kuffel et al. 1999; Lev, Onn et al. 2004).

4.9. Functional inactivation of p300 represents a possible mechanism that contributes to melanoma progression and metastatic transformation.

Our preliminary data of p300 knockdown experiments in the melanoma cell line A375 suggest that p300 has a crucial role in chemotherapy-induced apoptosis of melanoma cell lines (Figure 3.19). This might be explained by the co-activator role of p300 in p53-, or TAp73-mediated apoptosis after DNA damage (Costanzo, Merlo et al. 2002; Ianari, Gallo et al. 2004; Iyer, Chin et al. 2004). As TAp73 expression is mostly not detectable in melanoma, functional inactivation of p300 might contribute to the frequently observed inactivation of p53 then (Tsao, Zhang et al. 1999; Bardeesy, Bastian et al. 2001; Alla, Engelmann et al. 2010).

In line, some researchers discovered that functional inactivation of p53 in integrin-αV over-expressing melanoma cells is caused by the integrin-dependent functional inactivation of p300 (Bao and Stromblad 2004). They showed that integrin-αV prohibited p300-mediated acetylation of p53 at lysine residue 382, due to an integrin-dependent proteasomal degradation of the p300 protein. Accordingly, over-expression of integrin-αV can be frequently detected in melanoma and correlates with tumour growth, cell survival, cell invasion and promotion of metastasis (Hsu, Shih et al. 1998; Petitclerc, Stromblad et al. 1999).

Investigation of the proto-oncogene DEK in melanoma further underscores a possible role for p300 in determining the chemosensitivity of malignant melanoma. DEK constitutes a chromatin-remodelling factor that has been shown to be frequently over-expressed in melanoma due to chromosome 6p amplification (Santos, Zielenska et al. 2007; Khodadoust, Verhaegen et al. 2009). Interestingly, DEK over-expression leads to inhibition of DNA damage-induced apoptosis in melanoma, and this partially derives from DEK-mediated inhibition of the HAT activity of p300 (Ko, Lee et al. 2006; Wise-Draper, Allen et al. 2006; Khodadoust, Verhaegen et al. 2009).

In summary, integrin-αV as well as DEK over-expression can cause a functional inactivation of p300 in melanoma. As a consequence, the tumour suppressive function of p300 is impaired, thus contributing to p53 inactivation-dependent chemoresistance. Both studies validate p300 as a possible re-activation target in melanoma therapy. It might be worth to investigate if integrin-αV or DEK over-expression is present in those melanoma that retain normal iASPP level. Accordingly, low iASPP expression in melanoma could then correlate with moderate integrin-αV and DEK expression. Concluding, this correlation analysis would underscore our hypothesis that low iASPP expression might be a cause of functional inactivation of p300 in melanoma.

4.10. Treatment of low iASPP expressing melanoma with the p300 activator CTB fails to re-establish p300 level and function.

Recently, small molecules have been extracted from natural substances that specifically modulate the HAT activity of p300 and CBP (Balasubramanyam, Swaminathan et al. 2003). CTB [N-(4-chloro-3-trifluoromethyl-phenyl)-2-ethoxybenzamide] is a p300-activating substance that had been extracted from anacardic acid. Dissection of its binding properties showed that CTB enhances the HAT activity of p300 through conformational changes of the protein (Mantelingu, Kishore et al. 2007; Devipriya, Parameswari et al. 2010).

We investigated, if we could increase or re-establish p300 function in different cell lines by applying CTB alone or in combination with cisplatin. CTB treatment of MEF cells resulted in elevated expression of p300 as well as increased induction of cisplatin-mediated apoptosis (Figure 3.15). This finding motivated us to try CTB treatment in melanoma cells. However, CTB alone in combination with cisplatin could not re-establish p300 levels in low iASPP-expressing melanoma cells or iASPP knockdown HCT116 cells (Figure 3.16). One reason for this failure might derive from impaired expression of iASPP. We could show that iASPP does not only regulate p300 function but also controls the activity of p38 (Figure 3.17). Thus, if p38

contributes to both the regulation of p300 level and function, CTB-mediated re-activation of p300 will not compensate for diminished p38 activity.

Moreover, as CTB was shown to bind to the HAT domain rather than to the C-terminus of p300, we suggest that CTB treatment cannot abrogate BRMS1-mediated degradation of p300 in cisplatin-treated, iASPP knockdown cells. Following, CTB will bind p300 and partially activate the HAT domain, but it will fail to increase p300 expression on protein level.

Concluding, we suggest that CTB treatment of tumourigenic cell lines alone or in combination with other drugs does not constitute a reasonable therapeutically approach for re-activation of p300.

4.11. iASPP expression levels in melanocytes and melanoma may regulate the specific function of p300 in melanoma.

The function of p300 in melanocytes and melanoma development has not been intensively investigated. However, knockdown of p300 in melanocytes and melanoma cell lines resulted in cellular senescence due to inhibition of Cyclin E expression (Bandyopadhyay, Okan et al. 2002). Moreover, chemical inhibition of its HAT activity in melanoma cell lines resulted in both cell growth arrest and cellular senescence (Yan, Eller et al. 2013). Cellular senescence has been implicated as a tumour suppressive function of cells, thus abrogating uncontrolled proliferation of cells. Therefore, loss of p300 might trigger oncogene-driven cellular senescence in melanocytes and nevi. As a consequence, senescence prevents melanocyte transformation and subsequently the development of melanoma (Michaloglou, Vredeveld et al. 2005). In line with this argumentation, p300 might represent a proto-oncogene in melanocytes, and functional inactivation of p300 might contribute to the suppression of melanocyte transformation.

However, cellular senescence also implicates a low rate of apoptosis induction after treatment of the cells with chemotherapeutical drugs. Due to their quiescent status, senescent cells tolerate chemotherapeutical-drug induced DNA-damage, thereby failing to induce apoptosis after chemotherapy treatment (Achuthan, Santhoshkumar et al. 2011). Consequently, senescent cells might survive chemotherapy, followed by re-establishment of tumour cell proliferation and re-occurrence of tumours at a later time point. Therefore, loss of p300 function and following cellular senescence might promote chemoresistance and formation of metastasis in melanoma. Concluding, p300 might also be proclaimed as a tumour suppressor in primary and malignant melanoma.

Concluding, this possible proto-oncogenic and tumour suppressive role of p300 is likely to be cell context-dependent. P300-related co-factors might influence these functions of p300, and we suggest that iASPP represents such a regulatory switch for p300 function. IASPP could promote the tumour suppressive role of p300 in melanoma whereas it could suppress the proto-oncogenic functions of p300 in melanocytes and some subtypes of melanoma.

Summing up our findings, we showed that iASPP is regulating the protein stability and function of p300. Consequently, iASPP can promote TAp73 activation as well as TAp73`s pro-apoptotic role in cisplatin-induced apoptosis by regulation of p300 protein level. Moreover, iASPP expression is down-regulated in melanoma and might constitute a biomarker for the chemosensitivity of tumours. It still needs to be revealed if re-activation of p300 might be a new therapeutical approach for treatment of malignant melanoma, that display low expression levels of iASPP.

.

5. References

Achuthan, S., T. R. Santhoshkumar, et al. (2011). "Drug-induced senescence generates chemoresistant stemlike cells with low reactive oxygen species." J Biol Chem **286**(43): 37813-37829.

Adams, K. E., A. L. Medhurst, et al. (2006). "Recruitment of ATR to sites of ionising radiation-induced DNA damage requires ATM and components of the MRN protein complex." Oncogene **25**(28): 3894-3904.

Agami, R., G. Blandino, et al. (1999). "Interaction of c-Abl and p73alpha and their collaboration to induce apoptosis." Nature **399**(6738): 809-813.

Ahn, J., I.-J. L. Byeon, et al. (2009). "Insight into the structural basis of pro- and antiapoptotic p53 modulation by ASPP proteins." The Journal of biological chemistry **284**(20): 13812-13822.

Ait-Si-Ali, S., A. Polesskaya, et al. (2000). "CBP/p300 histone acetyl-transferase activity is important for the G1/S transition." Oncogene **19**(20): 2430-2437.

Alexandropoulos, K., G. Cheng, et al. (1995). "Proline-rich sequences that bind to Src homology 3 domains with individual specificities." Proc Natl Acad Sci U S A **92**(8): 3110-3114.

Alla, V., D. Engelmann, et al. (2010). "E2F1 in melanoma progression and metastasis." J Natl Cancer Inst **102**(2): 127-133.

Allocati, N., C. Di Ilio, et al. (2012). "p63/p73 in the control of cell cycle and cell death." Experimental cell research **318**(11): 1285-1290.

Arany, Z., W. R. Sellers, et al. (1994). "E1A-associated p300 and CREB-associated CBP belong to a conserved family of coactivators." Cell **77**(6): 799-800.

Avantaggiati, M. L., V. Ogryzko, et al. (1997). "Recruitment of p300/CBP in p53-Dependent Signal Pathways." Cell **89**(7): 1175-1184.

Avery-Kiejda, K. A., N. A. Bowden, et al. (2011). "P53 in human melanoma fails to regulate target genes associated with apoptosis and the cell cycle and may contribute to proliferation." BMC Cancer **11**: 203.

Balasubramanyam, K., V. Swaminathan, et al. (2003). "Small molecule modulators of histone acetyltransferase p300." J Biol Chem **278**(21): 19134-19140.

Bandyopadhyay, D., N. Okan, et al. (2002). "Down-regulation of p300/CBP histone acetyltransferase activates a senescence checkpoint in human melanocytes." Cancer research **62**(21): 6231-6239.

Bao, W. and S. Stromblad (2004). "Integrin alphav-mediated inactivation of p53 controls a MEK1-dependent melanoma cell survival pathway in three-dimensional collagen." J Cell Biol **167**(4): 745-756.

Bardeesy, N., B. C. Bastian, et al. (2001). "Dual Inactivation of RB and p53 Pathways in RAS-Induced Melanomas." Molecular and cellular biology **21**(6): 2144-2153.

Basu, A. and S. Krishnamurthy (2010). "Cellular responses to Cisplatin-induced DNA damage." Journal of nucleic acids **2010**.

Bedford, D. C. and P. K. Brindle (2012). "Is histone acetylation the most important physiological function for CBP and p300?" Aging (Albany NY) **4**(4): 247-255.

Bell, H., C. Dufes, et al. (2007). "A p53-derived apoptotic peptide derepresses p73 to cause tumor regression in vivo." The Journal of clinical investigation **117**(4): 1008-1018.

Bergamaschi, D., M. Gasco, et al. (2003). "p53 polymorphism influences response in cancer chemotherapy via modulation of p73-dependent apoptosis." Cancer cell **3**(4): 387-402.

Bergamaschi, D., Y. Samuels, et al. (2003). "iASPP oncoprotein is a key inhibitor of p53 conserved from worm to human." Nature genetics **33**(2): 162-167.

Bergamaschi, D., Y. Samuels, et al. (2006). "iASPP preferentially binds p53 proline-rich region and modulates apoptotic function of codon 72-polymorphic p53." Nature genetics **38**(10): 1133-1141.

Bernassola, F., P. Salomoni, et al. (2004). "Ubiquitin-dependent degradation of p73 is inhibited by PML." The Journal of experimental medicine **199**(11): 1545-1557.

Bhatia, S., S. Tykodi, et al. (2009). "Treatment of metastatic melanoma: an overview." Oncology (Williston Park.

Birkaya, B., K. Ortt, et al. (2007). "Novel in vivo targets of DeltaNp63 in keratinocytes identified by a modified chromatin immunoprecipitation approach." BMC Mol Biol **8**: 43.

Blagosklonny, M. V. (2000). "p53 from complexity to simplicity: mutant p53 stabilization, gain-of-function, and dominant-negative effect." FASEB J **14**(13): 1901-1907.

Blobel, G. A. (2002). "CBP and p300: versatile coregulators with important roles in hematopoietic gene expression." J Leukoc Biol **71**(4): 545-556.

Bode, A. M. and Z. Dong (2004). "Post-translational modification of p53 in tumorigenesis." Nat Rev Cancer **4**(10): 793-805.

Brosh, R. and V. Rotter (2009). "When mutants gain new powers: news from the mutant p53 field." Nat Rev Cancer **9**(10): 701-713.

Bulavin, D. V., S. Saito, et al. (1999). "Phosphorylation of human p53 by p38 kinase coordinates N-terminal phosphorylation and apoptosis in response to UV radiation." EMBO J **18**(23): 6845-6854.

Burge, S., D. Teufel, et al. (2009). "Molecular basis of the interactions between the p73 N terminus and p300: effects on transactivation and modulation by phosphorylation." Proceedings of the National Academy of Sciences of the United States of America **106**(9): 3142-3147.

Cai, Y., S. Qiu, et al. (2012). "iASPP inhibits p53-independent apoptosis by inhibiting transcriptional activity of p63/p73 on promoters of proapoptotic genes." Apoptosis **17**(8): 777-783.

Cao, L., Q. Huang, et al. (2013). "Elevated expression of iASPP correlates with poor prognosis and chemoresistance/radioresistance in FIGO Ib1-IIa squamous cell cervical cancer." Cell and tissue research **352**(2): 361-369.

Casciano, I., K. Mazzocco, et al. (2002). "Expression of DeltaNp73 is a molecular marker for adverse outcome in neuroblastoma patients." Cell Death Differ **9**(3): 246-251.

Chae, Y. S., J. G. Kim, et al. (2013). "PPP1R13L variant associated with prognosis for patients with rectal cancer." J Cancer Res Clin Oncol **139**(3): 465-473.

Chan, W. I., R. L. Hannah, et al. (2011). "The transcriptional coactivator Cbp regulates self-renewal and differentiation in adult hematopoietic stem cells." Mol Cell Biol **31**(24): 5046-5060.

Chen, J. and Q. Li (2011). "Life and death of transcriptional co-activator p300." Epigenetics **6**(8): 957-961.

Chen, J., J. St-Germain, et al. (2005). "B56 regulatory subunit of protein phosphatase 2A mediates valproic acid-induced p300 degradation." Molecular and cellular biology **25**(2): 525-532.

Chen, L. F., S. A. Williams, et al. (2005). "NF-kappaB RelA phosphorylation regulates RelA acetylation." Mol Cell Biol **25**(18): 7966-7975.

Chen, Y. J., Y. N. Wang, et al. (2007). "ERK2-mediated C-terminal serine phosphorylation of p300 is vital to the regulation of epidermal growth factor-induced keratin 16 gene expression." J Biol Chem **282**(37): 27215-27228.

Chikh, A., R. Matin, et al. (2011). "iASPP/p63 autoregulatory feedback loop is required for the homeostasis of stratified epithelia." EMBO J **30**(20): 4261-4273.

Cicek, M., R. Fukuyama, et al. (2009). "BRMS1 contributes to the negative regulation of uPA gene expression through recruitment of HDAC1 to the NF-kappaB binding site of the uPA promoter." Clin Exp Metastasis **26**(3): 229-237.

Cicek, M., R. S. Samant, et al. (2004). "Identification of metastasis-associated proteins through protein analysis of metastatic MDA-MB-435 and metastasis-suppressed BRMS1 transfected-MDA-MB-435 cells." Clin Exp Metastasis **21**(2): 149-157.

Codelia, V., M. Cisterna, et al. (2010). "p73 participates in male germ cells apoptosis induced by etoposide." Molecular human reproduction **16**(10): 734-742.

Conforti, F., A. E. Sayan, et al. (2012). "Regulation of p73 activity by post-translational modifications." Cell Death Dis **3**: e285.

Costanzo, A., P. Merlo, et al. (2002). "DNA damage-dependent acetylation of p73 dictates the selective activation of apoptotic target genes." Molecular cell **9**(1): 175-186.

Crowley, J. A., Y. Wang, et al. (2005). "Detection of MOZ-CBP fusion in acute myeloid leukemia with 8;16 translocation." Leukemia **19**(12): 2344-2345.

Daponte, A., P. A. Ascierto, et al. (2005). "Temozolomide and cisplatin in avdanced malignant melanoma." Anticancer Res **25**(2B): 1441-1447.

Das, C., M. S. Lucia, et al. (2009). "CBP/p300-mediated acetylation of histone H3 on lysine 56." Nature **459**(7243): 113-117.

de Vries, A., E. R. Flores, et al. (2002). "Targeted point mutations of p53 lead to dominant-negative inhibition of wild-type p53 function." Proc Natl Acad Sci U S A **99**(5): 2948-2953.

Debes, J. D., T. J. Sebo, et al. (2003). "p300 in prostate cancer proliferation and progression." Cancer Res **63**(22): 7638-7640.

Denissov, S., M. van Driel, et al. (2007). "Identification of novel functional TBP-binding sites and general factor repertoires." EMBO J **26**(4): 944-954.

Devipriya, B., A. Parameswari, et al. (2010). "Exploring the binding affinities of p300 enzyme activators CTPB and CTB using docking method."

Deyoung, M. and L. Ellisen (2007). "p63 and p73 in human cancer: defining the network." Oncogene **26**(36): 5169-5183.

di Bari, M. G., L. Ciuffini, et al. (2006). "c-Abl acetylation by histone acetyltransferases regulates its nuclear-cytoplasmic localization." EMBO Rep **7**(7): 727-733.

Douc-Rasy, S., M. Barrois, et al. (2002). "DeltaN-p73alpha accumulates in human neuroblastic tumors." Am J Pathol **160**(2): 631-639.

Eckner, R., M. E. Ewen, et al. (1994). "Molecular cloning and functional analysis of the adenovirus E1A-associated 300-kD protein (p300) reveals a protein with properties of a transcriptional adaptor." Genes Dev **8**(8): 869-884.

Elder, D. (1999). "Tumor progression, early diagnosis and prognosis of melanoma." Acta Oncol **38**(5): 535-547.

Espinosa, J. M. (2008). "Mechanisms of regulatory diversity within the p53 transcriptional network." Oncogene **27**(29): 4013-4023.

Faiola, F., X. Liu, et al. (2005). "Dual regulation of c-Myc by p300 via acetylation-dependent control of Myc protein turnover and coactivation of Myc-induced transcription." Mol Cell Biol **25**(23): 10220-10234.

Faridoni-Laurens, L., S. Tourpin, et al. (2008). "Involvement of N-terminally truncated variants of p73, deltaTAp73, in head and neck squamous cell cancer: a comparison with p53 mutations." Cell Cycle **7**(11): 1587-1596.

Fernandes-Alnemri, T., G. Litwack, et al. (1994). "CPP32, a novel human apoptotic protein with homology to Caenorhabditis elegans cell death protein Ced-3 and mammalian interleukin-1 beta-converting enzyme." Journal of Biological ….

Finn, L., S. Markovic, et al. (2012). "Therapy for metastatic melanoma: the past, present, and future." BMC medicine **10**: 23.

Fontemaggi, G., I. Kela, et al. (2002). "Identification of direct p73 target genes combining DNA microarray and chromatin immunoprecipitation analyses." The Journal of biological chemistry **277**(45): 43359-43368.

Franklin, C. C. and A. S. Kraft (1997). "Conditional expression of the mitogen-activated protein kinase (MAPK) phosphatase MKP-1 preferentially inhibits p38 MAPK and stress-activated protein kinase in U937 cells." J Biol Chem **272**(27): 16917-16923.

Galan-Moya, E. M., J. Hernandez-Losa, et al. (2008). "c-Abl activates p38 MAPK independently of its tyrosine kinase activity: Implications in cisplatin-based therapy." Int J Cancer **122**(2): 289-297.

Galluzzi, L., L. Senovilla, et al. (2012). "Molecular mechanisms of cisplatin resistance." Oncogene **31**(15): 1869-1883.

Garber, J. E. and K. Offit (2005). "Hereditary cancer predisposition syndromes." J Clin Oncol **23**(2): 276-292.

Gayther, S. A., S. J. Batley, et al. (2000). "Mutations truncating the EP300 acetylase in human cancers." Nat Genet **24**(3): 300-303.

Georgieva, J., P. Sinha, et al. (2001). "Expression of cyclins and cyclin dependent kinases in human benign and malignant melanocytic lesions." J Clin Pathol **54**(3): 229-235.

Gillotin, S. and X. Lu (2011). "The ASPP proteins complex and cooperate with p300 to modulate the transcriptional activity of p53." FEBS letters **585**(12): 1778-1782.

Gong, J., A. Costanzo, et al. (1999). "The tyrosine kinase c-Abl regulates p73 in apoptotic response to cisplatin-induced DNA damage." Nature **399**(6738): 806-809.

Goodman, R. H. and S. Smolik (2000). "CBP/p300 in cell growth, transformation, and development." Genes Dev **14**(13): 1553-1577.

Graham, F. L. and A. J. van der Eb (1973). "A new technique for the assay of infectivity of human adenovirus 5 DNA." Virology **52**(2): 456-467.

Grossman, S. (2001). "p300/CBP/p53 interaction and regulation of the p53 response." European journal of biochemistry / FEBS **268**(10): 2773-2778.

Gu, W. and R. G. Roeder (1997). "Activation of p53 sequence-specific DNA binding by acetylation of the p53 C-terminal domain." Cell **90**(4): 595-606.

Guan, M. and Y. Chen (2005). "Aberrant expression of DeltaNp73 in benign and malignant tumours of the prostate: correlation with Gleason score." J Clin Pathol **58**(11): 1175-1179.

Gusterson, R., B. Brar, et al. (2002). "The transcriptional co-activators CBP and p300 are activated via phenylephrine through the p42/p44 MAPK cascade." J Biol Chem **277**(4): 2517-2524.

Hanahan, D. and R. A. Weinberg (2000). "The hallmarks of cancer." Cell **100**(1): 57-70.

Haqq, C., M. Nosrati, et al. (2005). "The gene expression signatures of melanoma progression." Proc Natl Acad Sci U S A **102**(17): 6092-6097.

Haupt, Y., R. Maya, et al. (1997). "Mdm2 promotes the rapid degradation of p53." Nature **387**(6630): 296-299.

Hsu, M. Y., D. T. Shih, et al. (1998). "Adenoviral gene transfer of beta3 integrin subunit induces conversion from radial to vertical growth phase in primary human melanoma." Am J Pathol **153**(5): 1435-1442.

Huang, W. C. and C. C. Chen (2005). "Akt phosphorylation of p300 at Ser-1834 is essential for its histone acetyltransferase and transcriptional activity." Mol Cell Biol **25**(15): 6592-6602.

Hurst, D., Y. Xie, et al. (2013). "The C-terminal putative nuclear localization sequence of breast cancer metastasis suppressor 1, BRMS1, is necessary for metastasis suppression." PloS one **8**(2).

Hurst, D. R., Y. Xie, et al. (2009). "Multiple forms of BRMS1 are differentially expressed in the MCF10 isogenic breast cancer progression model." Clin Exp Metastasis **26**(2): 89-96.

Hurst, D. R., Y. Xie, et al. (2013). "The C-terminal putative nuclear localization sequence of breast cancer metastasis suppressor 1, BRMS1, is necessary for metastasis suppression." PLoS One **8**(2): e55966.

Ianari, A., R. Gallo, et al. (2004). "Specific role for p300/CREB-binding protein-associated factor activity in E2F1 stabilization in response to DNA damage." The Journal of biological chemistry **279**(29): 30830-30835.

Irwin, M., K. Kondo, et al. (2003). "Chemosensitivity linked to p73 function." Cancer cell **3**(4): 403-410.

Iwabuchi, K., P. L. Bartel, et al. (1994). "Two cellular proteins that bind to wild-type but not mutant p53." Proc Natl Acad Sci U S A **91**(13): 6098-6102.

Iwabuchi, K., B. Li, et al. (1998). "Stimulation of p53-mediated transcriptional activation by the p53-binding proteins, 53BP1 and 53BP2." J Biol Chem **273**(40): 26061-26068.

Iyer, N. G., S. F. Chin, et al. (2004). "p300 regulates p53-dependent apoptosis after DNA damage in colorectal cancer cells by modulation of PUMA/p21 levels." Proc Natl Acad Sci U S A **101**(19): 7386-7391.

Jiang, L., M. Siu, et al. (2011). "iASPP and chemoresistance in ovarian cancers: effects on paclitaxel-mediated mitotic catastrophe." Clinical cancer research : an official journal of the American Association for Cancer Research **17**(21): 6924-6933.

Kaghad, M., H. Bonnet, et al. (1997). "Monoallelically expressed gene related to p53 at 1p36, a region frequently deleted in neuroblastoma and other human cancers." Cell.

Kalkhoven, E. (2004). "CBP and p300: HATs for different occasions." Biochemical pharmacology **68**(6): 1145-1155.

Kay, B. K., M. P. Williamson, et al. (2000). "The importance of being proline: the interaction of proline-rich motifs in signaling proteins with their cognate domains." FASEB J **14**(2): 231-241.

Kelleher, F. C. and G. A. McArthur (2012). "Targeting NRAS in melanoma." Cancer J **18**(2): 132-136.

Khodadoust, M. S., M. Verhaegen, et al. (2009). "Melanoma proliferation and chemoresistance controlled by the DEK oncogene." Cancer Res **69**(16): 6405-6413.

King, K. E., R. M. Ponnamperuma, et al. (2003). "deltaNp63alpha functions as both a positive and a negative transcriptional regulator and blocks in vitro differentiation of murine keratinocytes." Oncogene **22**(23): 3635-3644.

Ko, S. I., I. S. Lee, et al. (2006). "Regulation of histone acetyltransferase activity of p300 and PCAF by proto-oncogene protein DEK." FEBS Lett **580**(13): 3217-3222.

Koeppel, M., S. van Heeringen, et al. (2011). "Crosstalk between c-Jun and TAp73alpha/beta contributes to the apoptosis-survival balance." Nucleic acids research **39**(14): 6069-6085.

Kovalev, S., N. Marchenko, et al. (1998). "Expression level, allelic origin, and mutation analysis of the p73 gene in neuroblastoma tumors and cell lines." Cell Growth Differ **9**(11): 897-903.

Kubbutat, M. H., S. N. Jones, et al. (1997). "Regulation of p53 stability by Mdm2." Nature **387**(6630): 299-303.

Kundu, S., K. Fan, et al. (2010). "Tyrosine phosphatase inhibitor-3 sensitizes melanoma and colon cancer to biotherapeutics and chemotherapeutics." Molecular cancer therapeutics **9**(8): 2287-2296.

Kung, A. L., V. I. Rebel, et al. (2000). "Gene dose-dependent control of hematopoiesis and hematologic tumor suppression by CBP." Genes Dev **14**(3): 272-277.

Lapi, E., S. Di Agostino, et al. (2008). "PML, YAP, and p73 are components of a proapoptotic autoregulatory feedback loop." Mol Cell **32**(6): 803-814.

Laska, M., U. Vogel, et al. (2010). "p53 and PPP1R13L (alias iASPP or RAI) form a feedback loop to regulate genotoxic stress responses." Biochimica et biophysica acta **1800**(12): 1231-1240.

Legha, S. S., S. Ring, et al. (1996). "Treatment of metastatic melanoma with combined chemotherapy containing cisplatin, vinblastine and dacarbazine (CVD) and biotherapy using interleukin-2 and interferon-alpha." Ann Oncol **7**(8): 827-835.

Lev, D. C., A. Onn, et al. (2004). "Exposure of Melanoma Cells to Dacarbazine Results in Enhanced Tumor Growth and Metastasis In Vivo." Journal of Clinical Oncology **22**(11): 2092-2100.

Levrero, M., V. De, et al. (2000). "The p53/p63/p73 family of transcription factors: overlapping and distinct functions." Journal of cell ….

Levy, D., Y. Adamovich, et al. (2007). "The Yes-associated protein 1 stabilizes p73 by preventing Itch-mediated ubiquitination of p73." Cell death and differentiation **14**(4): 743-751.

Levy, D., Y. Adamovich, et al. (2008). "Yap1 phosphorylation by c-Abl is a critical step in selective activation of proapoptotic genes in response to DNA damage." Molecular cell **29**(3): 350-361.

Ley, R., K. Balmanno, et al. (2003). "Activation of the ERK1/2 signaling pathway promotes phosphorylation and proteasome-dependent degradation of the BH3-only protein, Bim." J Biol Chem **278**(21): 18811-18816.

Li, G., R. Wang, et al. (2011). "RNA interference-mediated silencing of iASPP induces cell proliferation inhibition and G0/G1 cell cycle arrest in U251 human glioblastoma cells." Molecular and cellular biochemistry **350**(1-2): 193-200.

Li, M., R. Z. Luo, et al. (2011). "High expression of transcriptional coactivator p300 correlates with aggressive features and poor prognosis of hepatocellular carcinoma." J Transl Med **9**: 5.

Liu, G., S. Nozell, et al. (2004). "DeltaNp73beta is active in transactivation and growth suppression." Mol Cell Biol **24**(2): 487-501.

Liu, Y., C. E. Denlinger, et al. (2006). "Suberoylanilide hydroxamic acid induces Akt-mediated phosphorylation of p300, which promotes acetylation and transcriptional activation of RelA/p65." J Biol Chem **281**(42): 31359-31368.

Liu, Y., M. Mayo, et al. (2013). "BRMS1 suppresses lung cancer metastases through an E3 ligase function on histone acetyltransferase p300." Cancer research **73**(4): 1308-1317.

Liu, Y., P. Smith, et al. (2006). "Breast cancer metastasis suppressor 1 functions as a corepressor by enhancing histone deacetylase 1-mediated deacetylation of RelA/p65 and promoting apoptosis." Molecular and cellular biology **26**(23): 8683-8696.

Liu, Z. J., X. Lu, et al. (2005). "Downregulated mRNA expression of ASPP and the hypermethylation of the 5'-untranslated region in cancer cell lines retaining wild-type p53." FEBS Lett **579**(7): 1587-1590.

Llanos, S., C. Royer, et al. (2011). "Inhibitory member of the apoptosis-stimulating proteins of the p53 family (iASPP) interacts with protein phosphatase 1 via a noncanonical binding motif." The Journal of biological chemistry **286**(50): 43039-43044.

Lloyd, K. A. (2013). "A scientific review: mechanisms of valproate-mediated teratogenesis." Bioscience Horizons **6**.

Lokshin, M., Y. Li, et al. (2007). "p53 and p73 display common and distinct requirements for sequence specific binding to DNA." Nucleic acids research **35**(1): 340-352.

Lopez, C. D., Y. Ao, et al. (2000). "Proapoptotic p53-interacting protein 53BP2 is induced by UV irradiation but suppressed by p53." Mol Cell Biol **20**(21): 8018-8025.

Lu, M., H. Breyssens, et al. (2013). "Restoring p53 function in human melanoma cells by inhibiting MDM2 and cyclin B1/CDK1-phosphorylated nuclear iASPP." Cancer cell **23**(5): 618-633.

Luh, L., S. Kehrloesser, et al. (2013). "Analysis of the oligomeric state and transactivation potential of TAp73α." Cell death and differentiation **20**(8): 1008-1016.

Lunghi, P., A. Costanzo, et al. (2009). "The p53 family protein p73 provides new insights into cancer chemosensitivity and targeting." Clinical cancer research : an official journal of the American Association for Cancer Research **15**(21): 6495-6502.

Luo, J., M. Li, et al. (2004). "Acetylation of p53 augments its site-specific DNA binding both in vitro and in vivo." Proc Natl Acad Sci U S A **101**(8): 2259-2264.

Mantelingu, K., A. Kishore, et al. (2007). "Activation of p300 histone acetyltransferase by small molecules altering enzyme structure: probed by surface-enhanced Raman spectroscopy." The journal of physical chemistry. B **111**(17): 4527-4534.

Mantovani, F., S. Piazza, et al. (2004). "Pin1 links the activities of c-Abl and p300 in regulating p73 function." Molecular cell **14**(5): 625-636.

Mantovani, F., F. Tocco, et al. (2007). "The prolyl isomerase Pin1 orchestrates p53 acetylation and dissociation from the apoptosis inhibitor iASPP." Nature structural & molecular biology **14**(10): 912-920.

Marchesini, R., A. Bono, et al. (2007). "In vivo evaluation of melanoma thickness by multispectral imaging and an artificial neural network. A retrospective study on 250 cases of cutaneous melanoma." Tumori **93**(2): 170-177.

Martinez-Balbas, M. A., U. M. Bauer, et al. (2000). "Regulation of E2F1 activity by acetylation." EMBO J **19**(4): 662-671.

Melino, G., F. Bernassola, et al. (2004). "p73 Induces apoptosis via PUMA transactivation and Bax mitochondrial translocation." The Journal of biological chemistry **279**(9): 8076-8083.

Méndez, J. and B. Stillman (2000). "Chromatin Association of Human Origin Recognition Complex, Cdc6, and Minichromosome Maintenance Proteins during the Cell Cycle: Assembly of Prereplication Complexes in Late Mitosis." Molecular and Cellular Biology **20**(22): 8602-8612.

Michael, D. and M. Oren (2002). "The p53 and Mdm2 families in cancer." Curr Opin Genet Dev **12**(1): 53-59.

Michaloglou, C., L. C. Vredeveld, et al. (2005). "BRAFE600-associated senescence-like cell cycle arrest of human naevi." Nature **436**(7051): 720-724.

Molina, G., A. Vogt, et al. (2009). "Zebrafish chemical screening reveals an inhibitor of Dusp6 that expands cardiac cell lineages." Nat Chem Biol **5**(9): 680-687.

Mori, S., G. Ito, et al. (2004). "p53 apoptotic pathway molecules are frequently and simultaneously altered in nonsmall cell lung carcinoma." Cancer **100**(8): 1673-1682.

Morris, L., K. Allen, et al. (2000). "Regulation of E2F transcription by cyclin E-Cdk2 kinase mediated through p300/CBP co-activators." Nature cell biology **2**(4): 232-239.

Muller, M., E. S. Schleithoff, et al. (2006). "One, two, three--p53, p63, p73 and chemosensitivity." Drug Resist Updat **9**(6): 288-306.

Munshi, N., M. Merika, et al. (1998). "Acetylation of HMG I(Y) by CBP turns off IFN beta expression by disrupting the enhanceosome." Mol Cell **2**(4): 457-467.

Naldini, L., U. Blomer, et al. (1996). "In vivo gene delivery and stable transduction of nondividing cells by a lentiviral vector." Science **272**(5259): 263-267.

Naumovski, L. and M. L. Cleary (1996). "The p53-binding protein 53BP2 also interacts with Bc12 and impedes cell cycle progression at G2/M." Mol Cell Biol **16**(7): 3884-3892.

Nexo, B. A., U. Vogel, et al. (2008). "Linkage disequilibrium mapping of a breast cancer susceptibility locus near RAI/PPP1R13L/iASPP." BMC Med Genet **9**: 56.

Nicholson, D. W., A. Ali, et al. (1995). "Identification and inhibition of the ICE/CED-3 protease necessary for mammalian apoptosis." Nature **376**(6535): 37-43.

Notari, M., Y. Hu, et al. (2011). "Inhibitor of apoptosis-stimulating protein of p53 (iASPP) prevents senescence and is required for epithelial stratification." Proceedings of the National Academy of Sciences of the United States of America **108**(40): 16645-16650.

O'Shea, J. J., Y. Kanno, et al. (2005). "Cell signaling. Stat acetylation--a key facet of cytokine signaling?" Science **307**(5707): 217-218.

Ogiwara, H. and T. Kohno (2012). "CBP and p300 histone acetyltransferases contribute to homologous recombination by transcriptionally activating the BRCA1 and RAD51 genes." PLoS One **7**(12): e52810.

Oike, Y., N. Takakura, et al. (1999). "Mice homozygous for a truncated form of CREB-binding protein exhibit defects in hematopoiesis and vasculo-angiogenesis." Blood **93**(9): 2771-2779.

Petitclerc, E., S. Stromblad, et al. (1999). "Integrin alpha(v)beta3 promotes M21 melanoma growth in human skin by regulating tumor cell survival." Cancer Res **59**(11): 2724-2730.

Pillai, V. B., N. R. Sundaresan, et al. (2011). "Acetylation of a conserved lysine residue in the ATP binding pocket of p38 augments its kinase activity during hypertrophy of cardiomyocytes." Mol Cell Biol **31**(11): 2349-2363.

Poizat, C., P. Puri, et al. (2005). "Phosphorylation-dependent degradation of p300 by doxorubicin-activated p38 mitogen-activated protein kinase in cardiac cells." Molecular and cellular biology **25**(7): 2673-2687.

Poizat, C., V. Sartorelli, et al. (2000). "Proteasome-mediated degradation of the coactivator p300 impairs cardiac transcription." Mol Cell Biol **20**(23): 8643-8654.

Pollock, P. M. and P. S. Meltzer (2002). "A genome-based strategy uncovers frequent BRAF mutations in melanoma." Cancer Cell **2**(1): 5-7.

Reid, J. M., M. J. Kuffel, et al. (1999). "Metabolic Activation of Dacarbazine by Human Cytochromes P450: The Role of CYP1A1, CYP1A2, and CYP2E1." Clinical Cancer Research **5**(8): 2192-2197.

Riker, A. I., S. A. Enkemann, et al. (2008). "The gene expression profiles of primary and metastatic melanoma yields a transition point of tumor progression and metastasis." BMC Med Genomics **1**: 13.

Robertson, G., A. Coleman, et al. (1996). "A malignant melanoma tumor suppressor on human chromosome 11." Cancer Res **56**(19): 4487-4492.

Robinson, R., X. Lu, et al. (2008). "Biochemical and structural studies of ASPP proteins reveal differential binding to p53, p63, and p73." Structure (London, England : 1993) **16**(2): 259-268.

Röckmann, H. and D. Schadendorf (2003). "Drug Resistance in Human Melanoma: Mechanisms and Therapeutic Opportunities." Onkologie **26**(6): 581-587.

Roth, J. F., N. Shikama, et al. (2003). "Differential role of p300 and CBP acetyltransferase during myogenesis: p300 acts upstream of MyoD and Myf5." EMBO J **22**(19): 5186-5196.

Rufini, A., M. Agostini, et al. (2011). "p73 in Cancer." Genes & cancer **2**(4): 491-502.

Sakaguchi, K., J. E. Herrera, et al. (1998). "DNA damage activates p53 through a phosphorylation-acetylation cascade." Genes Dev **12**(18): 2831-2841.

Samuels-Lev, Y., D. O'Connor, et al. (2001). "ASPP proteins specifically stimulate the apoptotic function of p53." Molecular cell **8**(4): 781-794.

Sanada, M., M. Hidaka, et al. (2007). "Modes of actions of two types of anti-neoplastic drugs, dacarbazine and ACNU, to induce apoptosis." Carcinogenesis **28**(12): 2657-2663.

Sanchez-Prieto, R., V. Sanchez-Arevalo, et al. (2002). "Regulation of p73 by c-Abl through the p38 MAP kinase pathway." Oncogene **21**(6): 974-979.

Santos, G. C., M. Zielenska, et al. (2007). "Chromosome 6p amplification and cancer progression." J Clin Pathol **60**(1): 1-7.

Satake, N., Y. Ishida, et al. (1997). "Novel MLL-CBP fusion transcript in therapy-related chronic myelomonocytic leukemia with a t(11;16)(q23;p13) chromosome translocation." Genes Chromosomes Cancer **20**(1): 60-63.

Satoh, M. S. and T. Lindahl (1992). "Role of poly(ADP-ribose) formation in DNA repair." Nature **356**(6367): 356-358.

Schiltz, R. L., C. A. Mizzen, et al. (1999). "Overlapping but distinct patterns of histone acetylation by the human coactivators p300 and PCAF within nucleosomal substrates." J Biol Chem **274**(3): 1189-1192.

Seraj, M. J., R. S. Samant, et al. (2000). "Functional evidence for a novel human breast carcinoma metastasis suppressor, BRMS1, encoded at chromosome 11q13." Cancer Res **60**(11): 2764-2769.

Serrone, L. and P. Hersey (1999). "The chemoresistance of human malignant melanoma: an update." Melanoma Res **9**(1): 51-58.

Shevde, L. A., R. S. Samant, et al. (2002). "Suppression of human melanoma metastasis by the metastasis suppressor gene, BRMS1." Exp Cell Res **273**(2): 229-239.

Shi, D., M. S. Pop, et al. (2009). "CBP and p300 are cytoplasmic E4 polyubiquitin ligases for p53." Proc Natl Acad Sci U S A **106**(38): 16275-16280.

Shikama, N., W. Lutz, et al. (2003). "Essential function of p300 acetyltransferase activity in heart, lung and small intestine formation." EMBO J **22**(19): 5175-5185.

Shima, Y., T. Shima, et al. (2008). "PML activates transcription by protecting HIPK2 and p300 from SCFFbx3-mediated degradation." Mol Cell Biol **28**(23): 7126-7138.

Skaar, J. R., J. K. Pagan, et al. (2013). "Mechanisms and function of substrate recruitment by F-box proteins." Nat Rev Mol Cell Biol **14**(6): 369-381.

Slee, E., S. Gillotin, et al. (2004). "The N-terminus of a novel isoform of human iASPP is required for its cytoplasmic localization." Oncogene **23**(56): 9007-9016.

Slipicevic, A., R. Holm, et al. (2012). "Cytoplasmic BRMS1 expression in malignant melanoma is associated with increased disease-free survival." BMC cancer **12**: 73.

Smeenk, L., S. van Heeringen, et al. (2008). "Characterization of genome-wide p53-binding sites upon stress response." Nucleic acids research **36**(11): 3639-3654.

Soussi, T. and K. Wiman (2007). "Shaping genetic alterations in human cancer: the p53 mutation paradigm." Cancer cell **12**(4): 303-312.

St-Germain, J., J. Chen, et al. (2008). "Involvement of PML nuclear bodies in CBP degradation through the ubiquitin-proteasome pathway." Epigenetics.

Stefanaki, C., K. Stefanaki, et al. (2007). "Cell cycle and apoptosis regulators in Spitz nevi: comparison with melanomas and common nevi." J Am Acad Dermatol **56**(5): 815-824.

Stewart, S. A., D. M. Dykxhoorn, et al. (2003). "Lentivirus-delivered stable gene silencing by RNAi in primary cells." RNA **9**(4): 493-501.

Stiehl, D. P., D. M. Fath, et al. (2007). "Histone deacetylase inhibitors synergize p300 autoacetylation that regulates its transactivation activity and complex formation." Cancer Res **67**(5): 2256-2264.

Strano, S., O. Monti, et al. (2005). "The transcriptional coactivator Yes-associated protein drives p73 gene-target specificity in response to DNA Damage." Molecular cell **18**(4): 447-459.

Su, X. L., X. H. Ouyang, et al. (2009). "p73 expression and its clinical significance in colorectal cancer." Colorectal Dis **11**(9): 960-963.

Sullivan, A. and X. Lu (2007). "ASPP: a new family of oncogenes and tumour suppressor genes." British journal of cancer **96**(2): 196-200.

Takada, N., T. Sanda, et al. (2002). "RelA-associated inhibitor blocks transcription of human immunodeficiency virus type 1 by inhibiting NF-kappaB and Sp1 actions." J Virol **76**(16): 8019-8030.

Talantov, D., A. Mazumder, et al. (2005). "Novel genes associated with malignant melanoma but not benign melanocytic lesions." Clinical cancer research : an official journal of the American Association for Cancer Research **11**(20): 7234-7242.

Tannapfel, A., M. Wasner, et al. (1999). "Expression of p73 and its relation to histopathology and prognosis in hepatocellular carcinoma." J Natl Cancer Inst **91**(13): 1154-1158.

Teufel, D. P., S. M. Freund, et al. (2007). "Four domains of p300 each bind tightly to a sequence spanning both transactivation subdomains of p53." Proc Natl Acad Sci U S A **104**(17): 7009-7014.

Thompson, P. R., D. Wang, et al. (2004). "Regulation of the p300 HAT domain via a novel activation loop." Nat Struct Mol Biol **11**(4): 308-315.

Tidow, H., D. B. Veprintsev, et al. (2006). "Effects of oncogenic mutations and DNA response elements on the binding of p53 to p53-binding protein 2 (53BP2)." J Biol Chem **281**(43): 32526-32533.

Toh, W. H., E. Logette, et al. (2008). "TAp73beta and DNp73beta activate the expression of the pro-survival caspase-2S." Nucleic Acids Res **36**(13): 4498-4509.

Tomasini, R., K. Tsuchihara, et al. (2008). "TAp73 knockout shows genomic instability with infertility and tumor suppressor functions." Genes & development **22**(19): 2677-2691.

Tounekti, O., J. Belehradek, Jr., et al. (1995). "Relationships between DNA fragmentation, chromatin condensation, and changes in flow cytometry profiles detected during apoptosis." Exp Cell Res **217**(2): 506-516.

Trigiante, G. and X. Lu (2006). "ASPP [corrected] and cancer." Nature reviews. Cancer **6**(3): 217-226.

Truong, A. B., M. Kretz, et al. (2006). "p63 regulates proliferation and differentiation of developmentally mature keratinocytes." Genes & development **20**(22): 3185-3197.

Tsao, H., L. Chin, et al. (2012). "Melanoma: from mutations to medicine." Genes & development **26**(11): 1131-1155.

Tsao, H., X. Zhang, et al. (1999). "Mutational and expression analysis of the p73 gene in melanoma cell lines." Cancer Res **59**(1): 172-174.

Tschan, M. P., T. J. Grob, et al. (2000). "Enhanced p73 expression during differentiation and complex p73 isoforms in myeloid leukemia." Biochem Biophys Res Commun **277**(1): 62-65.

Uziel, T., Y. Lerenthal, et al. (2003). "Requirement of the MRN complex for ATM activation by DNA damage." EMBO J **22**(20): 5612-5621.

Vigneron, A., R. Ludwig, et al. (2010). "Cytoplasmic ASPP1 inhibits apoptosis through the control of YAP." Genes & development **24**(21): 2430-2439.

Vigneron, A. M. and K. H. Vousden (2012). "An indirect role for ASPP1 in limiting p53-dependent p21 expression and cellular senescence." EMBO J **31**(2): 471-480.

Wang, H. Y., Z. Cheng, et al. (2003). "Overexpression of mitogen-activated protein kinase phosphatases MKP1, MKP2 in human breast cancer." Cancer Lett **191**(2): 229-237.

Wang, Q.-E., C. Han, et al. (2013). "p38 MAPK- and Akt-mediated p300 phosphorylation regulates its degradation to facilitate nucleotide excision repair." Nucleic acids research **41**(3): 1722-1733.

Wang, X., J. Taplick, et al. (2004). "Inhibition of p53 degradation by Mdm2 acetylation." FEBS Lett **561**(1-3): 195-201.

Wise-Draper, T. M., H. V. Allen, et al. (2006). "Apoptosis inhibition by the human DEK oncoprotein involves interference with p53 functions." Mol Cell Biol **26**(20): 7506-7519.

Wong, P.-P., A. Pickard, et al. (2010). "p300 Alters Keratinocyte Cell Growth and Differentiation through Regulation of p21^{Waf1/CIP1}." PloS one **5**(1): e8369.

Yaciuk, P., M. C. Carter, et al. (1991). "Simian virus 40 large-T antigen expresses a biological activity complementary to the p300-associated transforming function of the adenovirus E1A gene products." Mol Cell Biol **11**(4): 2116-2124.

Yan, G., M. Eller, et al. (2013). "Selective Inhibition of p300 HAT Blocks Cell Cycle Progression, Induces Cellular Senescence, and Inhibits the DNA Damage Response in Melanoma Cells." The Journal of investigative dermatology.

Yang, A., M. Kaghad, et al. (1998). "< i> p63</i>, a< i> p53</i> Homolog at 3q27–29, Encodes Multiple Products with Transactivating, Death-Inducing, and Dominant-Negative Activities." Molecular cell **2**(3): 305-316.

Yang, J. P. (1999). "Identification of a Novel Inhibitor of Nuclear Factor-kappa B, RelA-associated Inhibitor." Journal of Biological Chemistry **274**.

Yao, T. P., S. P. Oh, et al. (1998). "Gene dosage-dependent embryonic development and proliferation defects in mice lacking the transcriptional integrator p300." Cell **93**(3): 361-372.

Yao, X., K. Panichpisal, et al. (2007). "Cisplatin nephrotoxicity: a review." Am J Med Sci **334**(2): 115-124.

Yin, J., L. Guo, et al. (2013). "Effects of PPP1R13L and CD3EAP variants on lung cancer susceptibility among nonsmoking Chinese women." Gene **524**(2): 228-231.

Yuan, L. W. and J. E. Gambee (2000). "Phosphorylation of p300 at serine 89 by protein kinase C." J Biol Chem **275**(52): 40946-40951.

Yuan, Z. M., H. Shioya, et al. (1999). "p73 is regulated by tyrosine kinase c-Abl in the apoptotic response to DNA damage." Nature **399**(6738): 814-817.

Zaika, A. I., S. Kovalev, et al. (1999). "Overexpression of the wild type p73 gene in breast cancer tissues and cell lines." Cancer Res **59**(13): 3257-3263.

Zeng, X., H. Lee, et al. (2001). "p300 does not require its acetylase activity to stimulate p73 function." J Biol Chem **276**(1): 48-52.

Zeng, X., X. Li, et al. (2000). "The N-terminal domain of p73 interacts with the CH1 domain of p300/CREB binding protein and mediates transcriptional activation and apoptosis." … and cellular biology.

Zhang, X., S. Diao, et al. (2007). "Identification of a novel isoform of iASPP and its interaction with p53." Journal of molecular biology **368**(4): 1162-1171.

Zhang, X., M. Wang, et al. (2005). "The expression of iASPP in acute leukemias." Leukemia research **29**(2): 179-183.

Zhao, J., G. Wu, et al. (2010). "Epigenetic silence of ankyrin-repeat-containing, SH3-domain-containing, and proline-rich-region- containing protein 1 (ASPP1) and ASPP2 genes promotes tumor growth in hepatitis B virus-positive hepatocellular carcinoma." Hepatology **51**(1): 142-153.

Appendix

Appendix Sup-1

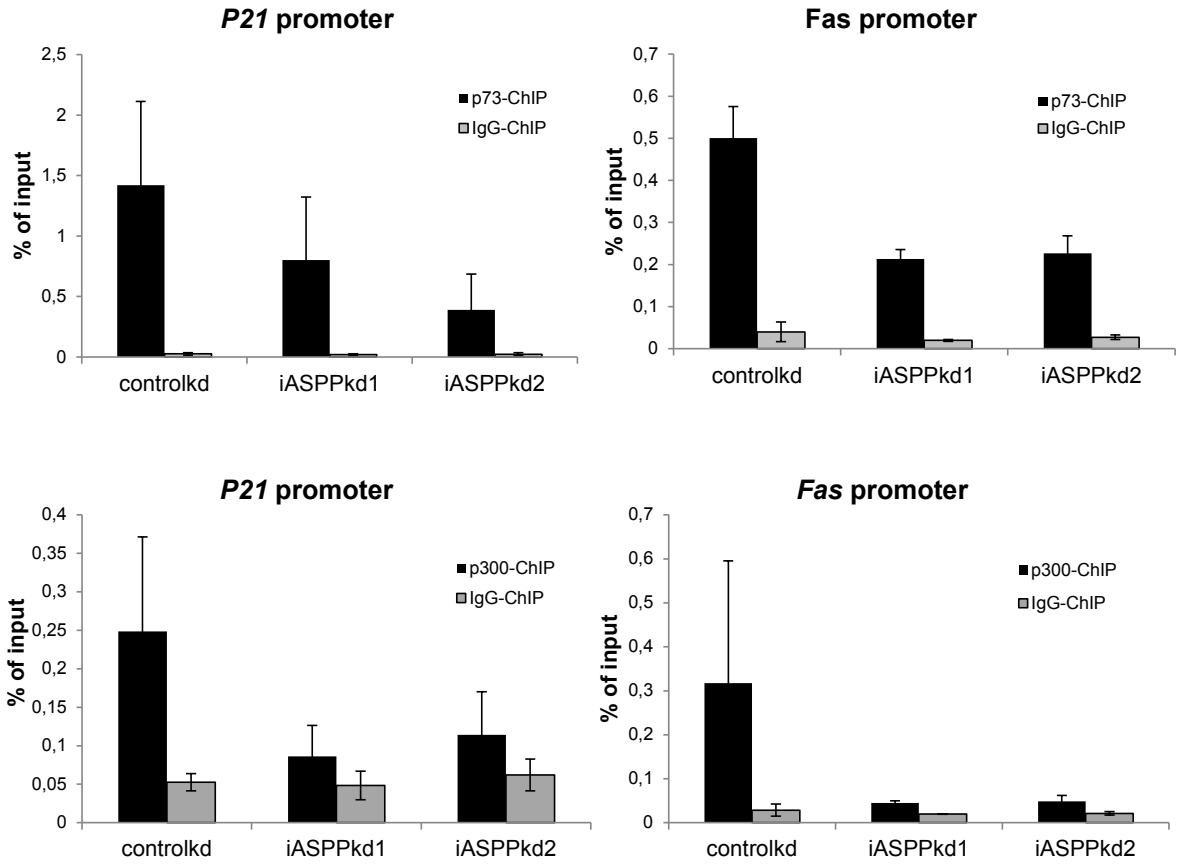

Appendix Sup-1. iASPP knockdown leads to an overlapping loss of p73 and p300 target site binding in cisplatin-treated HCT116 cells.
For chromatin immunoprecipitation HCT116 knockdown cells were treated for 8 h with 20 µM cisplatin prior to chromatin harvest. Chromatin immunoprecipitations were performed using a p73- as well as p300-specific antibody. For control, an IgG reaction was performed in parallel. The data is represented as the % of input sample of the respective target site. The *p21* and *fas* gene locus are depicted as two examples of the observed loss of p73 and p300 DNA-binding.

Appendix Sup-2

A

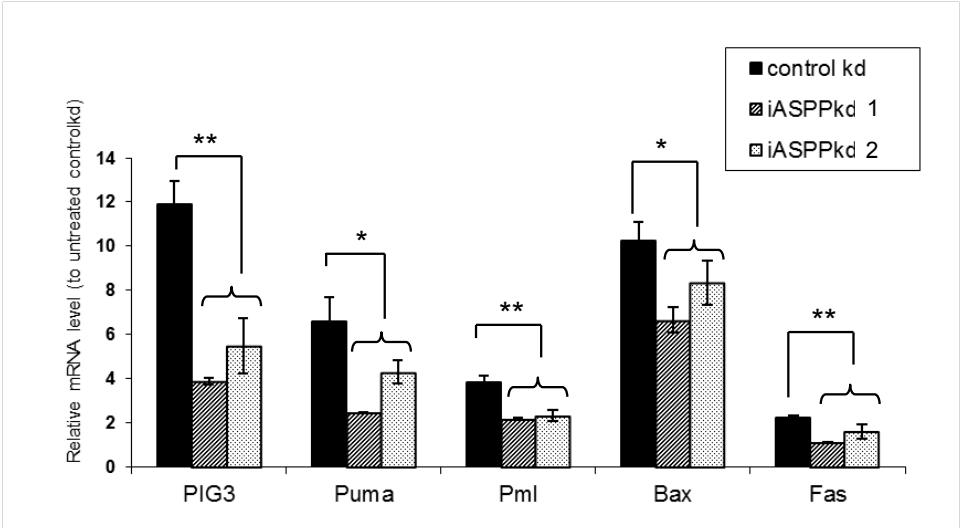

B

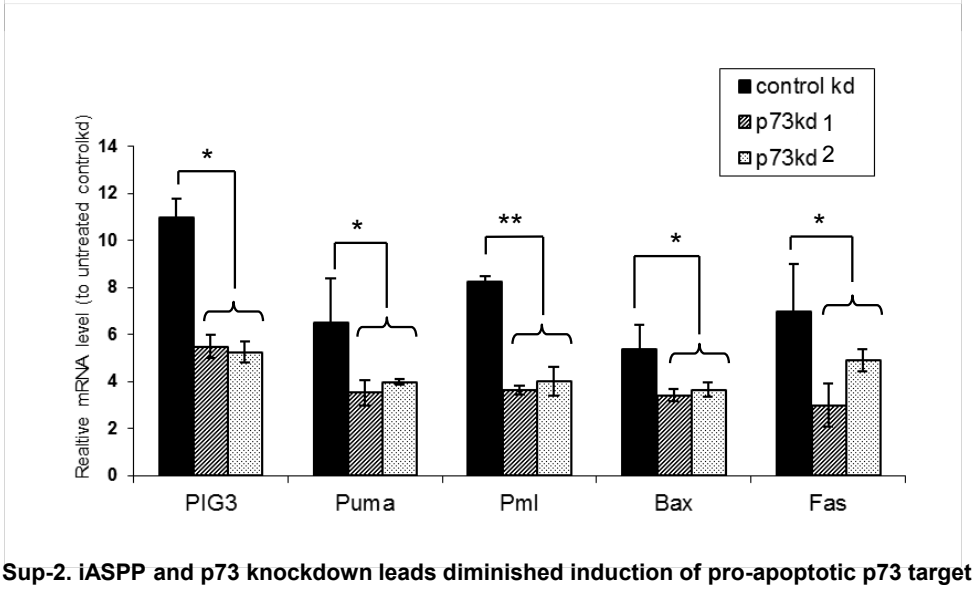

Appendix Sup-2. iASPP and p73 knockdown leads diminished induction of pro-apoptotic p73 target genes in cisplatin-treated HCT116 cells.
For RNA extraction cells were treated for 12 h with 20 μM cisplatin.
A. Gene expression of additional p73 target genes in cisplatin-treated iASPP knockdown cells.
For details see Figure 3.6.
B. P73 knockdown leads to a similar reduction in the mRNA levels of p73 target genes.
P73 was stably knockdown in HCT116 cells using two independent shRNA constructs.

Appendix Sup-3

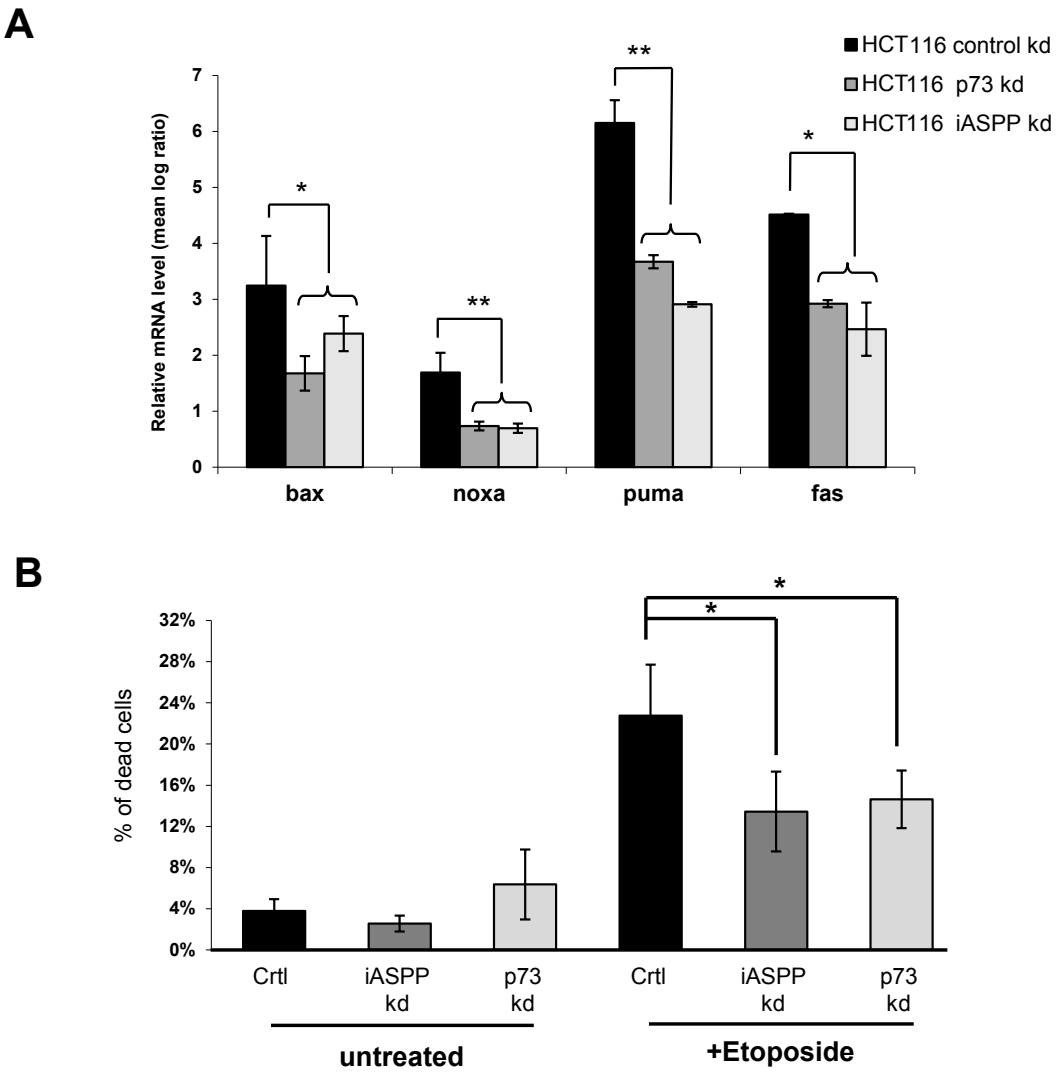

Appendix Figure Sup-3. iASPP and p73 knockdown leads diminished induction of pro-apoptotic p73 target genes and apoptosis in Etoposide-treated HCT116 cells.
IASPP and p73 knockdown cells were generated by pooling 3 different shRNA constructs for iASPP or p73 knockdown. Control knockdown was performed using shRNA for the luciferase gene. For RNA extraction and cell cycle analysis, cells were treated for 24 h with 30 µM Etoposide.
A. Gene expression analysis of p73 target genes in Etoposide-treated iASPPand p73 knockdown cells.
Bax, noxa, puma and fas mRNA level were analysied using gene-specific primer. HPRT1 served as a reference gene for normalization of the Ct values. Depicted are the relative mRNA level as the mean log ratio.
B. IASPP and p73 knockdown contributes to the apoptosis induction after Etoposide treatment.
Etoposide-treated control, iASPP and p73 knockdown cells were fixed with Ethanol and stained with Propidium iodied. Cell cycle profiles were generated by FACS analysis. For quantification of the % of dead cells, subG1 phase was quantified. Same gate settings were applied for all samples.

Appendix Sup-4

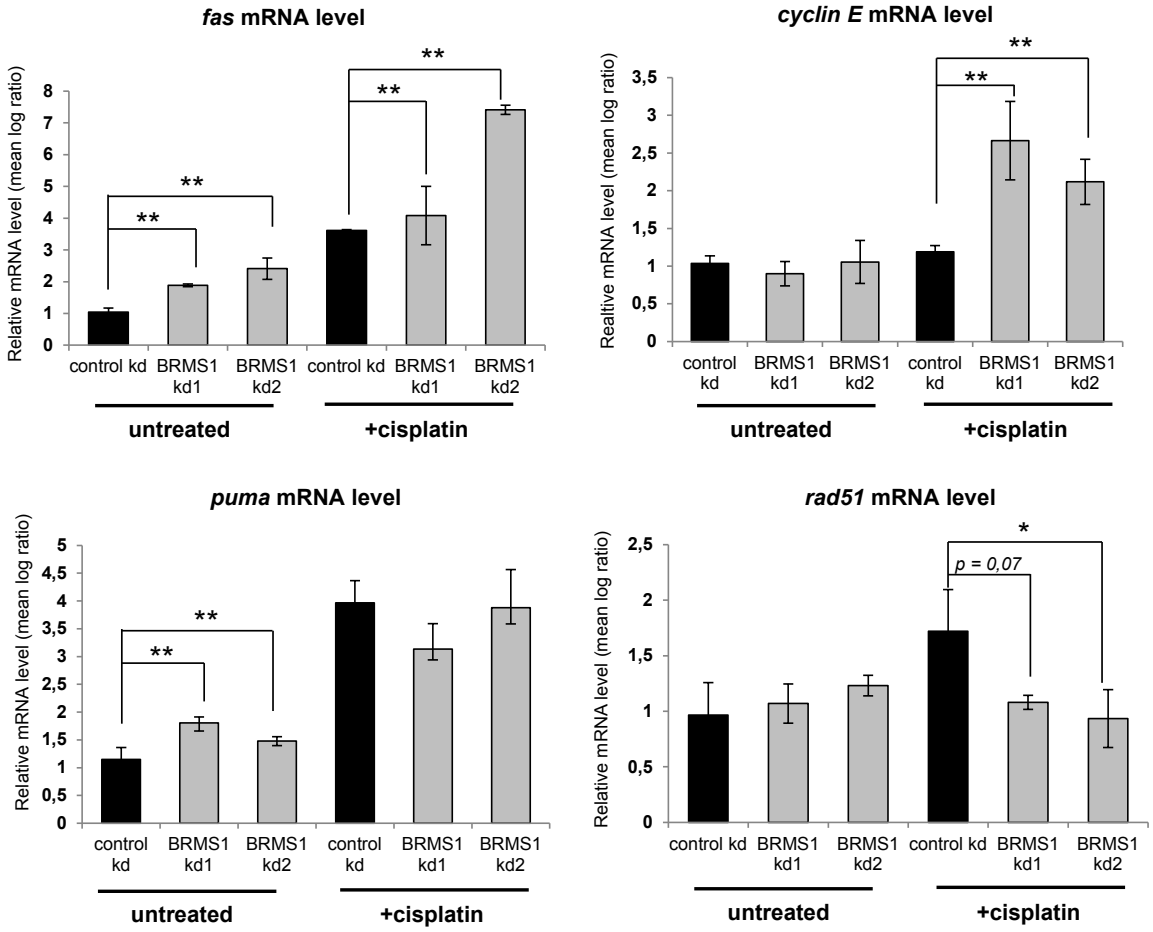

Appendix Sup-4. BRMS1 knockdown modifies the gene expression of a subset of p300/ p73 target genes. BRMS1 was transiently depleted using two different siRNAs and a scrambled siRNA as a control. 36 h after transfection, cells were treated for 8 h with 20 µM cisplatin. After RNA extraction and cDNA synthesis, the gene expression of various p73/ p300 target genes was analysed. Represented is *puma* and *fas* as p300 and p73 co-regulated, pro-apoptotic target genes. *Rad51* and *cyclin E* represents genes that are transcriptionally regulated by p300 only (according to Ogiwara et al, 2012; Bandyopadhyay et al, 2002).

Appendix Sup-5

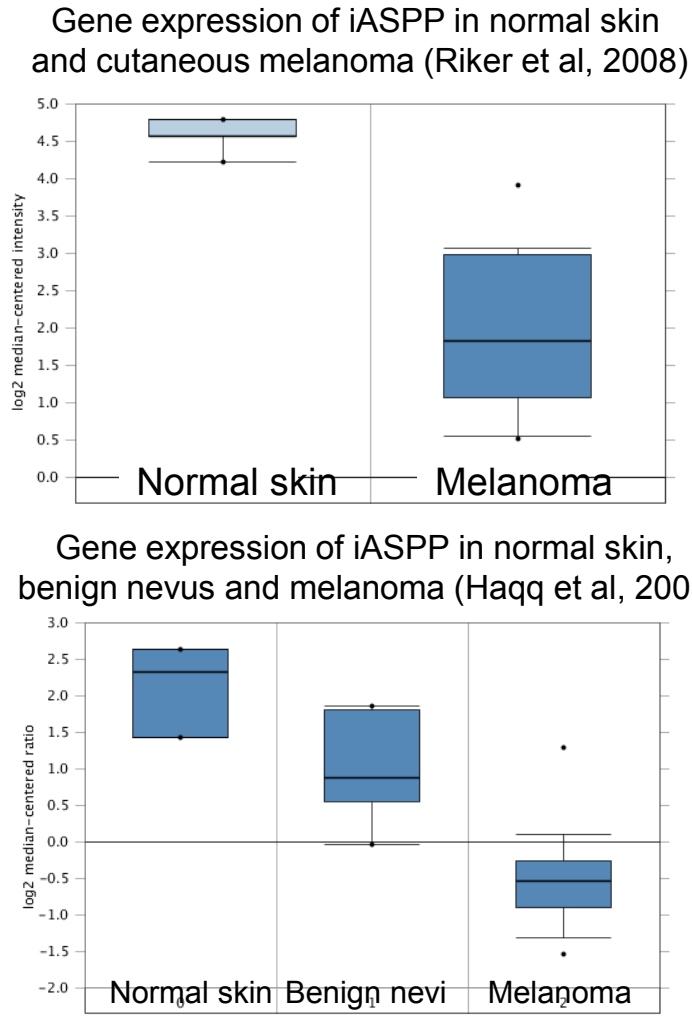

Appendix Sup-5. Down-regulation of iASPP mRNA level in two additional gene expression studies of malignant melanoma.
The figure displays the gene expression level of iASPP in multiple malignant melanoma samples compared to normal skin tissue and benign nevus samples of two independently performed microarray analysis (Riker et al, 2008; Haqq et al, 2005). These studies underscore the previously evaluated study of Talantov and colleagues; Figure 3.12), thereby confirming down-regulation of iASPP in the process of melanoma development.

Appendix Sup-6

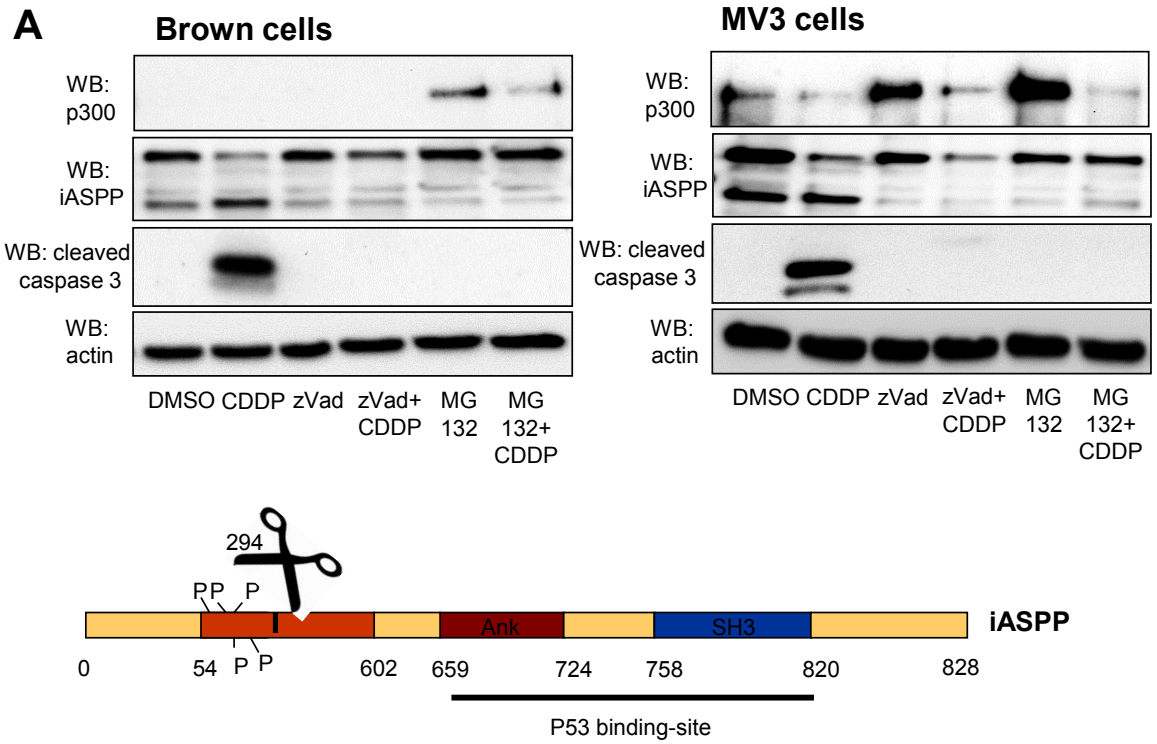

Appendix-Sup-6. IASPP is cleaved by caspases in some melanoma cell lines.
A. iASPP is subjected to caspase-cleavage in MV3 and Brown cells.
MV3 and Brown cells were treated for 24 h with 20 µM cisplatin. To proof cleavage of iASPP by caspases, cells were treated in parallel for 24 h with 40 µM Z-Vad or 40 µM Z-Vad and 20 µM cisplatin. Moreover cells were treated for 4 h with 10 µM MG132 or 10 µM MG132 and 20 µM cisplatin to visualize proteasomal degradation processes of p300 and iASPP. Protein lysates were prepared and immunoblotted. Detection of cleaved caspase 3 served as a control for effective inhibition of caspases by Z-Vad. Actin staining controls equal loading of the samples. (CDDP = cisplatin, zVAD = caspase inhibitor, MG132 = proteasome inhibitor)
B. *In-silico* analysis of the iASPP sequence detects a N-terminal caspase cleavage site.
The iASPP protein sequence was analysed with the CutDB program (http://cutdb.burnham.org/relation/show/21917). A caspase-cleavage site was detected at position 295 (sequence: SSLD-GLGG). (*Ank= ankryn-repeats, SH3= SH3-domain; P= phoshorylation site*)

.

Acknowledgements

First of all, I like to thank Prof. Dr. Matthias Dobbelstein for giving me the opportunity to finish my PhD thesis in his group. Without this chance, I would have never been able to submit my thesis. Also many thanks for his great supervision and support over the last two years.

Furthermore, I like to thank the other members of the thesis commitee, Prof. Heidi Hahn and Prof. Dr. Ralph Kehlenbach for their ideas and support during my thesis commitee meetings. I like to thank Prof. Dr. Holger Reichardt, Dr. Roland Dosch and Dr. Wilfried Kramer for their motivation to constitute my extended thesis committee and to attend my final thesis defense.

I especially like to thank my parents for all their motivation and help over the last years. Without your support, I would have never dared to start studying in the Netherlands, or moving to Frankfurt and Göttingen to complete my PhD. The same gratitude goes to my best friends, Saskia, Tina and Tanja. You always listened to my problems and doubts and convinced me to go on and look forward!

Moreover, I like to thank Dominik for his support. You were always there when I needed you.

Many thanks go to the whole Dobbelstein group as well. I really like the atmosphere in the group and the many discussions, ideas and help of all people from the group.

Last but not least, I like to thank Prof. Dr. Henk Stunnenberg and Dr. Martin Zörnig for their intermediate supervision during my PhD, as well as Nanni and Max for the help, support and ideas and motivation during the last years.